Territorial Robots

A Model Approach to the Ecology of Spatial Cognition

der Fakultät für Biologie
der Eberhard Karls Universität Tübingen

zur Erlangung des Grades eines Doktors
der Naturwissenschaften

von

Amelie Schmolke
aus Freiburg i. Br.

vorgelegte
Dissertation
2005

Tag der mündlichen Prüfung:	12. Juli 2005
Dekan:	Prof. Dr. F. Schöffl
1. Berichterstatter:	Prof. Dr. H. A. Mallot
2. Berichterstatter:	Prof. Dr. H.-U. Schnitzler

Summary

Territoriality represents an instance of a behaviour that is based on the ability of spatial learning. Thereby, no simple spatial goal can be defined, but territorial animals have to navigate between multiple places within their territory. They have to assess and learn characteristics of places, and have to memorise the relations between the places. In a simulation, specific cognitive abilities can be controlled and manipulated independent from the other traits of an individual, a condition not easily achievable in animal experiments. I explicitely modelled spatial information processing abilities in order to approach the cognitive ecology of territorial behaviour.

A common means of self-localisation in animals and robots is the measurement of egomotion, i.e. path integration. However, path integration is prone to accumulating errors if no external cues are available for recalibration. I introduced a polarisation compass for a miniature robot (Khepera) as an allocentric orientation measurement. The compass brought a significant reduction of the path integration error while claiming low energy supply and weight, properties that are essential in both miniature robots and animals.

The self-localisation in the environment provides the basis for the formation of an internal representation of the environment. Presumably, territoriality requires a map-like representation since the relation between many places does not allow the navigation by simple rules connecting defined starting and goal positions. Two alternatives of such a spatial memory, a graph and a grid structure, are combined with a model of territory establishment. Thereby, exclusive space use is achieved by the avoidance of competitors. The graph representation requires a lower memory capacity than the grid, and it was originally proposed as a solution for way-finding tasks. Nevertheless, both memory structures are equally suitable for territoriality, suggesting a graph as a favourable representation.

In simulation, I investigated the influences of information processing abilities and of external factors on space use. Higher learning rates as well as increased

amounts of memory retrieval resulted in more confined space use. The area used by more than one individual declined. Thus, higher information processing abilities led to an increasing stability of space use whereby competitors were avoided more efficiently. The individuals achieved exclusive ranges by decreased travelling distances.

On the other hand, a growing number of individuals competing for the same area led to an enlargement of the individual ranges whereby the territory sizes initially remained stable. However, if the population density did not allow the avoidance of competitors, the ranges used exclusively collapsed. This compares to conditional territoriality as found in animals. As an additional external factor, I investigated the effects of the structuring of the physical environment. If obstacles were present, the territory boundaries tended to line up with these obstacles.

The results emphasise the role of cognitive abilities in the understanding of animal behaviour. The amount of information available for decision making is crucial. The usage of simple rules might be more efficient than high problem-solving abilities since the computational complexity can be saved.

Contents

1 Preface **1**
- 1.1 The modelling approach 1
- 1.2 Thesis objectives and organisation 2

2 Polarisation compass **5**
- 2.1 Introduction 5
  - 2.1.1 Path integration in animals 6
  - 2.1.2 Compass orientation in animals 6
  - 2.1.3 Path integration in artificial systems 8
  - 2.1.4 Polarisation compass for the Khepera robot 9
- 2.2 Simulation environment 9
  - 2.2.1 Khepera robots 9
  - 2.2.2 Robot arena 10
  - 2.2.3 Calibration of the odometry 11
- 2.3 Polarisation compass 12
  - 2.3.1 Sensors 12
  - 2.3.2 Compass design 14
- 2.4 Quantification of the path integration error 14
- 2.5 Results 15
- 2.6 Discussion 16

3 Representations in spatial behaviour **19**
- 3.1 Introduction 19
- 3.2 Spatial memory 20
  - 3.2.1 Hierarchy of navigation by Trullier et al. (1997) 20
  - 3.2.2 Hierarchy of navigation by Mallot (1999) 21
  - 3.2.3 The cognitive map concept 21

3.2.4 Neuronal basis of spatial representations 22
3.2.5 Structure of spatial representations 24
3.2.6 Spatial representations in artificial systems 24
3.3 Territoriality 26
3.3.1 Ecology of territorial behaviour 26
3.3.2 Models of territoriality 27
3.3.3 Model by Stamps and Krishnan (1999) 28
3.3.4 Territorial behaviour and spatial representations 30
3.4 Goal of the simulation 30
3.5 Simulation 31
3.5.1 Simulation environment 31
3.5.2 Memory structures 33
3.5.3 Decision making 36
3.5.4 Algorithmic procedure 40
3.5.5 Model parameters 42
3.5.6 Territory establishment and internal representations 42
3.6 Results 44
3.6.1 Obstacle representation 44
3.6.2 Attractiveness distribution 46
3.7 Discussion 51

4 Space Use **53**
4.1 Introduction 53
4.2 Cognitive ecology 54
4.2.1 Benefits of cognitive abilities 54
4.2.2 Costs of cognitive abilities 55
4.2.3 Adaptivity of cognitive traits 56
4.3 External influences on territoriality 57
4.3.1 Competition for exclusive territories 57
4.3.2 Population density 57
4.3.3 Physical environment 58
4.4 Internal and external influences on space use 59
4.5 Home range analysis 60
4.5.1 Available methods 60
4.5.2 Methods applied 65
4.5.3 Quantification of the overlap 65
4.5.4 Statistics 66
4.6 Experimental design 66

4.6.1 Experiment 1: Learning rate . . . 67
4.6.2 Experiment 2: Memory retrieval . . . 69
4.6.3 Overview: Internal factors . . . 69
4.6.4 Experiment 3: Competitor number . . . 70
4.6.5 Experiment 4: Arena size . . . 70
4.6.6 Experiment 5: Habitat structuring . . . 70
4.6.7 Overview: External factors . . . 71
4.6.8 Experiment 6: Residents and newcomers . . . 71
4.6.9 Experiment 7: Long-term experiments . . . 72
4.7 Results . . . 72
4.7.1 Experiment 1: Learning rate . . . 72
4.7.2 Experiment 2: Memory retrieval . . . 78
4.7.3 Overview: Internal factors . . . 79
4.7.4 Experiment 3: Competitor number . . . 79
4.7.5 Experiment 4: Arena size . . . 81
4.7.6 Experiment 5: Habitat structuring . . . 83
4.7.7 Overview: External factors . . . 85
4.7.8 Experiment 6: Residents and newcomers . . . 86
4.7.9 Experiment 7: Long-term experiments . . . 88
4.8 Discussion . . . 91
4.8.1 Learning rate . . . 91
4.8.2 Memory retrieval . . . 92
4.8.3 Population density . . . 93
4.8.4 Habitat structuring . . . 94
4.8.5 Territory dynamics . . . 95

5 Conclusions and outlook **97**
5.1 Conclusions . . . 97
5.2 Outlook . . . 100

Bibliography **102**

A Implementation details **115**
A.1 Territory behaviour . . . 115
A.1.1 Attractiveness . . . 115
A.1.2 Occupancy . . . 115
A.1.3 BaseMap . . . 116
A.1.4 TerritoryNode . . . 118

A.1.5 FileMan 118
A.1.6 TerritoryBehave and SimBehave 118
A.1.7 TerritoryControl 118
A.1.8 sim 119
A.2 Control of the real Khepera robots 119
A.2.1 ComHand 119
A.2.2 TKhepera 120
A.2.3 TEnv 120
A.3 Simulation environment 121
A.3.1 sim 121
A.3.2 robot 121
A.3.3 multirobots 122
A.3.4 world 122
A.3.5 graphics 122
A.4 Initialisation files 123
A.4.1 Global initialisation file 123
A.4.2 Individual initialisation files 124

Danksagung **127**

Curriculum vitae **129**

Chapter 1

Preface

In many animals, behaviour is determined by cognitive processes, i.e. learning, memory, and decision making (Dukas, 1998a; Shettleworth, 2001; Dukas, 2004). Regarding spatial behaviour, the cognitive processes include the self-localisation in the environment. An animal can gain information about its location by measuring its egomotion, by retrieving allocentric information from a compass system, or by recognising places. The place recognition presupposes that the animal previously learned and memorised characteristics corresponding to the location. In complex spatial tasks, such as the establishment and maintenance of a territory, the animal has to memorise multiple places and the relations between them. Supposedly, such a spatial memory represents a cognitive adaptation to the animal's ecological niche. The shaping of information processing abilities by the niche is the concern of the field of cognitive ecology (Healy, 1992; Real, 1993; Dukas, 1998a).

1.1 The modelling approach

Individual-based modelling can be used as an approach to cognitive ecology since both internal factors, i.e. information processing, and external factors are completely controllable. Thus, simulation allows to quantitatively specify the influences of cognitive abilities on behaviours. Models based on individuals and their interactions have been proven a successful tool in ecological research (Judson, 1994; Grimm, 1999; Peck, 2004). The simulation of behaviour using robots or explicitely modelled agents with their sensors additionally allows the specification of the local interactions between the individuals. The influence of specific perception and information processing abilities on behaviour becomes measurable which

is not easily achievable in animal experiments (Webb, 2000).

Information processing abilities interact with the environment on different levels. The amount and quality of information available to an individual is determined by its sensors. Learning and memory allow it to set this information in the context of earlier experiences. The interactions between individuals lead to mutual influences on the cognitive systems involved.

1.2 Thesis objectives and organisation

Polarisation compass

The main subject of this thesis is the investigation of the influences of information processing abilities on spatial behaviour. The second Chapter is concerned with the benefit of a compass sense as integrated in a path integration system. The agents - Khepera miniature robots - have to assess their own position by measuring their egomotion. The additional information source, a polarisation compass, is added without altering any other aspects of the agent. Accordingly, the benefit of a defined sensory system on behavioural performance becomes measurable.

I will provide an introduction to path integration and compass systems in animals as well as in robots. The usage of a compass sense in other contexts of navigation will be discussed.

Representations in spatial behaviour

In a model of territory establishment, the role of learning and memory is investigated (Chapter 3). The agents are provided with one of two alternative memory structures. This allows the individuals to learn about their environment and to include previous experiences in their decisions. The internal representation formed by the individuals and the externally observable behaviour are compared.

Structures of spatial memory as applied in my simulation are usually referred to as cognitive maps. I will introduce the concept of the cognitive map, and set it in relation to other navigation mechanisms. Furthermore, I will give an overview of territorial behaviour and its causes in animals. Territoriality is mostly based on the ability of spatial learning, presumably claiming a map-like internal representation of space.

Space use

Within the model of territory establishment, the interactions of information processing abilities with the behaviour are quantified (Chapter 4). The individuals establish their territories using different learning rates as well as different amounts of information retrieved from memory for each movement decision. The changes in the externally observed behaviour are directly correlated to the manipulations of the defined cognitive abilities since modules of the cognitive equipment can be exchanged independent of the other aspects of the agent. The interactions between the individuals are manipulated by changing the number of competitors in the environment. Additionally, the individuals have to deal with different structures of the physical environment as achieved by the introduction of obstacles. The time dynamic of the territorial behaviour is investigated. The space used by the individuals serves as measure of the behaviour.

The field of cognitive ecology is concerned with the shaping of information processing abilities by the animal's ecological niche. I will introduce this field of research by giving examples of the benefits and costs of specific learning and memory tasks solved by animals. Additionally, an overview of the shaping of territorial behaviour by external factors will be given.

In Chapter 5, I will give an overview of the results as described in the Chapters 2 to 4, and I will summarise the main predictions of the simulation. Additionally, an outlook about the future development of the model will be given.

Chapter 2

Polarisation compass

2.1 Introduction

When moving in their environment, many animals rely on their ability to find back to specific places such as a nest, locations where they found food, or places providing shelter. Accordingly, the animals have to gather information about their own location. Path integration can provide such information by the measurement of the own movement. Additionally, the information can be achieved from external cues, for instance, a compass system. The information about space forms a basis for spatial behaviours such as territoriality. I will introduce a biologically inspired compass system for a miniature robot. Compass systems have been described in many animals. If included in path integration, animals are able to reliably find back to a starting position. In addition, the information gained from the compass can be included in an internal representation of space as I will introduce in the third Chapter. I assume the existence of a spatial representation as precondition for many appearances of territoriality. Sources of spatial information such as a compass system are the basis for spatial learning and memory, and thus, also essential for territoriality.

I will introduce path integration and compass systems in animals. The benefit of a similar system in robots will be demonstrated by applying a polarisation compass to a miniature Khepera robot. This robot provides the standard for the agents in the simulation of territorial behaviour.

2.1.1 Path integration in animals

Path integration is an idiothetic measurement of the own position relative to a fixed reference position (Benhamou and Seguinot, 1995). Animals can acquire this information by proprioception, e.g. by counting their own steps. The path integration has been extensively studied in the desert ant *Cataglyphis*. Single ants accomplish journeys up to $250m$ away from their nest searching for dead animals on the desert floor. While the outbound journey is characterised by many turns and twists, the ants return to their nest on a fairly straight line as soon as they found prey (Wehner and Srinivasan, 1981; Wehner, 1992). The ants are even able to project the path travelled over uneven terrain to the plane (Wohlgemuth et al., 2001, 2002).

Since path integration is based on proprioception, it is used by many mobile animals. Rodents are able to find their way back to a starting position in complete darkness (Etienne et al., 1996). However, the path integration system is prone to accumulate errors over time. Thus, the position estimate gained by proprioception is usually combined with allothetic information in animals. Place recognition by means of landmarks is an example for the navigation using allothetic information (Cartwright and Collett, 1983, 1987). Such allothetic position information is a possibility to recalibrate the path integration system (Etienne et al., 1996; Wehner, 2003).

A compass sense can be included in the path integration system. In this case, only the information about the distance travelled is gained from proprioception, while the heading information is retrieved from the compass. Thereby, the accumulation of a directional error is avoided. Additionally, visual place recognition is eased since the direction of memorised landmarks is independent of the own heading (Cartwright and Collett, 1983; Wehner, 2003)

2.1.2 Compass orientation in animals

Compass orientation can be found in a wide variety of animals. Birds are able to orient using the earth magnetic field. The birds perform head scans before choosing a direction (Mouritsen et al., 2004a) and their magnetoreception is light-dependent (Wiltschko and Wiltschko, 2001) suggesting that the receptor is located in the bird's eye. Mouritsen et al. (2004b) proposed cryptochromes in the retina as mediators of the magnetic sense. Birds migrating during the night can additionally use the stars as means for orientation (for review, see Papi and Wallraff, 1992). However, the most prominent allothetic compass cue used by animals appears to be the sun. In order to provide a real compass, the animal has to correct the sun's position ac-

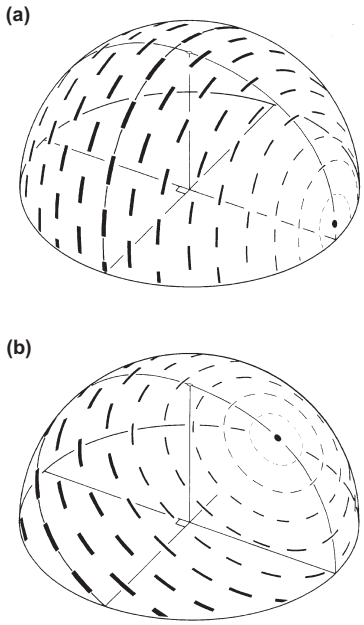

Figure 2.1: Skylight polarisation pattern for two elevations of the sun: **(a)** $6\,^{\circ}$, **(b)** 53°. The terrestrial observer is located in the centre of the sphere. The black disk denotes the sun's position, the bars show the polarisation plane. The bolder the bars, the stronger the polarisation of the sky light. Note that the polarisation plane in the zenith is rectangular to the sun's meridian irrespective of the sun's elevation (from Wehner, 1982).

cording to the time of day. Gould (1980) found that bees correct the sun's position even if they were unable to see the sun using a simple approximation rule.

The polarisation pattern of the sky light provides a further compass cue. The pattern occurs due to the scattering of the sunlight in the atmosphere and is organised in concentric circles around the sun. This results in a symmetry axes in the polarisation pattern that is described by the meridian running through the sun's azimuth. In the zenith, the polarisation plane is always rectangular to this meridian (Figure 2.1). Many insects use the polarisation pattern as orientation means. In bees, even small patches of blue sky are sufficient for orientation (Wehner, 1982; Rossel and Wehner, 1986). In the bee's compound eye, a specialised area, the dor-

sal rim area, acts as detector of the polarisation pattern. The receptors in this dorsal rim area are sensitive to linear polarised light which is not the case for the receptors in other parts of the eye. The absorption planes of the receptors are aligned in different orientations (Labhart, 1980). Amongst other insects, polarisation sensitivity is also found in vertebrates, e.g., in the sleepy lizard's parietal eye. As in bees, the polarisation vision appears to be involved in the animal's orientation (Chelazzi, 1992; Freake, 2001).

2.1.3 Path integration in artificial systems

In a wheeled mobile robot, path integration or odometry data can be gained by counting the wheel revolutions. While the translation can be computed from the sum of the wheel movements in the same direction, the rotation can be derived from the difference in the direction of rotation of the wheels. As in animals, the odometry of robots accumulates errors over time. These errors can be assigned to two different sources: systematic and unsystematic errors (Borenstein and Feng, 1996). Systematic errors arise due to an imprecise estimate of the distance between the wheels or due to different diameters of the wheels. The systematic errors can be measured and corrected by software. In contrast, unsystematic errors are provoked by noise in the wheel control, wheel slip or irregularities in the environment. Those errors cannot be corrected without allothetic information.

Compass devices in robotics. Since the heading information produces the highest error in odometry, different compass devices have been proposed for mobile robots (for review, see Franz and Mallot, 2000). Compass devices relying on the earth magnetic field have been used in robots. However, the existing sensors are very heavy and energy consuming. Additionally, the earth magnetic field is often distorted indoors by power lines or ferromagnetic structures (Borenstein et al., 1997). Gyroscopes provide an alternative, though they are also intrinsic (or idiothetic) sensors for the vehicle rotation, but can measure the rotation more accurately than this is possible with the wheel revolution counters.

Polarisation compass by Lambrinos et al. Lambrinos et al. (2000) introduced a compass device for mobile robots that used the polarised skylight. They equipped a robot with six polarisation sensors. The sensors consisted of photodiodes covered with a linear polariser each. The polarisation planes of two sensors in a pair were arranged in an angle of 90° in relation to the other sensor. In each pair, one sensor contributed a positive, the other a negative signal. The planes of the positive sensors were arranged in 60° angular distances to each other. The axis of the sensors' visual fields were pointing to the zenith. The data computed from

each sensor pair provides the input to an analytical procedure for the determination of the robot's heading. An ephemeris function was used for the compensation of the rotation of the polarisation plane in the azimuth caused by the azimuthal movement of the sun. Lambrinos et al. (2000) quantified the error in position estimation accumulated by the robot in a desert environment. The average error using exclusively proprioception was reduced to one quarter if the polarisation compass was added.

2.1.4 Polarisation compass for the Khepera robot

For the Khepera miniature robot, I introduced a polarisation compass for an indoor arena (Schmolke and Mallot, 2002a). The compass device is built of three sensors which is the minimal number of sensors needed for the determination of the polarisation plane (Kirschfeld, 1972). The robots were provided with an artificial source of polarised light mounted above the experimental arena. An optimisation procedure is introduced that allows non-fixed separation angles between the analyser directions. Comparable to the polarisation compass introduced by Lambrinos et al. (2000), I quantified the error of position estimate as gained from the wheel rotation counters alone, and from the combination of compass and odometry.

2.2 Simulation environment

2.2.1 Khepera robots

Miniature robot Khepera. The polarisation compass was mounted on Khepera robots as provided by the K-Team (Lausanne, Switzerland). These miniature robots have a diameter of $5.5cm$ and move on two wheels which are powered by a step motor each. The motors are combined with a counter which is used as basis for the odometry. The robots are built modular, i.e. for additional functions, turrets are available. The Khepera base is equipped with eight infrared sensors as described below. For the wireless communication with the host computer, a radio communication turret was used. All robots sent and retrieved the information via a radio base. Only one robot could be processed at a time. A linear camera module provided 64 light sensors. The polarisation compass was mounted on top the linear camera. In Figure 2.2a, a Khepera robot with the polarisation compass mounted on top of the linear camera module is depicted. A scheme of the Khepera base with the infrared sensors in shown in Figure 2.2b.

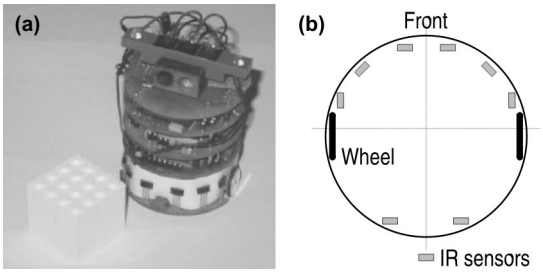

Figure 2.2: (a) Khepera miniature robot. The polarisation compass is mounted on top of the linear camera device. **(b)** Scheme of the Khepera base with wheels and infrared sensors.

Infrared sensors. The infrared sensors of the Khepera robot can be used in two ways: as detectors of the ambient infrared light, or as active sensors that emit a beam of infrared light and measure the intensity of reflection. In the experiments described here, only the active infrared sensing was employed. The sensors detect obstacles up to a distance of about $4cm$. White plastic thereby yields the strongest sensor reply. The furthest distance detectable decreases with darker colouring and with the roughness of the object's surface (Figure 2.3). The reply of the infrared sensors ranges from 0 (no infrared light detected) to 1023. In the experiments, the robots stopped if the frontal sensors exceeded a value of 400 in active sensing in order to avoid collisions with obstacles.

2.2.2 Robot arena

The robots were housed in a rectangular ($140 \times 118cm^2$) arena with white walls. Obstacles of different sizes were constructed of white plastic bricks (Lego). Obstacles could be placed in the arena at arbitrary places according to the experiment. The arena could easily be scaled down by inserting additional walls. The position of the robots was observed externally by a tracking system. The robots were equipped with two LEDs. Their different colours, red and green, allowed to determine the robot's heading as well as its position. The LEDs were facing up to be detectable for the tracker camera which was mounted above the arena. From the calibrated camera image, the position of the LEDs in the arena was calculated.

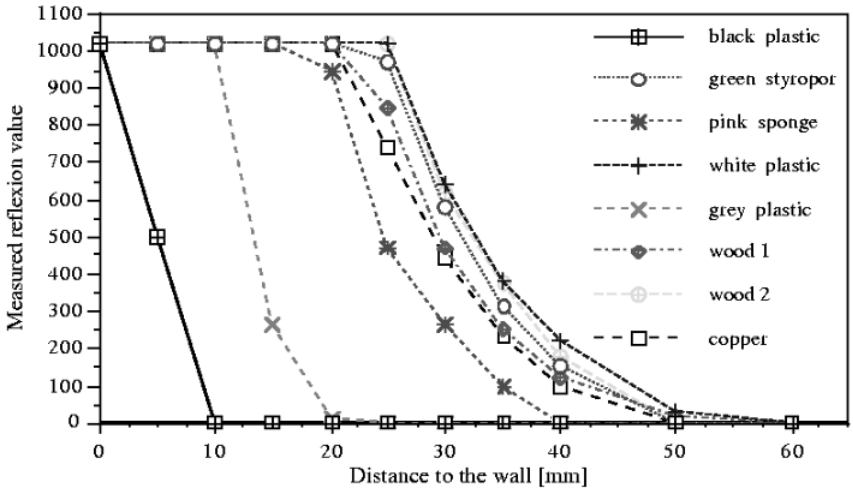

Figure 2.3: Measurements of the light reflected by various kinds of objects versus the distance to the object (from the Khepera user manual).

2.2.3 Calibration of the odometry

Borenstein and Feng (1994, 1996) introduced a method, the UMBmark test, for the calibration of the odometry in wheeled robots. This method allows the correction of the systematic odometry errors. The deviation in the distance between the wheels (wheelbase) and the differences in wheel diameters can be extracted separately, and thus, be corrected by software. I used the method for the calibration of the Khepera's odometry.

The robots drove along a square, resuming their starting position again in the end. The distance between the starting position and the final position of the robot was measured ($\Delta x, \Delta y$). The square track was accomplished by the robot in both senses, clockwise (cw) and counter clockwise (ccw). One leg of the square was $L = 50cm$ long. The position error after completing the square in two orientations reveals the two systematic errors. If the errors in clockwise and counter clockwise runs have the same sign, the wheelbase b was imprecise. In this case, the robot makes a systematic error α during the rotations. On the other hand, different signs of the errors indicate unequal wheel diameters. The robot was actually driving along a bended track when it should accomplish the straight legs of the square causing the error β. These two errors, α and β are calculated according to Equations 2.1 and 2.2.

$$\alpha = \frac{\Delta x_{cw} + \Delta x_{ccw}}{-4L} \tag{2.1}$$

$$\beta = \frac{\Delta x_{cw} - \Delta x_{ccw}}{-4L} \tag{2.2}$$

$E_b = b^*/b$ denotes the error of the wheelbase estimate. b^* is the actual wheelbase while b denotes the nominal value. It holds that

$$\frac{b^*}{90^\circ} = \frac{b}{90^\circ - \alpha} \tag{2.3}$$

$$E_b = \frac{90^\circ}{90^\circ - \alpha} \tag{2.4}$$

A difference in the wheel diameters cause a curvature of the straight tracks by the radius $R = L/(2\sin(\beta/2))$. Accordingly, the difference E_d of the wheel diameters D_r and D_l can be calculated with Equation 2.5.

$$E_d = \frac{D_r}{D_l} = \frac{R + \frac{b}{2}}{R - \frac{b}{2}} \tag{2.5}$$

In order to achieve a reliable measure of the difference, I used the averaged values of five runs in each orientation. I determined the difference between starting and end position using the data from the tracking system.

2.3 Polarisation compass

2.3.1 Sensors

To determine the E-vector direction of linear polarised light without rotating the sensor, the data of at least three sensors have to be taken simultaneously. Accordingly, three photodiodes were mounted on the top of the Khepera robot and covered by linear polarising filters oriented in three different angles φ_k. The sources of polarised light were two lamps emitting white light, also combined with a linear polarising filter in the orientation φ, above the robot's arena. If a polarisation filter is rotated beneath a source of polarised light, the light intensity measured behind the filter shows a sinusoidal behaviour, reaching its maximum I_{max} if the E-vector direction and the filter orientation are parallel, and its minimum I_{min} if they are

separated by an angle of $90°$. The light intensity measured by sensor k can be calculated as follows (Kirschfeld, 1972):

$$I_k(\varphi) = I_{min} + (I_{min} - I_{max}) \sin^2(\varphi - \varphi_k) \tag{2.6}$$

Minimal and maximal intensity measured are dependent on the overall light intensity and the polarisation degree of the light. These factors can also be subsumed by two constants, a and b. Differences in the behaviour of the individual sensors k are taken into account by introducing the constants c_k (see also Lambrinos et al., 2000).

$$I_k(\varphi) = c_k(a + b \cos 2(\varphi - \varphi_k)) \tag{2.7}$$

I assume that a and b are equal for all sensors, i.e. $\tilde{I}_k = \frac{I_k}{c_k}$. From the data I_k of the three sensors, φ can be computed independently of the overall light intensity and degree of polarisation as follows:

$$\begin{aligned}
\tilde{I}_k(\varphi) &= a + b \cos 2(\varphi - \varphi_k) \\
&= a + b \cos(2\varphi)\cos(2\varphi_k) + \sin(2\varphi)\sin(2\varphi_k) && (2.8)\\
\tilde{I}_2(\varphi) - \tilde{I}_1(\varphi) &= b \cos(2\varphi)(\cos(2\varphi_2) - \cos(2\varphi_1)) \\
&\quad + b \sin(2\varphi)(\sin(2\varphi_2) - \sin(2\varphi_1)) && (2.9)\\
\tilde{I}_3(\varphi) - \tilde{I}_1(\varphi) &= b \cos(2\varphi)(\cos(2\varphi_3) - \cos(2\varphi_1)) \\
&\quad + b \sin(2\varphi)(\sin(2\varphi_3) - \sin(2\varphi_1)) && (2.10)\\
b \cos(2\varphi) &= -[(\tilde{I}_1(\varphi) - \tilde{I}_2(\varphi)) \sin(2\varphi_3) \\
&\quad + (\tilde{I}_2(\varphi) - \tilde{I}_3(\varphi)) \sin(2\varphi_1) \\
&\quad - (\tilde{I}_3(\varphi) - \tilde{I}_1(\varphi)) \sin(2\varphi_2)] \\
&\quad / [4 \sin(\varphi_1 - \varphi_2) \sin(\varphi_2 - \varphi_3) \sin(\varphi_1 - \varphi_3)] && (2.11)\\
b \sin(2\varphi) &= [(\tilde{I}_1(\varphi) - \tilde{I}_2(\varphi)) \cos(2\varphi_3) \\
&\quad + (\tilde{I}_2(\varphi) - \tilde{I}_3(\varphi)) \cos(2\varphi_1) \\
&\quad + (\tilde{I}_3(\varphi) - \tilde{I}_1(\varphi)) \cos(2\varphi_2)] \\
&\quad / [4 \sin(\varphi_1 - \varphi_2) \sin(\varphi_2 - \varphi_3) \sin(\varphi_1 - \varphi_3)] && (2.12)\\
\tan(2\varphi) &= [(\tilde{I}_1(\varphi) - \tilde{I}_2(\varphi)) \cos(2\varphi_3) \\
&\quad + (\tilde{I}_2(\varphi) - \tilde{I}_3(\varphi)) \cos(2\varphi_1) \\
&\quad + (\tilde{I}_3(\varphi) - \tilde{I}_1(\varphi)) \cos(2\varphi_2)] \\
&\quad / [(\tilde{I}_1(\varphi) - \tilde{I}_2(\varphi)) \sin(2\varphi_3) \\
&\quad + (\tilde{I}_2(\varphi) - \tilde{I}_3(\varphi)) \sin(2\varphi_1) \\
&\quad - (\tilde{I}_3(\varphi) - \tilde{I}_1(\varphi)) \sin(2\varphi_2)] && (2.13)
\end{aligned}$$

A systematic error in this computation can arise due to differences in the gain characteristic of the photodiodes and due to deviations from the ideal angle separations by $60°$ between the transmission axes of the analysers. I eliminated this error E by introducing a minimisation procedure. For this procedure, the variables $p_k = c_k a$, $q_k = c_k b \cos(2\varphi_k)$ and $r_k = c_k b \sin(2\varphi_k)$ are applied to the Equations 2.14 - 2.17. n denotes the number of measurements.

$$E = \sum_{i=1}^{n} \sum_{k=1}^{3} (I_{ki} - p_k - q_k \cos(2\varphi_i) - r_k \sin(2\varphi_i))^2 \quad (2.14)$$

$$\frac{\delta E}{\delta p_k} = -2 \sum_{i=1}^{n} (I_{ki} - p_k - q_k \cos(2\varphi_i) - r_k \sin(2\varphi_i) = 0 \quad (2.15)$$

$$\frac{\delta E}{\delta q_k} = -2 \sum_{i=1}^{n} (I_{ki} - p_k - q_k \cos(2\varphi_i) - r_k \sin(2\varphi_i) \cos(2\varphi_i) = 0 \quad (2.16)$$

$$\frac{\delta E}{\delta r_k} = -2 \sum_{i=1}^{n} (I_{ki} - p_k - q_k \cos(2\varphi_i) - r_k \sin(2\varphi_i) \sin(2\varphi_i) = 0 \quad (2.17)$$

Since a is a constant for all sensors k, it can be assumed that $p_k = c_k$. Thence, the sensor angles φ_k can be calculated after the optimisation using Equation 2.18.

$$\tan(2\varphi_k) = \frac{\sin(2\varphi_k)}{\cos(2\varphi_k)} = \frac{r_k}{q_k} \quad (2.18)$$

The detector angles as gained from the optimisation procedure were used for the calculation of the robot's heading (Equation 2.8 - 2.13).

2.3.2 Compass design

The Khepera robot provides three channels for external input on its extension bus. These channels were used for the three diodes of the polarisation compass. A bar containing three notches for the photodiodes was prepared. The diodes were placed in the notches facing to the ceiling and were covered by the polarisation filters. The bar was plugged on top of the Khepera's linear camera device.

2.4 Quantification of the path integration error

In order to quantify the performances of the path integration system with and without polarisation compass, the robot completed 20 random tracks consisting of 15

segments each. The robot started with a turn between $5°$ and $175°$ clockwise or counter clockwise and proceeded with a forward translation of $0.3cm$ to $10.2cm$ (for an example, see Figure 2.4). The actual end position was determined by the tracking system and compared to the robot's two position estimates.

The odometry of the robot was previously calibrated using the UMBmark procedure as described above (Section 2.2.3). In each randomly assembled track, the robot returned two estimates of its own position. The first estimate was exclusively derived from the wheel revolution counters. The second estimate was gained by combining the translation measurement from the wheel revolutions with the heading estimate of the polarisation compass. The angle calculated from the polarisation sensors is ambiguous in $180°$. Thus, the heading information from the odometry was used to solve the ambiguity.

2.5 Results

The presented polarisation compass is a device applicable indoors to miniature robots such as the Khepera. I designed the compass such that it is mountable on the Khepera without changing the robot's hardware. With the introduced optimisation procedure, differences of the individual sensors and deviations from the optimal separation between their transmission axis were corrected.

The heading estimate from the polarisation compass was compared to the actual robot's heading measured with the tracking system. The average deviation amounted to $2.7°$ from the actual heading. After about a full turn on the spot, the compass device exceeded the accuracy of the heading estimation from the wheel revolution counters.

The position estimate gained exclusively from the Khepera's odometry was compared to the actual final position as measured by the tracking system for the 20 tracks. The mean error amounted to $1.03cm$. Simultaneously, a second position estimate was achieved by combining the heading information gained from the compass and the translation estimate from the robot's odometry. The usage of the compass reduced the error of the position estimate significantly to a mean error of $0.66cm$ (paired t-test, $p = 0.015$). The analysis of the position estimates are summarised in Table 2.1. An example track with the two position estimates is depicted in Figure 2.4.

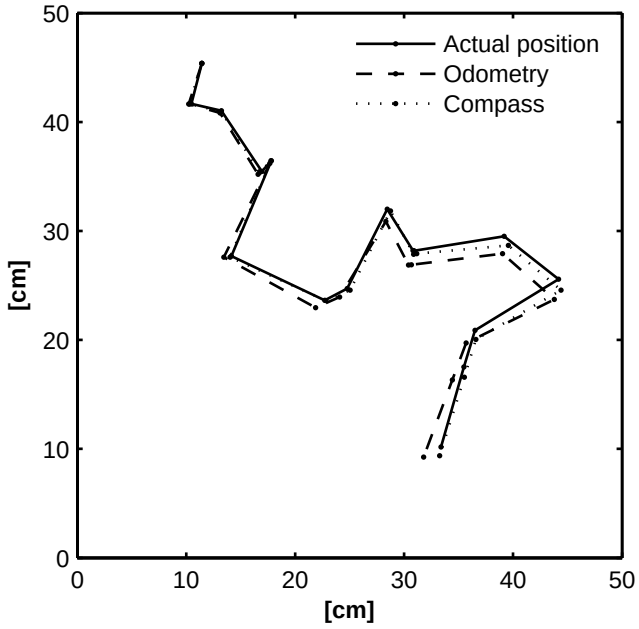

Figure 2.4: Example track with 15 rotations and translations. The tracked robot positions, the positions estimated by the robot using exclusively proprioception, and the position estimates gained by using the compass for the orientation information are depicted.

2.6 Discussion

In order to reduce the error accumulation occurring in path integration based on proprioceptive motion detection, I designed a polarisation compass for the Khepera miniature robot. The application of additional sensory devices to the Khepera robot is strongly constrained. Weight and energy consumption have to be low, ruling out magnetic field measurements or gyroscopes (Borenstein et al., 1997).

A polarisation compass implies few sensors and low energy consumption. Lambrinos et al. (2000) could show the benefit of a compass device using the polarised skylight. The usage of a polarisation compass on a miniature robot requires a further reduction of the sensory need, and the installation of an artificial source of

Table 2.1: Performance of the path integration system without and with polarisation compass.

	Proprioception	Compass
Average error [cm]	1.03	0.66
Standard deviation [cm]	0.67	0.35
Min [cm]	0.07	0.22
Max [cm]	2.15	1.67
n	20	20

polarised light. The polarisation compass applied to the Khepera used the minimal number of three sensors. No extensions of the robot's hardware were needed.

The mounting of the small compass device was simplified by introducing an optimisation procedure. The optimal angular sensor separation is 60° between the polarisation planes. Deviations from these optimal angles between the sensors were not critical due to the optimisation procedure. Thus, a systematic error in the measurement of the heading angle due to the arrangement of the sensors was avoided. Additionally, differences between the characteristics of the individual sensors were also corrected by the optimisation procedure. The polarisation compass as applied to the Khepera robot displays a high accuracy. Accordingly, the combination of the compass with the odometry results in a significant improvement of the position estimate (Schmolke and Mallot, 2002a).

An individual relying on an accurate path integration system is able to return safely to its home after a wide-ranging excursion, or to keep track of its own position within a limited range or territory. Nevertheless, even if compass information is available, an error of the position estimate still accumulates. This problem can only be solved by the recalibration using additional external cues. Cartwright and Collett (1983) found that bees can use visual landmarks for this task. They developed a model for the underlying mechanism used by the bees. According to the model, the bees store a visual snapshot of the goal position as, for instance, their hive. When approaching the goal, the insects may find the exact position again by comparing the current image of their environment with the stored snapshot. The goal direction can be computed from the azimuth and the size change of the landmarks in the image (Cartwright and Collett, 1983). Other approaches were

introduced for the estimation of the optimal movement direction that allows to resume the position where the original snapshot was taken (for review, see Franz et al., 1998; Franz and Mallot, 2000). These different simulation studies have proven the feasibility of the scene-based homing. The scene-based homing is simplified if a compass is available. No rotation of the images has to be considered if the current and the snapshot heading are known (Franz and Mallot, 2000).

The path integration system does not merely provide a possibility to find one's way back home, but it can also be used for the formation of an internal representation of the environment as introduced in Chapter 3. Metric distances between places can be determined by path integration. The combination of metric and visual information allows the formation of a reliable map-like representation of places (Hübner and Mallot, 2002). Internal representations without explicit distance information might still include direction information as available from a compass. Since a compass sense can be found in a wide variety of animals, the inclusion of directional information in spatial memory is very likely.

Chapter 3

Representations in spatial behaviour

3.1 Introduction

A wide variety of navigation mechanisms are used by animals. In the second Chapter, I described a model of path integration combined with a compass system as it is found in many animal species. Additionally, animals can find a goal using landmarks either by estimating their own position relative to these cues or by following extended landmarks according to simple rules. In territorial behaviour, no simple goal can be defined. Nevertheless, the animals have to learn about their environment. But how can animals achieve area-based behaviour, i.e. behaviour that does not only include the navigation from a fixed start position (e.g. the nest) to a goal (e.g. a feeder)?

I will approach this question by combining spatial memory with territorial behaviour in a simulation. The simulation is based on the assumption that territorial animals memorise spatial information in a memory structure, i.e. an internal map. I will introduce hierarchies of navigation mechanisms in animals and classify map-like representations within these hierarchies. Additionally, I will give an introduction to territorial behaviour. Existing models of territoriality do not include the spatial abilities of the individuals. Thus, I modelled the cognitive demands of territorial behaviour, and included them in a model of territory establishment. The simulation allows the observation of the individual behaviour, i.e. the pattern of space use, as well as the internal state of the individuals, i.e. the internal representation of space.

3.2 Spatial memory

Tolman (1948) first introduced the concept of a cognitive map as framework of spatial learning in animals. In Tolman's sense, rats can learn a map of their environment that is not dependent on the task. He used the notion of the cognitive map in a general sense, i.e. not restricted to spatial tasks, and proposed it as alternative hypothesis to simple stimulus-response chains explaining animal behaviour. O'Keefe and Nadel (1978) defined the cognitive map as an "information structure from which map-like images can be reconstructed and from which behaviour dependent upon place information can be generated" (p.78). The information stored in the map thereby comes from multisensory input. Maps are flexible and do not define goals, hence maps are context independent. The representation consists of a set of connected places which are systematically related to each other by a group of spatial transformation rules. This requires a special coding system.

However, in order to explain animal behaviour, a cognitive map in the sense of O'Keefe and Nadel is not necessary. O'Keefe and Nadel presented the route navigation as mechanism that does not require a special coding system. As in Tolman (1948), route navigation as stimulus-response chain opposes the cognitive map.

3.2.1 Hierarchy of navigation by Trullier et al. (1997)

Trullier et al. (1997) provide a more sophisticated hierarchy of navigation that is classified in levels of complexity. Thereby, guidance represents the simplest level. A goal is reached by the optimisation of some sensor-related criterion, i.e. memorised sensory information is restored. The place-recognition triggered response combines multiple goals, and thus corresponds to route-learning as described by O'Keefe and Nadel (1978). These two levels do not allow planning or flexibility. The third level postulated by Trullier et al. (1997), the topological navigation, allows planning and flexibility of behaviour, i.e. the representation is not goal-dependent. Routes include the expectation of subgoals and can be connected if the connecting paths are known. The representation may include bifurcations. The fourth and highest level, the metric navigation, additionally includes metric information. The individual is able to take shortcuts using unknown paths. The metric navigation claims a cognitive map representation in the sense of O'Keefe and Nadel (1978).

3.2.2 Hierarchy of navigation by Mallot (1999)

Another hierarchy of navigation mechanisms in animals has been introduced by Mallot (1999). In this system, the simplest level of navigation is represented by taxis. Sensor and effector are not distinguishable though they might be physically separated. The behaviour can be achieved by a single cell. Very impressive illustrations of taxis behaviour have been given by the simple vehicles described by Braitenberg (1984). The drives of the vehicles' wheels were directly coupled with the sensory input. Braitenberg demonstrated that a wide variety of behaviours can be produced in his vehicles. However, no integration of information over time and space is possible. Such integration represents the second level of complexity in the hierarchy presented by Mallot (1999). An example provides the path integration as described in Chapter 2. The third level includes learning, i.e. the animal's behaviour changes due to prior experience. While integration only assumes a working memory, learning requires a long-term memory. The animal has to memorise information about its goal. Thus, the third level of Mallot's hierarchy subsumes guidance and place-recognition triggered response of the system proposed by Trullier et al. (1997). As fourth level in the hierarchy, Mallot introduces cognition. It allows the animal to display goal-dependent flexibility. At bifurcations, an animal is able to decide for a path dependent on its goal although the goal is currently unperceivable. The cognition level subsumes all behaviours that do not follow a mere stimulus-response mechanism, and thus includes topological and metric navigation as proposed by Trullier et al. (1997) and would include the cognitive map as defined by O'Keefe and Nadel (1978).

3.2.3 The cognitive map concept

The cognitive map is a concept that is not uniformly used or defined. O'Keefe and Nadel (1978) propose the cognitive map as a set of ordered and connected places which are represented by means of external and internal information. The external information includes input from multiple sensors. These allow place recognition even if parts of the input are missing. Additionally, internal cues from the motor system, i.e. path integration, provide metric information. O'Keefe and Nadel (1978) assume that explorative behaviour is a means to built up a map of the environment. The map allows the generation of new paths, i.e. also of previously unknown shortcuts between known places. Additionally, sensitivity to novelty in the environment can be attributed to the existence of a cognitive map.

However, in other concepts, metric information is not necessarily included in

the cognitive map. The cognitive level of navigation as introduced by Mallot (1999) merely requires the ability to choose a path from memory in favour of an invisible goal starting at a arbitrary location of the known environment. Thus, task-independence of the map is assumed, but the ability to generate completely new shortcuts is not necessary. Gallistel (1990) even used the cognitive map as synonym for any internal representation of space in animals.

The concept of an internal map-like representation has been criticised. Wehner and Menzel (1990) argued that, for instance, shortcut behaviour as used as indicator of a cognitive map might also be achievable by path integration or guidance by extended landmarks. Bennett (1996) extended the critique by assuming that the cognitive map concept does not provide any testable predictions for animal behaviour.

Nevertheless, path planning and novel shortcuts are not easily explainable by simple recognition-triggered response chains if extended landmarks or path integration mechanisms can be excluded. Menzel (1973) showed that chimpanzees can relocate multiple hiding places for food. Thereby, the apes did not visit the places in the same sequence as they were presented to them previously, i.e. the apes did not follow a simple rule. Gould (1986) described that bees can resume a feeder location although they were caught at the hive and released at arbitrary places, i.e. they were using novel shortcuts. These experiments were criticised since extended landmarks might have played a role (Wehner and Menzel, 1990; Dyer, 1991). However, tracking the whole flight paths of displaced bees reveals that they might be able to choose between alternative destinations (Menzel et al., 2005). Bees were caught at a feeder and set loose at arbitrary positions within a radius of a about $200m$ from the hive. The bees first flew in the direction of the hive as seen from their capture site. At the estimated location of the hive, they started slow search flights. Finally, they flew straight back to the hive (at its real position) or used a detour that led them via the location of the feeder where they had been caught previously. Menzel et al. (2005) concluded that the bees can choose between alternative paths back to the hive, and thus, possess a map-like spatial memory. However, the neuronal basis and the structure of such a map-like representation in bees remains unclear.

3.2.4 Neuronal basis of spatial representations

Place cells. While the existence of some form of spatial representation in many animals is not challenged, the structure of such a representation remains unclear. The hippocampus has been the focus in the search for the neuronal basis of spatial representations in vertebrates, especially in rodents. O'Keefe and Nadel (1978)

assumed to have discovered the cognitive map in the hippocampus of rats. Single cells fired according to the rat's location in its environment. They could show that this place cell activity was dependent on the input from multiple sensors. For instance, the place-specific firing even lingered if the light was turned off in the experimental arena. It was suggested that the place cells correspond to modules of a map.

Yet the place cells do not appear topologically in the hippocampus. Changes in the environment yield different reactions of the place cells. Some cells fire at a place relative to a displaced visual cue while others are unaffected by the change. If the animal has to solve a specific task, goal-independent place cells become rare. Instead, cells firing dependent on location *and* task are observed (Hölscher, 2003). A map is used for the generation of expectations about places that are currently not perceivable, and it allows to plan ahead. However, place cells are only active when the animal has reached the corresponding place field in the environment. Thus, the pattern of place cell activity is not sufficient for the notion of a cognitive map as proposed by O'Keefe and Nadel (1978).

The hippocampus and spatial behaviour. Although the place cell system as described in the rat does not hold as a direct correlate of the cognitive map, the hippocampus nevertheless appears to be strongly involved in the processing of spatial information. Lesions of the hippocampus lead to impairments in spatial tasks though the lesioned rats do not loose their spatial abilities completely (for review, see Hölscher, 2003). The bird's hippocampus is supposedly homologous to the mammalian hippocampus (Jacobs, 2003). Accordingly, impairments in spatial behaviour due to the loss of the hippocampus were also observed in birds (Colombo et al., 2001).

Hippocampal size was correlated with the spatial learning demand of the animal's ecological niche (see also Section 4.2). Polygynous vole males possess a larger hippocampus than the females of the same species. The males regularly visit the nests of their females that are spread over an extended area. In contrast, the females usually stay close to their nest. Monogynous vole males display the same spatial range as their females and the same hippocampal size (Jacobs et al., 1990). Similar correlations could be found in birds. Food hoarding species have a larger hippocampus than their non-storing relatives (Hampton et al., 1995; Shettleworth, 2003; Healy et al., 2005). In black-capped chickadees, the Alaskan population relies strongly on their food caches during winter while their conspecifics from Colorado are only mildly dependent on their stored food. Birds from both populations performed equally well in non-spatial learning tasks. However, the birds

from Alaska performed better in food caching and retrieval as well as in spatial memory tasks compared to birds from Colorado. Accordingly, the northern birds had larger hippocampi (Pravosudov and Clayton, 2002).

The involvement of the hippocampus in spatial learning is not limited to mammals and birds, but was also found in reptiles and fish. The processing of spatial information in the brain area homologous to the hippocampus might thus be a preserved trait in the vertebrate evolution (Rodríguez et al., 2002; Jacobs, 2003).

3.2.5 Structure of spatial representations

An internal representation of the environment that exceeds mere stimulus-response chains would claim a special coding structure (O'Keefe and Nadel, 1978). A structure of the spatial representation in the brain of mammals and birds was hypothesised by Jacobs and Schenk (2003). In their parallel map theory, they assume three parts of representation linked to the hippocampal formation. A bearing map represents metrical position cues derived from compass systems in a grid-like structure. The second kind of representation, the sketch map, denotes a topographical representation of the local cues, e.g. proximal landmarks. Lesion studies show that the behavioural abilities derived from the two representation types are dissociable, i.e. they are mediated by different hippocampal structures. The loss of dentate gyrus function and the CA3-region of the hippocampus cause the impairment of global bearing abilities. However, the affected animals still orient well according to local cues. In contrast, animals with lesions of the CA1-region are unable to use local cues to find their goal though displaying a good orientation within coarse-grained directions.

According to the theory of Jacobs and Schenk (2003), the bearing and the sketch map are linked into an integrated map. The consolidation of the sketch map in the framework of the bearing map is mediated by the CA3-region. The integrated map corresponds to the cognitive map in the sense of Trullier et al. (1997).

3.2.6 Spatial representations in artificial systems

As animals, robots that have to solve spatial tasks rely on internal representations of their environment. If no map of the environment is provided from outside, i.e. by the programmer, the representation has to be built up by the robot while exploring the environment. As in animals, information about self-motion, sensory cues, and compass information can be used for this task. The complexity of the representation built can be classified in a hierarchy that follows the complexity of

navigation mechanisms proposed for animals. Kuipers (2000) suggested a spatial semantic hierarchy, i.e. an ontology of information processing and storage for spatial behaviour. He defines five levels: sensory, control, causal, topological and metric level. The sensory level denotes the interface of the agent with the sensory system. The control level binds the agent to its environment by continuous control laws. The control laws may include local sensor maps as comparable to the sketch map introduced by Jacobs and Schenk (2003). On this level, goals can be reached, e.g., by resuming a pattern of sensory input. This can be solved by hill-climbing in the sensory space (compare scene-based homing, Section 2.6; Franz et al., 1998). Wall-following represents another instance of behaviour achievable by control laws. Compared to hierarchies of navigation mechanisms as presented above, the control level corresponds to the level of guidance according to Trullier et al. (1997) and learning after Mallot (1999).

The causal level in the hierarchy introduced by Kuipers (2000) adds abstractions of the continuous environment to the control laws. Places can be coupled with actions, and thus, the control laws can be abstracted into routines. The routines in the spatial semantic hierarchies has characteristics comparable to the route navigation described by O'Keefe and Nadel (1978) and Trullier et al. (1997). However, Kuipers (2000) allows bifurcations of the representation at the causal level, already adding a level of abstraction that would only arise at the topological level in the other hierarchies presented. In Kuipers' topological map, places and paths are stored in combination with additional information or attributes. These attributes can separate the map into regions, i.e. two-dimensional subsets of the environment, or might even include metric information about neighbouring places. In the sense of the hierarchies presented above, the level of the cognitive map is achievable with Kuipers' topological level. Nevertheless, in robotics, a global metric map is commonly applied as representation. The agent's position as well as the positions of environmental features are stored relative to a global frame of reference.

Grid representations often serve as structure of the global metric map. Every cell of the grid corresponds to a location in the environment. In an occupancy grid, a value associated with each cell provides information about obstacle locations in the environment (Moravec and Elfes, 1985; Elfes, 1987; Thrun and Bücken, 1996). Since grid maps require high computational space and time costs, graph-like representations have been used for robot navigation, adding metric information to a topological structure (Franz et al., 1998a). Both representation structures have also been combined (Thrun, 1998). I will introduce both structures, the grid and the graph, more thoroughly in Section 3.5.2 as potential memory structures underlying

territorial behaviour.

3.3 Territoriality

Many animals confine their activities to a delimited area, the home range. They abide to their home range for a certain period or season or even their whole life. Although home ranges may shift over a longer time interval or may be abandoned and reestablished at another location, they can be distinguished from occasional forays or migratory routes (Burt, 1943). The home ranges of several individuals may overlap partly or completely ("neutral ranges"). However, in many species, solitary individuals or groups defend their whole home range or parts of it against conspecific intruders. The range used exclusively by an individual or group is defined as its territory (Maher and Lott, 1995).

3.3.1 Ecology of territorial behaviour

Territoriality subsumes several behaviours. The individual range of sessile animals can be labelled as territory since they prevent other individuals from settling. Some mobile species defend small areas that they can fully survey. Such territories might even shift with the position of the animal as observed in butterflies (Davies, 1978). In other cases, males gather in an area and set up tiny territories, the leks, in order to attract females (Bradbury, 1977). However in many species, individuals or groups defend foraging territories that vastly exceed their perceptive range. The defence of such territories is often correlated with high energetic costs. Hence, the benefit gained by monopolising food must exceed the costs of fighting. The costs of territory defence have been demonstrated in Yarrow's spiny lizards. The testosterone levels of the males were increased artificially during the season when the lizards usually are only weakly territorial. The manipulated males invested a third more energy in territorial defence than the controls. The aggressive displays additionally decreased the time available for capturing insects. Accordingly, the males with elevated testosterone levels built up smaller fat reserves and were prone to an earlier death than their unmanipulated conspecifics (Marler and Moore, 1991; Marler et al., 1995).

Since the costs of territorial defence change according to the competitor-to-resource ratio, some animals only defend territories during certain periods of the year. Armstrong (1992) could demonstrate that in nectar-feeding birds, New Holland honeyeaters and white-cheeked honeyeaters, aggression against intruders was

dependent on the season, but not on the actual food availability. Since the time of year usually might provide a reliable cue for the food distribution, it may not be necessary for the birds to assess the actual food availability and adjust their behaviour accordingly. Instead, the adaptive behaviour can be achieved by following a simple rule, i.e. by following an annual rhythm in the case of the honeyeaters.

3.3.2 Models of territoriality

As discussed above, exclusive ranges or territories allow the monopolisation of resources, and thus, may be energetically advantageous for the resident even if it has to invest in the defence. Yet how do individuals achieve exclusive ranges in the first place? Territories are usually no predefined patches of the environment, but have to be negotiated between the individuals. Maynard Smith (1982) presented a game-theoretic model for the negotiation of territory borders between two individuals. Both and Visser (2003) included the population density in a model, and tested the effects of divisible and indivisible resources, i.e. food and nest sites, respectively. Dependent only on divisible resources, they were able to predict an optimal territory size which decreased with an increasing competitor number. This corresponds to a decreased fitness of the territory holder due to increased population density. Such a correlation was described in great tits. These birds suffered a declining breeding success with increasing population density (Both and Visser, 2000). However, food availability is not always the main factor influencing the fitness of the territory holder. If nest sites were rare, they had a stronger influence on territory formation and fitness in the modelled individuals than the divisible resources. This finding is comparable to the situation found in pied flycatchers (Both and Visser, 2003).

Indivisible resources might not be crucial for many species since most resources are divisible, for instance food. The inhomogeneous distribution of divisible resources might have a strong impact on the territory establishment. Pereira et al. (2003) modelled a heterogenous habitat by applying a linear gradient of resource abundance along the available space. The negotiation of the border between the territories was dependent on the energy budget of the individuals. In most cases, the competition between the two modelled individuals settled, and the space was divided between them. However in extreme cases, one individual “died” or the contestants remained in constant fight over the border. In a comparable approach, Morrell and Kokko (2003) tested different territorial strategies in a model including the costs of fights. The individuals divided the space by avoiding each other if the fighting costs were high. Otherwise, the partitioning of the space occurs by

winning fights whereby the winner takes hold of the corresponding area.

The models presented above demonstrate how the division of space can be achieved. However, the interactions between multiple competitors in a two-dimensional area are not regarded. White et al. (1996) presented a mathematical model for wolf pack territories. They included the scent markings of the territory borders in their model. The wolf packs were assumed to return to a central den on a regular basis. The distribution of three wolf packs dependent on their relative den locations were predicted. The model predicts the division of space with a marked buffer zone between the territories as observable in wolf packs (White et al., 1996; Lewis et al., 1997).

A mechanism for the division of space between ant colonies was demonstrated by Adams (1998). The interactions between neighbouring colonies were modelled explicitely in two dimensions. Since both ant and wolf territories are centred around a den or nest site, respectively, these cases of territoriality are comparable as described by the models. This includes that the presence of the residents is nearly always perceivable for neighbours and intruders. In the wolf case, the scent marks persist, and in the ants, the individuals disperse over the colony's range.

The model of territory establishment introduced by Stamps and Krishnan (1999) acts on less assumptions about the individuals. Thus, it is applicable to a wider range of species than the models by White et al. (1996) and Adams (1998). The two-dimensional model by Stamps and Krishnan (1999) allows the interactions of an arbitrary number of individuals. I chose this model as basis for the investigation of cognitive abilities within spatial behaviour. In the following, I will present the model of Stamps and Krishnan (1999) in detail. A review of their model is also given by Sih and Mateo (2001). Adams (2001) gave a review about model approaches to territoriality.

3.3.3 Model by Stamps and Krishnan (1999)

Stamps and Krishnan (1999) presented a general model of territory establishment and maintenence. Since it is based on few assumptions concerning the individuals, it comprises the territorial behaviour of a wide range of species. However, it is preassumed that the individuals have the capability of spatial learning. The model includes territorial species that remain mobile after their settlement. The habitat is assumed to be heterogeneous on a small scale, i.e. the individuals have to keep moving in order to achieve food or shelter. They have to learn about the corresponding places and motor programs (Stamps, 1995). In contrast, resources are supposedly distributed homogeneously on a large scale, i.e. two territories of

the same size yield the same fitness for the territory holder irrespective of the territory's location in the habitat. Furthermore, single patches of the habitat can support multiple individuals which is the requirement for potential encounters between individuals. Though mainly based on the investigation of anolis lizards behaviour (Stamps and Krishnan, 1990, 1994a,b; Stamps, 1994; Stamps and Krishnan, 1995, 1998, 1997), the model excludes only a small portion of territorial species, mainly sessile animals (e.g. polyps), species that defend only tiny or shifting patches of their environment (e.g. aphids and butterflies) and animals that defend discrete sites without neighbour contact as can be observed in a couple of wasp species.

Encounters between individuals are assumed to lead to fights or aggressive displays. These are energetically costly for each individual, even if it might win a fight. As simplest case, a balanced energy cost for both individuals involved is supposed in the model. Accordingly, the individuals tend to avoid such encounters by avoiding the locations where they took place. On the other hand, individuals have the opportunity to learn food and shelter locations as well as motor programs adjusted to a patch. Thus, they will prefer to return to known places where no competitor encounter is expectable.

In the model of Stamps and Krishnan (1999), each patch of the environment is associated with an attractiveness value which reflects the probability of future visits. The attractiveness changes gradually according to the individual's experiences at each patch. Since it is assumed that all patches yield equal fitness values, a visit to a patch is reckoned positive, i.e. the attractiveness of the patch rises, if no competitor is met. In contrast, a patch will loose attractiveness for an individual due to competitor encounters. The individuals adjust the attractiveness A_i of a patch i each time they visit it according to Equation 3.1.

$$\begin{aligned} A_i^* &= P_{max}(1 - e^{-\frac{N_{pi}}{R_p}}) - F_{max}(1 - e^{-\frac{N_{fi}}{R_f}}) \\ A_i &= \max(0, A_i^*) \end{aligned} \tag{3.1}$$

The constant R_p determines the rate of attractiveness learning. The larger R_p, the slower is the increase of the attractiveness due to the number of positive visits N_{pi} to patch i. The attractiveness cannot exceed a maximum given by P_{max}. Competitor encounters decrease the attractiveness in a comparable way, i.e. the impact of the number of fights N_{fi} is defined by the constant R_f. The overall attractiveness loss maximally amounts to F_{max}. The attractiveness A_i reflects how likely the resident will return to the associated patch i. Thus, A_i cannot drop below zero. The individuals continuously move in their environment staying at each place for one time step. In each time step, an individual chooses an adjacent place and moves

there. The goal locations are chosen stochastically according to the attractiveness values. The probability p_i for area i as subsequent destination is given by Equation 3.2.

$$p_i = \frac{A_i}{\sum_{j=1}^{n} A_j} \tag{3.2}$$

n is the number of reachable areas; in the model $n = 8$, since the environment is subdivided into uniform squares. Unknown patches are given a low default attractiveness A_0. Note that A_i depends only on the number of positive and negative visits, not on their temporal order. The territory of each individual is defined as the part of its range which it uses exclusively.

3.3.4 Territorial behaviour and spatial representations

Animals with stable home ranges or territories use their familiar environment more efficiently than unfamiliar areas (for review, see Stamps and Krishnan, 1999). Chipmunks escape more successfully from predators the more familiar they are with their environment (Clarke et al., 1993). Another example is given by hummingbirds that improve their foraging efficiency due to spatial learning (Healy and Hurly, 1995). Song birds even know about the borders of their territories. Song sparrows weakly respond to the song of a neighbouring bird singing in its territory. However, if the same song is played from within the own territory or an unfamiliar direction, the resident shows the same reaction as if a foreign bird was singing (Beecher et al., 1998).

These examples demonstrate the involvement of spatial learning in the establishment of stable home ranges and territories. The behaviours cannot be explained by simple route-learning mechanisms, but suggest a map-like memory structure. While the hypothesis about the structure of spatial memory are mostly developed from experiments wherein the animals have to learn defined goal locations, the interactions between spatial information processing abilities and the establishment of stable home ranges or territories remain unclear.

3.4 Goal of the simulation

In order to investigate the influences of different representation structures on area-based spatial behaviour, I combined the model of territory establishment introduced by Stamps and Krishnan (1999) with spatial learning based on two alternative memory structures: a graph and a grid map. While the grid structure is a

commonly used mapping means in robotics claiming a high memory capacity, the graph structure is a less memory-consuming solution for way-finding tasks. I tested whether these memory structures are also suited to support area-based spatial behaviour such as territoriality. I compared the internal state of the agents, i.e. their memory content with their space use.

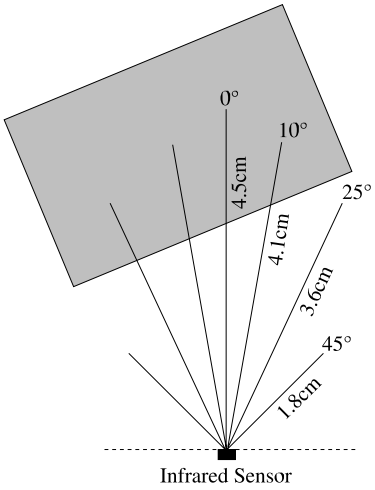

Figure 3.1: Single infrared sensor modelled by seven lines. The number of lines that intersect with an obstacle determine the sensor response. In this example, the sensor response would be 650, since four lines intersect with the obstacle here depicted as gray rectangle (compare Table 3.1).

3.5 Simulation

3.5.1 Simulation environment

A simulation of Khepera miniature robots was used for the experiments with the territorial behaviour. The simulation provided by Olivier Michel (MAGE team, i3S laboratory, CNRS, University of Nice - Sophia Antipolis, France, 1995) was adapted to the demands of the model of territoriality. The simulated robots were equipped with eight infrared sensors, as are the real Khepera robots (Figure 2.2).

Table 3.1: The number of rays of the modelled infrared sensor intersecting with the outline of an obstacle and the returned sensor value. The maximum sensor value is 1023.

Ray intersections	Sensor value
0	0
1	100
2	200
3	400
4	650
5	900
6	1000
7	1023

The control module could be used with both the simulated and the real robots (compare Section 2.2.1). The simulated arena corresponded to a square area of $1m^2$, the robots had a diameter of $5.5cm$. Obstacles could be placed at arbitrary positions and orientations in the arena. The robots relied on their infrared sensors for the detection of obstacles. They received their own (exact) position from the simulated environment, as comparable to the tracking system if the real Khepera robots were used. Additionally, the proximity ($< 15cm$) of competitors was notified externally. The basic simulation results were confirmed in experiments with the real Khepera robots (Schmolke and Mallot, 2002b).

The infrared sensors have been remodelled for the application in the territorial context. The simulated infrared beam consisted of seven rays of different lengths and angles: the central ray spread out for $4.5cm$ and was aligned with the sensor orientation. Two rays deviated from the central ray by $10°$ in each direction and had a length of $4.1cm$. The next pairs had a bearing of $25°$ and $45°$ as referred to the central ray and spread out from the sensor by $3.6cm$ and $1.8cm$, respectively (Figure 3.1). The simulated sensor response values, as listed in Table 3.1, were dependent on the number of rays that intersected with the outline of an obstacle. This sensor simulation was tightly justified to the sensor behaviour of the Khepera robots (compare Section 2.2.1), and yielded enough detail for the determination of the obstacle position needed especially for the occupancy grid map (see Section 3.5.2).

The simulation has the advantage that experiments could be conducted much

faster than using the real robots. However, neither linear camera nor the polarisation compass were available. The path integration provided position information without errors. The infrared sensor data were combined with a small amount of noise which simulates the situation in the real robot running under constant infrared light conditions.

3.5.2 Memory structures

In my simulation presented here, I explicitly modelled the spatial memory. Since the memory structure itself might influence the behaviour, two alternative memory types, a graph and a grid structure, were tested. These two memory structures used identical interfaces with the other modules of the simulation, allowing to study the effects of memory structure independent of other factors.

Grid structure

The grid structure consisted of an array of regularly spaced cells ($2cm$). Each cell (or node) acted as a memory container for the information collected at the corresponding location of the environment including the position, the occupancy probability, and the attractiveness value (as described in Section 3.3.3).

Occupancy probability. The occupancy probability reflected the probability that the area corresponding to the grid cell was occupied by an obstacle (Moravec and Elfes, 1985; Elfes, 1987). Whenever no information about the area was available, as it was initially the case, this probability was set to 50%. If an obstacle was detected via the robot's infrared sensors, the probability was increased. It was decreased if the sensors could not detect anything at the location corresponding to the cell. The occupancy probability $P(occ_{x,y})$ of a cell with the coordinates (x, y) was calculated conditioned on all T sensor readings $s^{(1)}, \cdots, s^{(T)}$ available for the cell. Assuming the independence of the sensor readings, the occupancy probability was calculated by applying Bayes' rule (Equation 3.3; Thrun and Bücken, 1996).

$$P(occ_{x,y} \mid s^{(1)}, \cdots, s^{(T)}) = \\ 1 - \left[1 + \frac{P(occ_{x,y})}{1 - P(occ_{x,y})} \prod_{\tau=1}^{T} \left(\frac{P(occ_{x,y} \mid s^{(\tau)})}{1 - P(occ_{x,y} \mid s^{(\tau)})} \frac{1 - P(occ_{x,y})}{P(occ_{x,y})} \right) \right]^{-1} \quad (3.3)$$

This computation can be simplified given the primary probability of $P_0(occ_{x,y}) = 0.5$, and converted to an incremental form:

$$P(occ_{x,y} \mid s^{(1)}, \cdots, s^{(T)}) =$$

$$1 - \left(1 + \frac{P(occ_{x,y} \mid s^{(T)})}{1 - P(occ_{x,y} \mid s^{(T)})} \frac{P(occ_{x,y} \mid s^{(1)}, \cdots, s^{(T-1)})}{1 - P(occ_{x,y} \mid s^{(1)}, \cdots, s^{(T-1)})}\right)^{-1} \quad (3.4)$$

Detection of obstacles. In order to determine the occupancy probability of a grid cell from a single measurement, a sensor model was needed, i.e. a rule that allowed the inference of the obstacles in the sensor's range from the sensor's reply. A sensor model applicable to both the real Khepera robot and the simulation was designed for this purpose. It did not only allow the determination of the occupancy probability independent of the used robot (real or simulated), but also rendered the obstacle detection in the simulation more realistic. Note that the sensor replies of the real Khepera robot can take any value between 0 and 1023.

For the determination of the occupancy probability, as a first step, the possible responses of the infrared sensors were divided into five groups that approximated the distance to a potential obstacle (Table 3.2). Note that the sensor response was not only dependent on the distance to an obstacle, but was also reduced if the obstacle was small or if it stood in an angle relative to the sensor axes.

Table 3.2: Infrared sensor model used for the occupancy grid. The range of possible sensor replies is subdivided into groups that correspond to distances between sensor and obstacle. The model applies for both the simulated and the real infrared sensors.

Sensor response	Assumption	Estimated area occupied by an obstacle	Illustration
0 - 50	no obstacle detected	$8cm^2$ free	Fig. 3.2a
50 - 600	obstacle location unclear	no occupation probability assumed	
600 - 900	obstacle detected	$0.75cm^2$ occupied	Fig. 3.2b
900 - 1000	obstacle detected	$3.72cm^2$ occupied	Fig. 3.2c
1000 - 1023	obstacle detected	$8cm^2$ occupied	Fig. 3.2a

In the second step, a certain area in the sensor's range was assumed either as occupied by an obstacle or as free, dependent on the sensor response. If the sensor response did not exceed a value of 50 (compare Table 3.2), it was assumed that no obstacle can be found in the reach of the sensor, and thus, an area of $8cm^2$ was assigned with a zero occupancy probability (Figure 3.2a). Since the sensor curve is steep in the medium range of values, no assumption was made if the sensor re-

sponse fell between 50 and 600, i.e. the occupancy probability remained unaltered. If the value exceeded 600, an obstacle in the vicinity of the sensor reflected the infrared light beam. If the sensor response fell between 600 and 900, a small area ($0.75cm^2$) at a distance of $4.1cm$ from the sensor was assumed to be occupied by an obstacle (Figure 3.2b). A larger area ($3.72cm^2$) was marked as occupied if the sensor response was between 900 and 1000 (Figure 3.2c). A sensor response above 1000 indicated an obstacles very close to the sensor. Accordingly, an area close to the sensor was assumed to be occupied (distance: $1.3cm$, area: $8cm^2$; Figure 3.2a). The estimated occupancy areas in the sensor model follow the implementation of the sensor response (compare Section 3.5.1; Figure 3.1). Areas that were covered by the robot itself were assumed not to be occupied by obstacles.

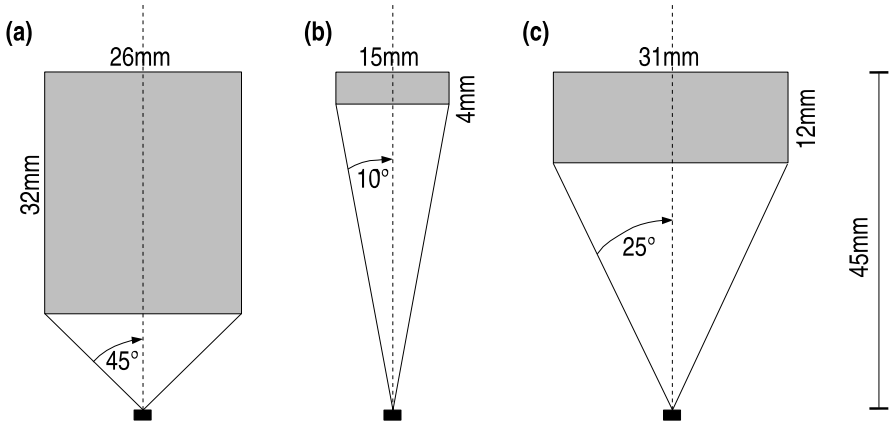

Figure 3.2: Areas (depicted in gray) assumed as occupied by an obstacle dependent on the response of a single infrared sensor. The dashed line shows the axes of the sensor's perceptive field. The sensor position is depicted by the black rectangle. **(a)** Sensor response is very low (< 50) or very high (> 1000). The gray area is assumed to be free or occupied by an obstacle, respectively. **(b)** Sensor response between 600 and 900, and **(c)** between 900 and 1000. The gray areas are assumed to be occupied by an obstacle.

The free and occupied areas of the eight sensors were combined to a local occupancy grid in a third step. The local occupancy grid was aligned with the global grid structure, but only reached as far as the ranges of the infrared sensors. All cells of the local occupancy grid were initially assigned with neutral occupancy probability. The area of each grid cell was represented by nine reference points that subdivided the cell into nine equal-sized areas. For each reference point in each

grid cell, it was checked if it fell in the area of a sensor rectangle as determined in the second step. The number of reference points within each grid cell determined its occupancy probability. If no reference point fell in any sensor rectangle or in the area covered by the robot, the occupancy remained unaltered.

In the last step of the calculation of the current occupancy grid, the local occupancy grid, as built from the current sensory input, was merged with the global occupancy grid. The new occupancy probabilities of each cell that had a correspondence in the local grid was calculated according to Equation 3.4.

Graph structure

In contrast to the grid map, the graph did not presuppose a fixed pattern of nodes. The graph structure used was based on the model of spatial memory as introduced by Franz et al. (1998a). If a place was visited for the first time, a node was added to the graph. There were only as many nodes in the graph as places visited, i.e. the graph map grew with the explored area. As in the grid map, a node acted as a memory container storing the position and the attractiveness value. Connections were formed between two nodes if the agent had travelled between the corresponding locations before. A circular area, the catchment area, with a fixed radius of $1.8cm$ was associated to each graph node. The agent moved to the location of a node if it entered the catchment area.

Obstacles in the environment were represented only indirectly. If the robot detected an obstacle in front of it during a step, i.e. the value of at least one of the most frontal 4 sensors exceeded 400, the step was interrupted. The robot set a new node at its current position. Since the path in the direction of its current heading was blocked, it labelled the nodes which fell in the angular area of $\pm 10^{\circ}$ of its heading as unreachable from the current node. Hence, the obstacle positions were mirrored in the graph structure as edges between nodes that could not be passed by the robot.

3.5.3 Decision making

In each time step, the agents had to decide for their next destination. Since the attractiveness was the crucial information for this decision, they had to recall the memorised attractiveness of the surrounding places. A robot's step always consisted of a rotation followed by a translation. The translation was interrupted if the robot detected an obstacle in front of it. The robot assumed that its path was blocked by an obstacle if at least one of the four frontal infrared sensors exceeded

a value of 400. The robot's behaviour after such an interruption was similar to that following a completed step.

(a)

0.2	0.2	0.2	0.2	0	0	0	0	0.2
0.2	0.2	0	0	0	0	0.2	0.2	0.2
0.2	0.2	0	1.13	0	0.2	0.2	0.2	0.2
0.2	0.2	0	0.58	1.08	0.81	0.61	1.46	1.46
0.2	0	0.2	0.49	×	0.85	1.25	0.2	0
0	0.2	0.2	0.75	0.78	0.75	1.04	0.2	0.85
0.2	0	0.2	2.21	1.06	0	2.71	2.43	0.85
0	0.2	0.2	0.2	1.46	0.97	1.9	2.71	0.85
0.2	0.2	0.2	0.2	0.2	2.21	2.71	2.21	1.9

(b)

0.2	0.2	0.2	0.2	0	0	0	0	0.2
0.2	0.2	0	0	0	0	0.2	0.2	0.2
0.2	0.2	0.13 *0*	0.93 *1.13*	0 *0*	0.07 *0.2*	0.2 *0.2*	0.2	0.2
0.2	0.2	0.13 *0*	1.17 *0.58*	1.21 *1.08*	1.04 *0.81*	1.03 *0.61*	1.46	1.46
0.2	0	0.13 *0.2*	0.38 *0.49*	×	2.14 *0.85*	1.67 *1.25*	0.2	0
0	0.2	0.07 *0.2*	1.49 *0.75*	2.45 *0.78*	2.7 *0.75*	1.78 *1.04*	0.2	0.85
0.2	0	0.13 *0.2*	2.63 *2.21*	1.74 *1.06*	1.24 *0*	3.0 *2.71*	2.43	0.85
0	0.2	0.2	0.2	1.46	0.97	1.9	2.71	0.85
0.2	0.2	0.2	0.2	0.2	2.21	2.71	2.21	1.9

Figure 3.3: Grid map with attractiveness values. In both cases, the same section of a grid is depicted. The white areas are included in the movement decision. **(a)** Only the neighbouring nodes ($N = 1$) form the basis for the movement decision. **(b)** Nodes up to distance $N = 3$ contribute to the movement decision. The gray numbers depict the original attractiveness values A of the cells. The black numbers denote the directional attractiveness B (see text).

Grid structure

In the grid map, the agent chose one of the eight neighbouring cells as its subsequent destination. Cells exceeding 60% probability of occupancy by an obstacle were excluded from the decision as well as the cell visited in the last step. From the remaining cells, the agent chose stochastically according to the attractiveness values (Figure 3.3a). Attractiveness values of more distant places were taken into account by defining a "directional attractiveness" B for each of the eight possible movement directions, i.e. for the eight nearest neighbours. Assume that nodes in an N-neighbourhood around the current node are to be taken into account, i.e. all nodes up to a maximal distance $D = N$ from the current location. Here, distance D between nodes was measured using the maximum norm, i.e. the ring of eight nearest neighbours had $D = 1$, the surrounding 2nd order neighbourhood (16 cells)

had $D = 2$, and so forth. The directional attractiveness was calculated iteratively starting with the most distant cells of the neighbourhood, at distance N. Let j be a cell in the $N-1$ neighbourhood. The attractiveness values of the three nearest neighbours of j in the N-neighbourhood were averaged, yielding a value $\bar{A}$. The directional attractiveness was then calculated as $B_j = A_j + (\bar{A} - A_0)/(D+1)$, where A_0 is the default attractiveness defined above, and initially, $D + 1 = N$. The procedure was iterated towards the centre, using in further steps the previously computed directional attractiveness B instead of the place attractiveness A (Figure 3.3b).

Graph structure

For the graph memory, the notion of directional attractiveness was generalised to continuous directions, yielding an attractiveness panorama $B(\varphi)$. The N-neighbourhood was defined as the set of all nodes that could be reached from the current node in at most N steps; I denoted this set of nodes as V_N. The directional attractiveness panorama was then computed according to Equation 3.5.

$$
\begin{aligned}
B^*(\varphi) &= A_0 + \sum_{i \in V_N}^{n} \left((A_i - A_0) \exp^{-\frac{(\varphi - \theta_i)^2}{2\sigma_i^2}} \right) \qquad (3.5)\\
B(\varphi) &= \begin{cases} 0 & if \quad B^*(\varphi) < 0 \\ B^*(\varphi) & if \quad 0 \le B^*(\varphi) \le P_{max} \\ P_{max} & if \quad B^*(\varphi) > P_{max} \end{cases}
\end{aligned}
$$

Each node i contributed to the panorama according to its direction θ_i. The width of the Gaussian in Equation 3.5 was proportional to the angular extend of the catchment area of node i as seen from the current node, $\sigma_i = k \tan^{-1}(\frac{r_i}{d_i})$, where r_i is the radius of the catchment area and d_i denotes the euclidian distance of node i from the current position. The constant $k = 0.233$ was chosen to maximise the similarity of the graph scheme with the grid scheme; k determines the relative width of the Gaussian of each attractiveness value in the panorama. For a single attractiveness value, $B(\varphi)$ reaches 10% of its maximum value at the angle $\varphi - \theta = \frac{1}{2} \tan^{-1}(\frac{r_i}{d_i})$. In Figure 3.4, a section of a graph is depicted, and the attractiveness panorama for $N = 1$ and $N = 3$ is shown.

Nodes that were labelled as unreachable due to previous obstacle encounters contributed to the panorama with zero attractiveness, $A_i = 0$. Thence, obstacles acted as repulsive forces in the attractiveness panorama (compare Pipe, 2000). In order to avoid the oscillation between two nodes, the node visited in the previous

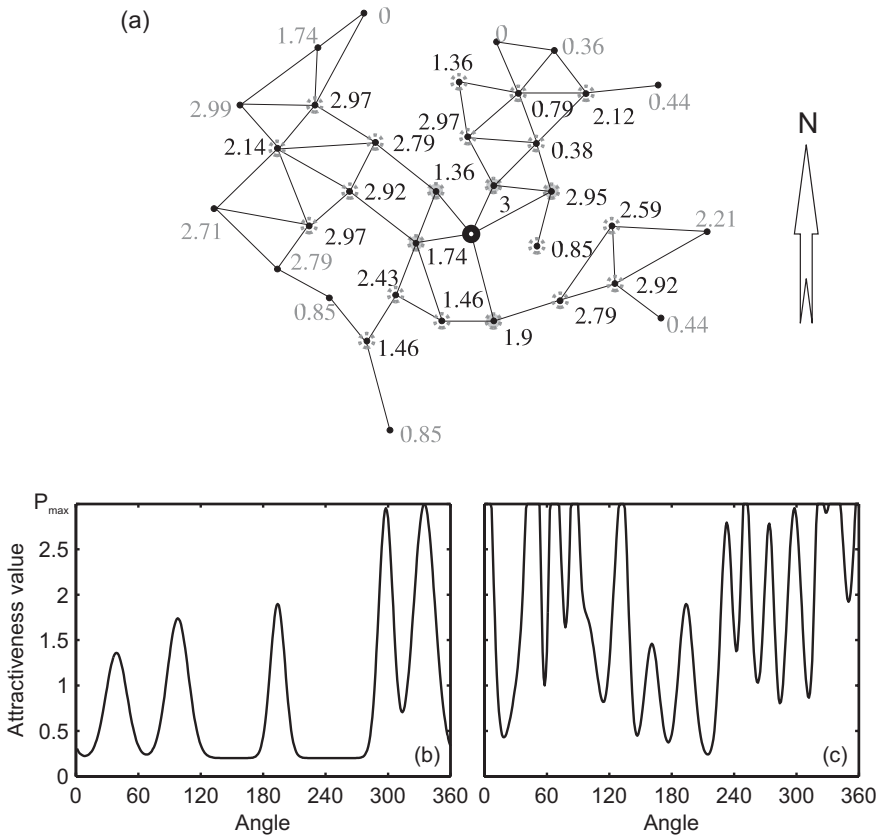

Figure 3.4: (a) Section of a graph structure. The circle in the middle denotes the current position. The numbers are the attractiveness values of the nodes. Nodes with a distance $N = 1$ relative to the current node are marked by filled circles, nodes with distance $N = 3$ by open circles. The north direction is chosen arbitrarily. **(b)** Attractiveness panorama if an neighbourhood of $N = 1$ is included in the movement decision. **(c)** Attractiveness panorama including a neighbourhood of $N = 3$. An angle of zero corresponds to the north direction in the graph.

step was given the default attractiveness, $A_i = A_0$. The panorama was sampled in steps of $10°$. From these samples, one direction was chosen stochastically whereby directions with high attractiveness in the panorama were more likely to be chosen than directions assigned with a low attractiveness. The robot moved in the chosen

direction by a distance fixed to $2cm$, or until it entered the catchment area of a node. In the latter case, the agent moved towards the node's position. Detecting an obstacle during movement, the agent stopped.

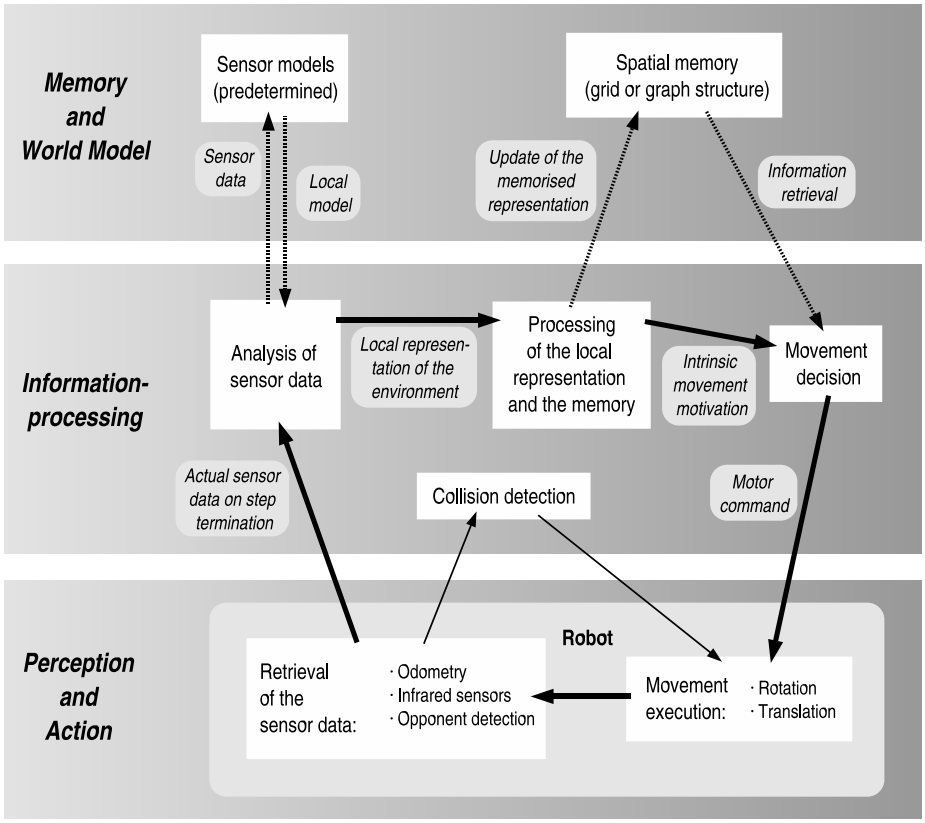

Figure 3.5: Procedure conducted by each robot during the territorial behaviour. Each time step corresponds to a loop in the procedure as marked by bold arrows. The collision detection can interrupt a translation, i.e. the collision detection is embedded in the main loop. The dashed arrows mark information retrieval and update of the memory content.

3.5.4 Algorithmic procedure

The programming language used was C++. The simulation of the Khepera robot as provided by Olivier Michel (compare 3.5.1) was written in C. From this Khepera

simulation environment, I used the modules building the robot and its environment as well as the graphical user interface in my simulation. I integrated these modules in the class system of the territorial behaviour that controlled multiple robots simultaneously. Alternative to the simulation, modules could be used that controlled real Khepera robots.

A step of a single robot in the territorial behaviour is presented schematically in Figure 3.5. After each movement decision as described above, the robot rotated in the chosen direction and performed a translation. During the translation, it retrieved the data from its infrared sensors. If an obstacle was detected in the movement direction, the translation was interrupted. As soon as the translation was completed, position, competitor presence, and sensor information were retrieved. In Figure 3.5, movement and sensor retrieval were classified in the level of perception and action. In the next step, the sensor data was processed whereby predefined sensor models were used (compare Section 3.5.2). The information processing resulted in a local representation of the environment. The local representation was then merged with the memorised information as stored in the memory structure. The following movement decision was based on the information retrieved from the updated memory (or internal world model). This decision preceeded a new step. The three levels suggested in Figure 3.5 are comparable to the levels introduced by the hierarchy of Kuipers (2000). Perception and action corresponds to the sensory and control levels, information processing subsumes the causal level, and memory and world model fulfil the metrical level.

The robots were subordinated to a control unit. The robot's steps were processed consecutively, i.e. only one robot moved at a time. The control unit tracked the positions of the robots (either using the tracker camera if real robots were used, or retrieving it from the environment control). If two robots came closer than $15cm$ to each other, the robots got the information that a competitor is present, i.e. both individuals rated the visit to the current location as a fight (compare Section 3.3.3).

The position data of each robot was monitored during the experiments. Additionally, information stored in the memory structure was read out and saved by the experimental computer every 200 steps. The model parameters used were determined in an initialisation table before an experiment was started. The parameters were set individually for each robot in the experiment (compare Tables 3.3 and 3.4). Additionally, the number of robots and the layout of the environment could be varied (compare Table 3.5). An overview of the main classes controlling the territorial behaviour is given in the Appendix. The functions crucial for the algorithmic procedure are described. Additionally, the parameters determined in the

initialisation tables are listed.

Table 3.3: Parameters of the model of territoriality (compare Equation 3.1). The values marked in bold font are used as default.

Parameter	Description	Possible value range	Applied values
R_p	Parameter determining the attractiveness gain per positive visit	$)0, \infty)$	0.5, 1, **3**, 5, 10, 20, ∞
R_f	Parameter determining the attractiveness decline per fight	$)0, \infty)$	0.5, 1, **3**, 10, ∞
P_{max}	Parameter determining the maximal attractiveness of a node	$(0, \infty)$	**3**
F_{max}	Parameter determining the maximal attractiveness loss of a node by fights	$(0, \infty)$	**3**
A_0	Default attractiveness value assigned to unknown areas	$(0, \infty)$	**0.2**

3.5.5 Model parameters

From each robot, the positions after the accomplishment of each step were tracked externally and stored in chronological order. The experiments were usually conducted over 1000 steps; for exceptions, see Chapter 4. These were subdivided into five time intervals of 200 steps each. At the end of an interval, the robots' internal representation was written to a file. In the representations, the robocentric positions of the nodes were stored in conjunction with the attractiveness value and the local sensor data.

3.5.6 Territory establishment and internal representations

I tested if the robots were able to establish home ranges and territories while building an internal representation of the environment. For this task, the robots' positions during 1000 steps were monitored. The robots used either the graph or the

Table 3.4: Parameters of the spatial memory. The values marked in bold font are used as default.

Parameter	Description	Possible value range	Applied values
N	Amount of memory retrieval for each movement decision (see Section 3.5.3)	1, 2, 3, ..., ∞	**1**, 2, 3, 4, 5
Map	Memory structure (see Section 3.5.2)	*Grid*, *Graph*	***Grid, Graph***
Grid: Occupancy	Minimum occupancy probability that causes the avoidance of a grid cell	$(0, 1)$	**0.6**
Grid: Cell size	Edge length of a single cell in the grid map (see Section 3.5.2)	$)0, \infty)$	**2*cm***
Graph: k	Parameter determining the width of the Gaussian in the attractiveness panorama (see Section 3.5.3)	$)0, \infty)$	**0.233**

grid structure as internal representation. For the other parameters of the model, the default values were used (see Tables 3.3, 3.4, and 3.5). The sensitivity analysis of the model parameters is described in Chapter 4.

In order to visualise the representation of obstacles in the memory structures, four robots were set in the arena containing a regular array of obstacles (see Figure 3.6). In the graph structure, obstacles were represented by special connections between nodes. If two nodes are connected by such special edges, the direct path between them could not be passed by the robot. I present the graph structure with the two types of connections, and the area used by the robot as observed from the outside. Correspondingly, the obstacle representation, i.e. the occupancy grid, and the area used will be shown if the grid structure was used by the robots.

The attractiveness of a place changed with the number of visits. Thus, the attractiveness distribution in the internal representation is compared to the utilisation distribution in the arena. In order to visualise the effect of competitor encounters on

Table 3.5: Parameters of the simulation environment. The values marked in bold font are used as default.

Parameter	Description	Possible value range	Applied values
Robots	Individuals with sensory equipment (see Section 2.2.1 and 3.5)	Simulated or real Khepera robots	**Simulated** and real Khepera robots
Competitor number	The number of robots exploring the arena in the same time	1, 2, ..., 50	1, 2, **4**, 8
Arena size	Area of the environment available to the robots	$(0.01m^2$,$1m^2)$	$0.25m^2$, $0.5m^2$, **1**m^2
Habitat structuring	Number and arrangement of obstacles in the arena	*arbitrary, 800 obstacles fill the arena*	**Empty**, regular quadrants, random

the attractiveness of places in the memory, the attractiveness distribution achieved by an individual roaming solitarily in the environment will be shown as well as the attractiveness distribution of an individual competing with seven others for the available space.

3.6 Results

3.6.1 Obstacle representation

Graph structure. In Figure 3.6a, the ranges of four robots after completing 1000 time steps are depicted. The arena was structured by regularly arranged obstacles which are marked by black rectangles. Overlap areas between the individuals are depicted in gray.

The graph structure built as internal representation by a single individual is shown in Figure 3.6b. The graph consists of 100 nodes, i.e. places were often revisited. Each connection in the graph marked by a solid line corresponds to at least one direct journey of the robot between the connected nodes. The dotted lines

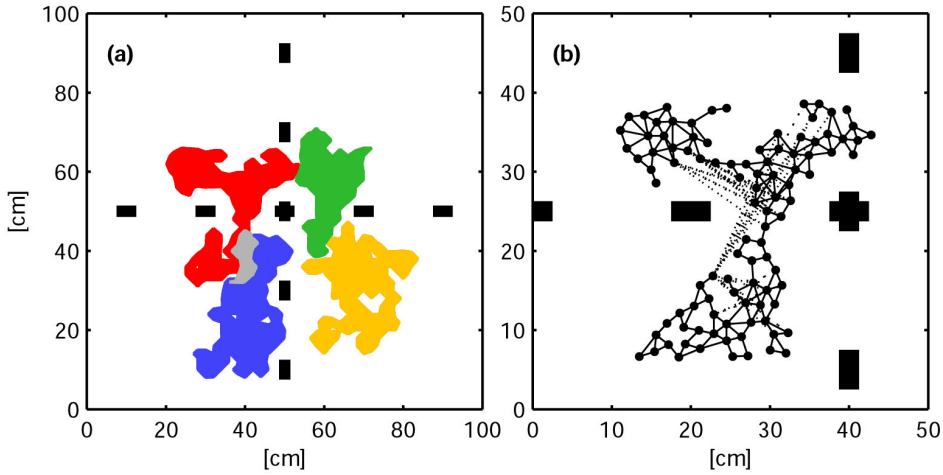

Figure 3.6: (a) Ranges of four robots using the graph as memory structure. Obstacles (black rectangles) were placed in the arena in a regular layout. The ranges are derived from the positions visited by the robots during 1000 steps. Areas visited by more than one robot are shown in gray. **(b)** Graph structure as formed by the robot whose home range was depicted in red in (a). The circles mark the positions of the graph nodes, the solid lines denote the edges that connect the nodes. The dotted lines denote obstacle encounters: the robot could not pass in the corresponding directions. Mind the robot's diameter and the range of its infrared sensors. Note the different scales in (a) and (b).

mark obstacle encounters. The path between nodes connected by dotted lines could not be passed by the robot. Since the robots avoided collisions with obstacles, they assumed paths as blocked if an obstacle came in the range of the infrared sensors during their translations (compare Section 3.5.2). Note that all nodes in the travelling direction were marked as unreachable, even if they did not fall in the reach of a single step of the robot.

Grid structure. The ranges of robots relying on the grid structure as spatial representation are shown in Figure 3.7a. As for the graph structure, the ranges of the robots were derived from their positions after completing 1000 steps. The obstacles were arranged in the same way as in Figure 3.6.

The robots assessed the occupancy by obstacles for a larger range than they visited due to the range of their infrared sensors. In Figure 3.7b, the occupancy

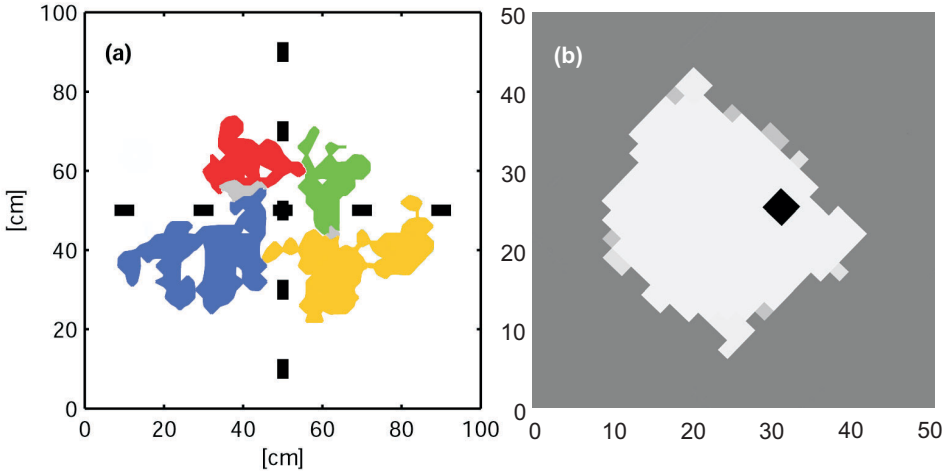

Figure 3.7: (a) Ranges of four robots in the arena with regularly placed obstacles. Gray areas correspond to overlapping ranges between two or more individuals. All robots use a grid map as spatial representation. **(b)** Representation of the occupancy by the robot depicted in red in (a). Black cells denote a high occupancy probability while white areas reflect empty places. Note the different scales.

probabilities of cells in the grid are reflected by different gray values. White areas were assumed to be free. Obstacles were located at places corresponding to black areas. Unknown areas were assigned with the neutral occupancy probability of 50%.

3.6.2 Attractiveness distribution

Graph structure. In Figure 3.8, ranges, utilisation distribution, and the attractiveness in the graph representation are demonstrated. For the solitary and the competitive situation, the areas used by the individuals are depicted (Figure 3.8a and d). For a single individual, the utilisation distribution is shown (Figure 3.8b and e). Red areas denote many visits while blue areas were visited only a few times. The attractiveness in the maps is displayed in Figure 3.8c and f. Areas of high attractiveness appear in red while low attractiveness is depicted in blue.

The individual roaming solitarily in the environment displayed a high correspondence between the utilisation distribution as observed externally and the attractiveness distribution in the graph memory (Figure 3.8a-c). On the other hand, if an individual often encountered competitors in the environment, the utilisation distribution and the attractiveness distribution deviated from each other. Overlap areas as marked in Figure 3.8d led to a disjunction of the utilisation distribution, i.e. the individuals preferably moved away from strongly crowded areas (Figure 3.8e). In the graph memory, those areas appeared with a very low attractiveness (Figure 3.8f). The areas of highest attractiveness did not necessarily coincide with the peaks of the utilisation distribution. Solely if an individual found an area of low crowding, the attractiveness of this area rose due to repeated visits. In the situation with many competitors present in the arena, no coherent attractiveness distribution was formed due to repeated interactions with the competitors.

Grid structure. As for the graph structure, the ranges, utilisation distribution, and the attractiveness distribution in the memory were compared if the grid structure was used by the individuals (Figure 3.9). Similar results as for the graph structure were observed. A solitary individual displayed a confined space use (Figure 3.9a). The utilisation distribution was highly correspondent to the attractiveness distribution in the memory (Figure 3.9b and c). As for the graph structure, this correspondence diminished if the individual was exposed to strong competition for space (Figure 3.9e and f). Additionally, the range used by the individual was disjunct in contrast to the solitary situation (Figure 3.9d).

Figure 3.8 (Page 49): Ranges, utilisation distribution and attractiveness distribution with the graph map. **(a)-(c)** Robot roaming solitary in the arena. **(a)** Range used during 1000 steps. **(b)** Utilisation distribution. Key for colours on the right. **(c)** Attractiveness distribution in the graph. Key for colours on the right. **(d)-(f)** Competitive situation. **(d)** Ranges of eight robots in the environment (1000 steps). The range of the focal individual is marked in red while the ranges of the other seven individuals are subsumed in black. Overlap areas between the focal individual and at least one of the others is marked in gray. **(e)** Utilisation distribution of the focal individual. **(f)** Attractiveness distribution in the focal individual's graph memory. Note the different scales.

Figure 3.9 (Page 50): Ranges, utilisation distribution and attractiveness distribution with the grid map. **(a)-(c)** Robot roaming solitary in the arena. **(a)** Range used during 1000 steps. **(b)** Utilisation distribution. Key for colours on the right. **(c)** Attractiveness distribution in the grid. Key for colours on the right. **(d)-(f)** Competitive situation. **(d)** Ranges of eight robots in the environment (1000 steps). The range of the focal individual is marked in red while the ranges of the other seven individuals are subsumed in black. Overlap areas between the focal individual and at least one of the others is marked in gray. **(e)** Utilisation distribution of the focal individual. **(f)** Attractiveness distribution in the focal individual's grid memory. Note the different scales.

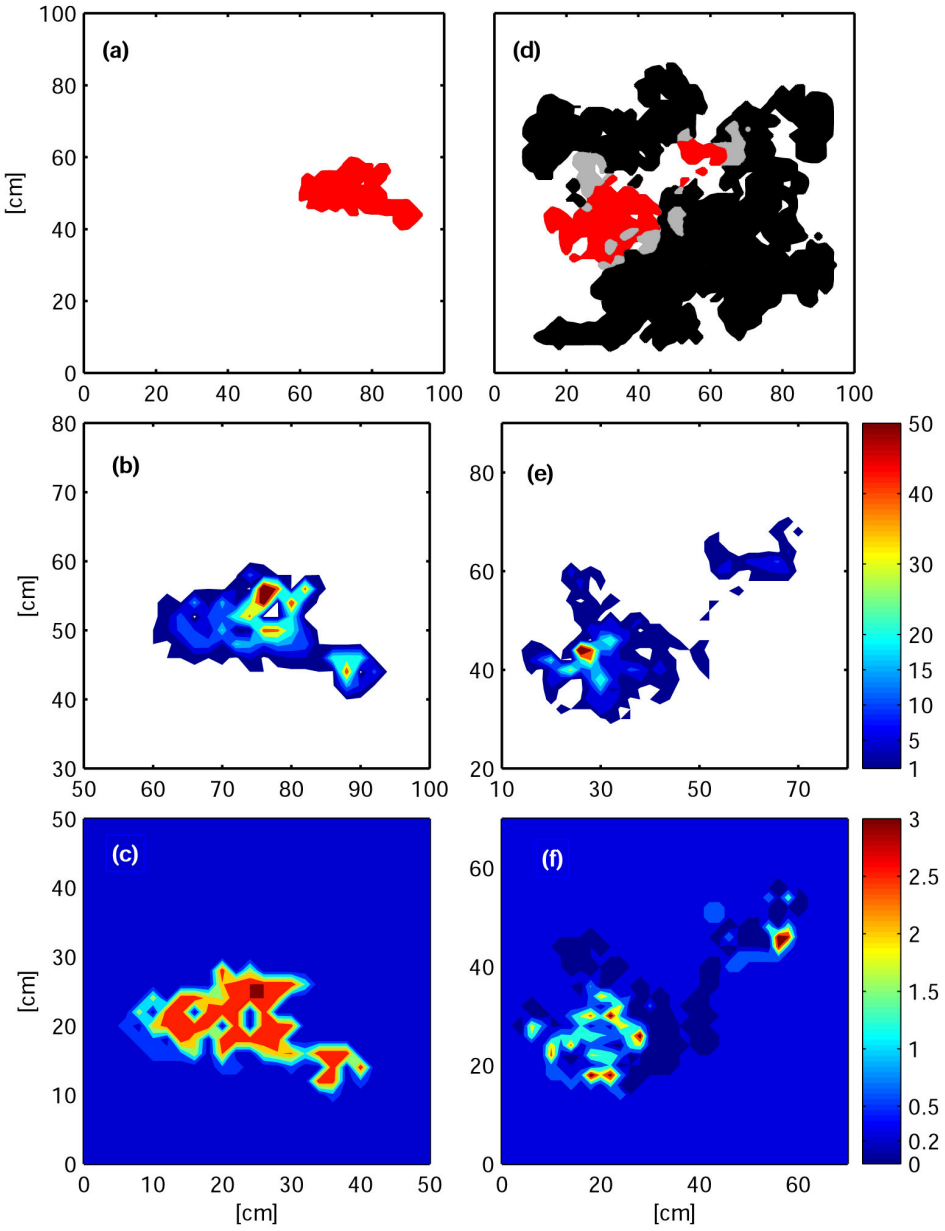

Figure 3.8: For description, see page 48.

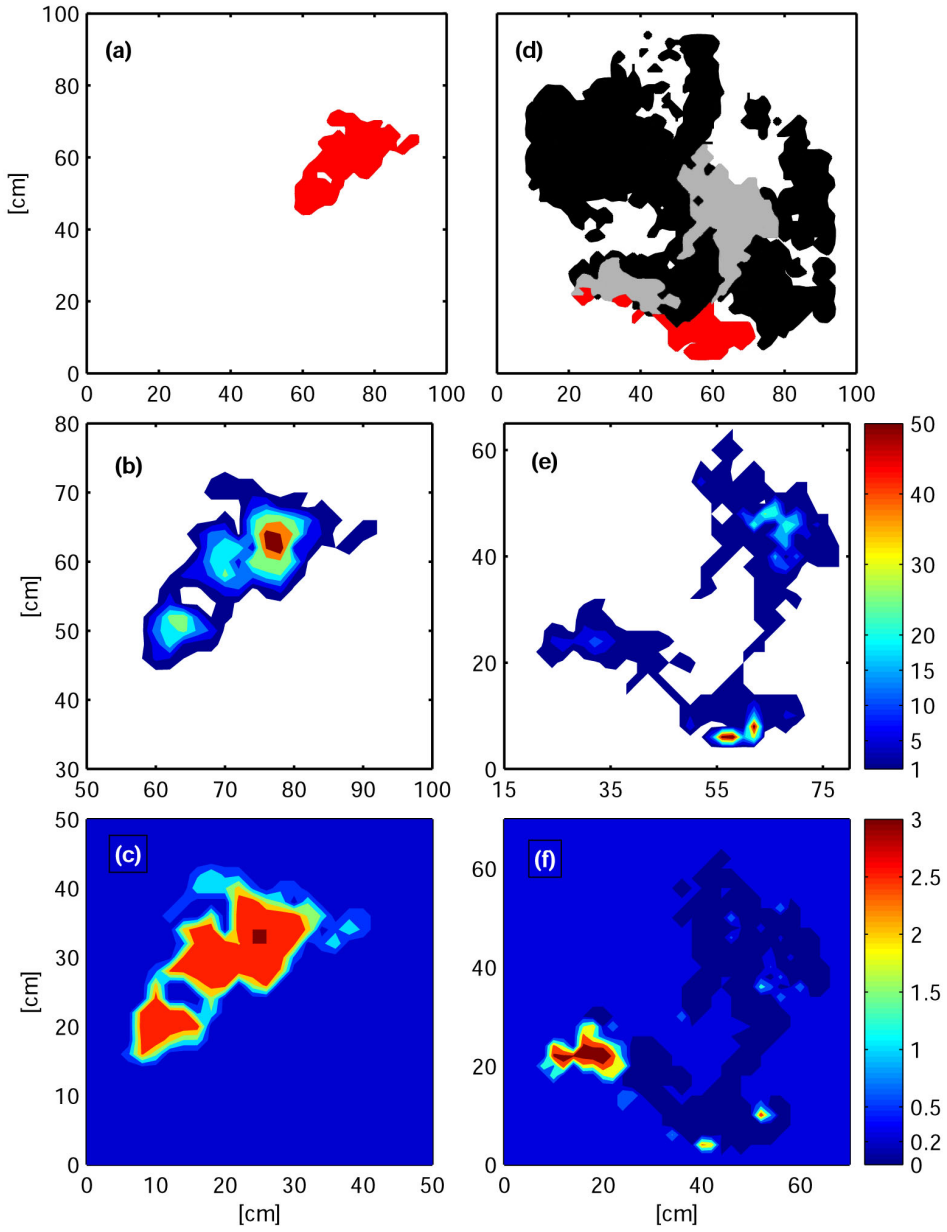

Figure 3.9: For description, see page 48.

3.7 Discussion

The establishment of stable home ranges and territories within a model combining spatial learning with territoriality is shown. With both memory structures applied, the graph and the grid map, a suitable representation for space is provided.

In the grid structure, the reachable space is fully represented. The regularly arranged cells of the grid map cover the represented space completely. This results in an area-based representation. Metric information, i.e. distances and directions, are essential for the grid map. Its storage is memory consuming since information is stored even if it is redundant with the information in the neighbouring cells which even applies if no information about the corresponding area is yet available. Hence, the grid does not represent any weighting of the information which leads to high computational demands if information is retrieved from the grid. For instance, path planning would be costly. Thus, the computational demands of grid-like representations should be considered in cognitive map theories. In their parallel map theory, Jacobs and Schenk (2003) hypothesise a combination of a grid-like global map and local sketch maps in the mammalian and avian brain, but they do not treat the computational costs of such a representation.

In contrast to a grid, in the graph representation, space is only represented if information about it is available. The agent sets a node in its graph that is associated with the information gained about the corresponding location. Thus, information about the environment is not stringently continuous or area-based. Thence, the graph representation is less memory consuming than the grid map, and allows memory retrieval for tasks such as path planning with low computational demands. Metric information is not obligatory for a graph representation. Instead, topological information based on the sensory input is sufficient for its formation (Schölkopf and Mallot, 1995). Graph structures as spatial representation were originally introduced as a means for solving path planning.

The model of territory establishment as described above does not include tasks as path planning, but claims area-based spatial learning. The grid structure thus meets the requirements for this kind of behaviour. Accordingly, I observe the formation of stable home ranges and territories in my model with the usage of the grid as memory structure. The attractiveness values of the internal representation correspond to the pattern of space use including the competitor encounters. Nevertheless, the agents using a graph as internal representation of space display a similar stability in space use as the individuals relying on the grid map. Thus, computationally costly area-based memory structures as the grid map are not required to explain stable space use.

Both memory structures applied in my model do store information that would qualify them as cognitive maps, i.e. as belonging to the most complex navigation strategies of the hierarchies presented in Section 3.2. However, this information is not used in the context of shortcut or detour behaviour which is often stated as the criterion for the existence of a cognitive map. Though a map-like structure is apparently essential for territorial behaviour, the metric information might be negligible. As mentioned above, a graph representation does not rely on metric information. Following the assumption of the model introduced by Stamps and Krishnan (1999), the establishment of home range and territory is based on local movement decisions and not on forward planning of paths or actions. I introduced the attractiveness panorama as potential solution of this decision process. For the panorama, the compass information is important while the metric information, i.e. the distance of a possible goal from the current location, is less crucial. Applying the hierarchies of navigation mechanisms, territorial behaviour demands the topological navigation in the sense of Trullier et al. (1997) or the cognitive level of the levels introduced by Mallot (1999).

The combination of both spatial and non-spatial information in a graph framework has been proposed as a qualitative model of motivational learning in spatial behaviour. Arbib and Lieblich (1977) postulated a "world graph" as internal representation used by animals. In their model, the behaviour of the animals is controlled by a set of drives. Each place in the world graph is associated with position information and an expectation of drive reduction. The animal would aim at the place that promises the highest drive reduction in relation to the travelling time needed to reach it. The potential field map as introduced by Arkin (1989) follows similar ideas though the non-spatial information displays less complexity. Obstacles in the environment were associated with repulsive forces while a goal position had attracting forces. The agents could reach the goal without planning a path. Pipe (2000) used a potential field map as learning scheme in a robot experiment. By learning obstacle locations and assigning them with repulsive forces, the robot was able to navigate efficiently around the obstacles. Pipe (2000) compared the simulation to reward-free learning in animals.

In my simulation, I showed that both a graph and a grid structure support area-based behaviour without the previous knowledge of the environment as it is available to the agents in the model by Arkin (1989). No explicit goals have to be defined in order to account for a behaviour such as territoriality. The only drive, spoken in terms of the ideas of Arbib and Lieblich (1977), is the drive to keep moving to places of the environment assigned with a high attractiveness.

Chapter 4

Space Use

4.1 Introduction

In the context of many behaviours, animals rely on spatial learning. In Chapter 3, I could show that a map-like representation provides a suitable framework for spatial learning in territoriality. However, storage and retrieval of the information in the representation can vary, and thus, influence the behaviour. Additionally, the individuals have to deal with external factors such as competitors and the physical environment. Such cognitive abilities in animals are traits adapted to the ecological niche. This assumption represents the basis of the field of cognitive ecology (Healy, 1992; Real, 1993; Dukas, 1998a).

In this chapter, I will introduce the ideas of cognitive ecology by presenting potential benefits and costs of information processing in animals. Using the simulation of territorial behaviour, I investigated the effects of defined cognitive abilities, i.e. learning rate and memory retrieval, on the individuals' behaviour as measured by the space use. Additionally, I focused on the interactions between external factors and territorial behaviour. I will give an overview of reactions of territorial animals according to external factors, and I will present the space use of the simulated individuals exposed to varying population densities and structurings of the physical environment.

4.2 Cognitive ecology

4.2.1 Benefits of cognitive abilities

Learning and memory can be regarded as phenotypic plasticity enabling an animal to adapt to changing environmental conditions (Dukas, 1998b). This plasticity can be observed in a wide variety of animals and contexts. Food-storing birds and mammals are able to bridge lean seasons by caching food while it is available. Individuals often set up several hundred hiding places. A high memory capacity is vital for the later retrieval of the food (compare Section 3.2.4; for review, see e.g., Giraldeau, 1997).

As introduced in Chapter 3, learning and memory is needed for many navigation tasks. For instance, bees exploit sources that provide nectar or pollen over a longer time period. Accordingly, bees visit such food sources over and over again (von Frisch, 1965), i.e. they learned the way between the source and their hive. Ants of the genus *Ectatomma* are even able to adjust their foraging behaviour according to multi-event past experience. Food locations were manipulated by the experimenter following a predictable rule. The ants were able to increase their foraging success by learning this rule (Franz and Wcislo, 2003). Regarding a whole ant colony, Haefner and Crist (1994) could demonstrate in a simulation study that the inclusion of learning and memory distinctly increased the foraging success of the colony.

Hummingbirds are not only able to return to locations of profitable flowers, but also remember which flowers they recently emptied. Hence, the birds were able to avoid foraging at momentarily unrewarding sites (Healy and Hurly, 1995). This ability was also found in flower bats (Winter and Stich, 2005). Additionally, foraging presents instances of the advantage of learning in a non-spatial context. The theory of optimal foraging implies phenotypic plasticity according to past experiences. Bélisle and Cresswell (1997) demonstrated in a simulation study that optimal foraging behaviour can only be achieved if memory is included. Increasing memory capacity went hand in hand with increasing energy intake of the individuals.

Learning and memory also appears to be particularly useful in social contexts. Whenever an animal interacts with the same individuals repeatedly, it may be favourable to adjust the own behaviour according to the past experiences with these individuals (Pusey and Packer, 1997; Dukas, 1998b). An instance for the benefit of learning in a social context is the dear-enemy phenomenon. In a territorial system, the neighbours might impose a different threat on a resident than

strangers (Temeles, 1994). If a neighbour can be assumed as a minor threat since it will not dispute for a territory, no reaction is needed if the neighbour comes close to the borders of the own territory (Getty, 1987; Heinze et al., 1996; Beecher et al., 1998; Langen et al., 2000). However, if competing for food, the neighbours might be the strongest rivals. In this case, increased aggression against neighbours might yield the highest benefit (Gordon, 1989; Temeles, 1994; Knaden and Wehner, 2003; Sanada-Morimura et al., 2003). Both the dear-enemy phenomenon and its opposite require the discrimination between neighbours and strangers, and thus, memory.

The examples demonstrate that learning and memory strongly influence behaviour. Animals can only achieve optimal behaviour within the limits of their information processing abilities. In reverse, alterations of cognitive traits should lead to marked changes in behaviour.

4.2.2 Costs of cognitive abilities

The examples presented above indicate the benefit of learning and memory, especially in the context of spatial behaviour. However, this kind of phenotypic plasticity also has drawbacks. The complexity of processing requires the corresponding neural complexity, i.e. number of processing units (neurons) and their connections (synapses). Thus, higher cognitive abilities imply a larger neural machinery (Jerison, 2001). We have seen an example for an enlarged brain area due to higher processing demands in the hippocampal sizes of food storing birds as compared to non-storers (compare Section 3.2.4). Even a small amount of tissue that has to be sustained additionally by an animal might be costly, and thus, have distinct fitness consequences (Dukas, 1999). Neural tissue appears to be especially expensive. In humans, the brain avails 15% of the total metabolic activity, but contributes less than 2% to the body weight (Aiello and Wheeler, 1995).

Mery and Kawecki (2004) could even demonstrate that learning claims immediate costs. *Drosophila* flies were either exposed to an ongoing conditioning treatment or achieved equal amounts of food without any learning. The conditioning treatment led to a reduced egg laying rate, reflecting a direct fitness reduction. Additionally, the learning procedure itself might be costly (Dukas, 1998b). Laverty and Plowright (1988) compared bumble bees feeding primarily on monkshood (*Aconitum* spp.) with generalistic species feeding on a wide variety of flowers. Previously naive bees were allowed to search for nectar in the morphologically complex flowers of the monkshood. Bees of the generalist species needed a search time during their first visits that was thrice as long than observable in the bees of the specialist species. Hence, by relying on inherited abilities, the specialists save

learning time (Laverty and Plowright, 1988; Dukas, 1998b).

The costs associated with cognitive abilities entail that the optimal solution to behavioural tasks might not be achievable by animals. In order to economise neural machinery, they should forgo, for instance, high learning abilities or memory capacity.

4.2.3 Adaptivity of cognitive traits

Correspondingly, learning and memory abilities should be adapted to the animal's niche as much as any other trait. This hypothesis led to the foundation of the field of cognitive ecology or neuroecology (Healy, 1992; Real, 1993). Although evidences for the correlations between specialised cognitive abilities and the ecological niche have been presented (Healy and Braithwaite, 2000; Healy et al., 2005), the modular evolution of brains and intelligence remains a subject of discussion. Bolhuis and Macphail (2001) criticised the neuroecological approach, and assumed that the evolution of intelligence was a general process. In their view, all learning tasks are based on similar processes. Complexity of information processing thus goes hand in hand with a general growth of the brain (Macphail and Bolhuis, 2001).

Flombaum et al. (2002) defended the idea of psychological modularity as favoured by the neuroecological approach. He argues that psychological modularity is not necessarily innate. Conversely, modules might also be acquired by learning. Additionally, the idea of psychological modules as adapted traits does not imply that such modules have to be strictly restricted to a single task. Instead, a module might serve in different contexts. A psychological module might not have a particular neural counterpart, i.e. not every cognitive ability is strictly associated with a single specialised brain region. Hence, the cognitive ecology approach does not oppose to the existence of multiple-purpose information processing abilities. However, these abilities cannot be viewed outside the evolutionary context. At some point of a species' evolutionary history, an information processing ability appeared as an adaptation to the confined problems posed by the ecological niche.

Thus, the neuroecological approach predicts that the cognitive abilities in animals as well as their brains are shaped by both their evolutionary descent and their current niche. Indeed, an investigation of mammalian brains supports this view. The sizes of brain areas in different mammalian species are not merely scaled with the size of the whole brain. The brain parts rather allow a grouping of the investigated species according to both their phylogeny and their particular adaptations (de Winter and Oxnard, 2001; Brown, 2001).

4.3 External influences on territoriality

4.3.1 Competition for exclusive territories

Territorial behaviour is not only influenced by the cognitive abilities of the individuals, but space use will also depend on external factors such as the competitor density and the structuring of the physical environment. Animals defend territories in order to monopolise the resources of the area (see also Section 3.3). However, the defence itself is costly for the individual since it risks injuries in fights and looses the time for foraging. Thus, home ranges of individuals might be disjunct without actual defence of an exclusive territory. Since an area used by several individuals usually provides less benefit for the single animal, such overlap areas might be avoided. The active defence of resources is called interference competition while exploitation competition is the notion for the depletion of the same resources by several individuals (Begon et al., 1990). Both types of competition are strongly dependent on the population density (Kawata, 1997). As soon as the animals actively defend resources, the two processes are hard to separate. Nevertheless, disjoint foraging ranges which are not actively defended can be observed suggesting the avoidance of exploitation competition. In Bechstein's bats, females maintain fairly stable foraging ranges. Although no aggressive interactions between the females were observed during foraging, their foraging ranges are mostly exclusive. Only a mother may widely share a foraging area with her daughter (Kerth et al., 2001; Rossiter et al., 2002). In the model of territoriality as presented in Chapter 3, the individuals achieve exclusive ranges by avoidance. Thus, the model does apply to both interference and exploitation competition.

4.3.2 Population density

The defence and maintenance of exclusive access to a resource is strongly dependent on the population density. If too many individuals compete for the same resource, the energy needed for its defence will override the benefit achievable from the resource. Craig and Douglas (1986) described conditional territoriality in New Zealand bellbirds. These nectar feeding birds defended largely exclusive ranges when the *Dysoxylum* trees found scattered in the forest were in flower. Earlier in the season, a single *Vitex* found in the observation area attracted most of the birds. In this case, they were not able to defend exclusive ranges, but mostly dispersed over the whole tree. Grant et al. (2000) described comparable behaviour in the Japanese medaka. These fish initially spent more time chasing competitors if

the competitor-to-resource ratio increased. Thereby, the resources in these experiments were the number of potential mates. However, if the competitor-to-resource ratio exceeded three, the level of aggression declined again (scramble competition). Chapman and Kramer (1996) tested the effects of scramble competition in an experiment with interspecies competition. A single food source was provided in an aquarium which initially housed a giant danio fish. Successively, individuals of the smaller zebrafish were introduced. With up to five of the smaller competitors, the giant danio was able to monopolise the resource completely. However, if the competitor number exceeded ten, each fish, including the giant danio, obtained an equal share of the food.

Conclusively, exclusive space use is achievable by defending a defined range, the territory, but might also arise only due to exploitation competition. In the latter case, exclusive areas arise because the individuals tend to avoid each other. In both cases, the exclusive space use due to interference and/or exploitation competition, the exclusivity is not maintainable if the competitor number becomes too high.

4.3.3 Physical environment

Not only the competitors might influence the space use as an external factor, but also the layout of the physical environment might come into play. Landmarks and obstacles can be used as markers for territory borders or may direct migration movements. The dispersal of butterflies is hampered by edges such as treelines or field borders in a fragmented habitat. The butterflies stopped their movement according to patterns that do not necessarily hinder their movement as it is the case for field borders (Ries and Debinski, 2001; Schultz and Crone, 2001).

In territorial species, the preferred establishment of territory borders along landmarks or visual barriers was observed. Cicada killer wasps readjusted the boundaries between their territories according to sticks on the ground that were introduced by the experimenter. Aggressive encounters between the territorial residents declined along the borders defined by the landmarks (Eason et al., 1999). Correspondingly, an elongated landmark on the ground of an otherwise homogenous aquarium was used as territorial border location by buckheads. Pairs of these fish establish territories. While one of the two pairs introduced in the aquarium usually claimed the whole available space as its territory if no visual cues were provided, the two pairs divided the available space along the added landmark. This even held true if the landmark location distinctly deviated from the mid of the aquarium. The fish rather accepted a smaller territory than risking elongated fights with the competitors (LaManna and Eason, 2003). Lizards were introduced in

an environment that was subdivided by opaque barriers. Although the sight was blocked, the animals could easily pass beneath the barriers. The territories established by the lizards in this environment were lined up with the barriers. In comparison to an environment without the barriers, the lizards established on average smaller territories (Eason and Stamps, 1992). In a field study of sparrow territories, a high consistency of the territory locations was found over 14 years. The territory borders were mostly aligned with ridges or hills. These topographical constraints apparently influenced the territory sizes more than the resource holding potential of the residents (Reid and Weatherhead, 1988).

The landmarks or barriers might provide a local position cue for both of the competitors. Hence, both individuals are able to locate their border, and thus, fights around the border might be reduced. This reduced investment in the border defence may pay even in case of a decreased territory size.

4.4 Internal and external influences on space use

As discussed in Chapter 3, territorial behaviour presupposes spatial learning and memory in most cases (Stamps and Krishnan, 1999). How do the cognitive abilities influence spatial behaviour such as territoriality? Such a question is hard to approach in animal experiments. Instead, the simulation as presented in Chapter 3 allows the alteration of independent modules of information processing abilities. Additionally, effects of the structuring of the physical environment can be tested by the explicit simulation of the individuals with their sensors.

Using the individual space use and the areas frequented by more than one individual as behavioural measures, I investigated the influences of cognitive and external factors in the simulation. The two memory structures applied were compared under the different conditions. I altered the learning rate of place attributes, i.e. the learning rate of the attractiveness. Additionally, I investigated the influence of different amounts of memory retrieval on the behaviour. As external factors, the population density and the structuring of the physical environment were studied (Schmolke et al., 2004; Schmolke and Mallot, submitted). The time dynamic of the territories in the model was approached by observing the development of the space use over long time periods. Additionally, I analysed the effects of the removal of single individuals as well as the retarded introduction of individuals in the experimental arena.

4.5 Home range analysis

The analysis of bivariate data is of high importance for studies of space use in animals. From the positions where individuals were observed, the underlying utilisation distribution has to be concluded. This also holds true for the analysis of the robots' space use. Since several methods have been proposed for this task (for review see Powell, 2000; Silverman, 1986), I will present the three methods the most commonly used in the analysis of animal home range data. For the illustration of the methods, I applied them to an example data set drawn from the robots' home ranges.

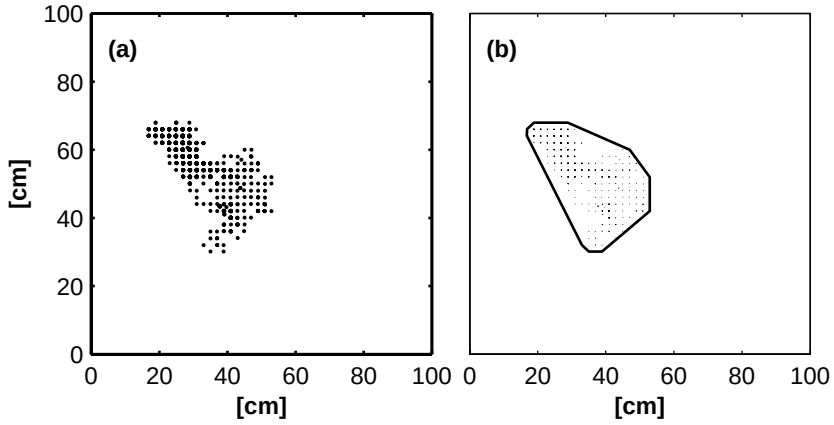

Figure 4.1: Area estimation by a minimum convex polygon **(a)** Positions visited by one robot in 1000 steps. **(b)** Minimum convex polygon with an area of $846.4cm^2$

4.5.1 Available methods

Minimum convex polygon

The bivariate data points can be surrounded by a minimum convex polygon (Figure 4.1). The home range is then defined as the area of the polygon.
Problems: The area of the minimum convex polygon usually overestimates the area

covered by the data points since gaps as they appear if the used range is concave are neglected (compare Figure 4.1). No utilisation distribution can be derived.
Advantages: This method is applicable to any bivariate data set. The polygon and its area can be easily computed.

The minimum convex polygon is well suited for the area estimate if few data points are available. For larger data sets, especially if the point cloud diverges from a convex form, another method should be applied.

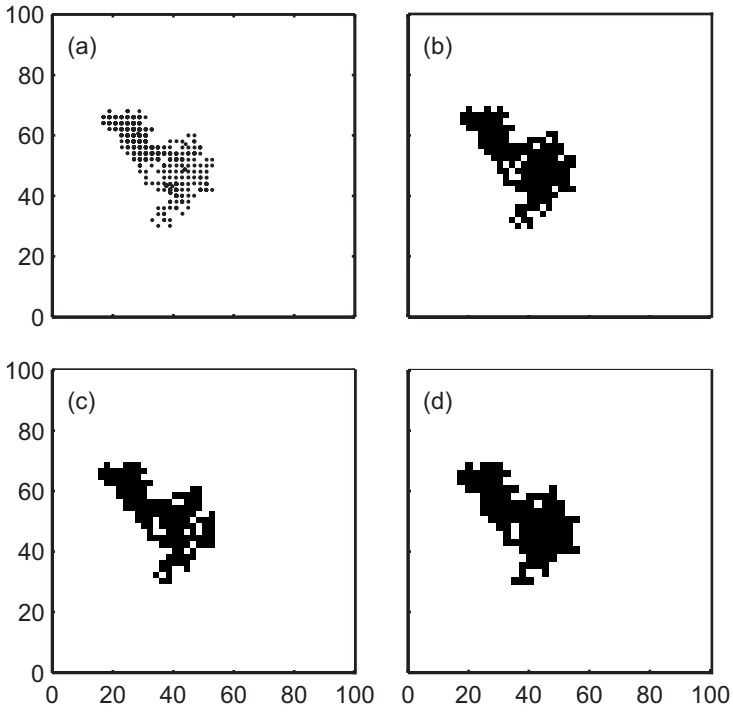

Figure 4.2: Area estimation using the histogram method. **(a)** Positions visited by one robot in 1000 steps. **(b)** Histogram with $2cm$ cell spacing; total area: $612cm^2$. **(c)** Grid shifted by $1cm$ compared to (b); total area: $584cm^2$. **(d)** Cell spacing of $2.5cm$; total area: $706cm^2$.

Histogram method

In order to generate a histogram of a bivariate data set, a grid is superimposed on the data. For each grid cell, the number of measurements falling in the area of this cell are counted. The area of the home range is reflected in the sum of all cell areas that have at least one count. The probability that the animal is observed in the area of one grid cell can be calculated.
Problems: The results of this method are strongly dependent on the chosen size of the grid cells and the positioning of the grid (compare Figure 4.2).
Advantages: The method has no restrictions concerning the bivariate data and is easily computable. In the histogram, the utilisation distribution is represented (compare Figure 4.3).

With the histogram method, a large data set can be handled. In contrast to the minimum convex polygon, concave ranges are not overestimated and the utilisation distribution is available. If the grid spacing can be determined beforehand, this is a very useful method for home range analysis.

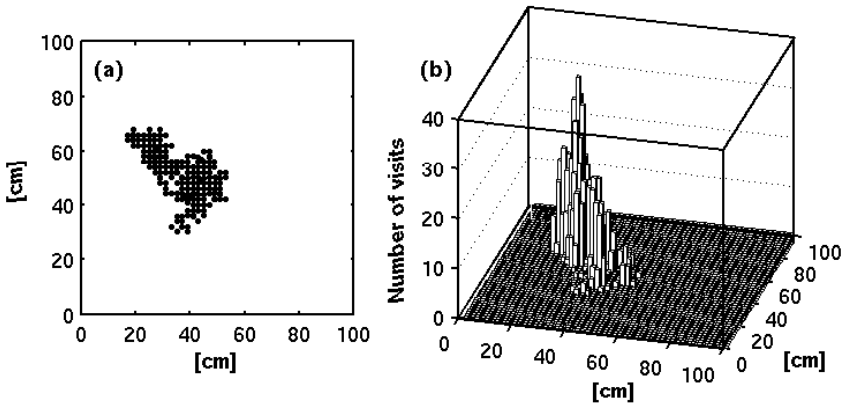

Figure 4.3: Utilisation distribution gained by the histogram method. **(a)** Positions visited by one robot in 1000 steps. **(b)** Number of visits in each cell; cell spacing: $2cm$

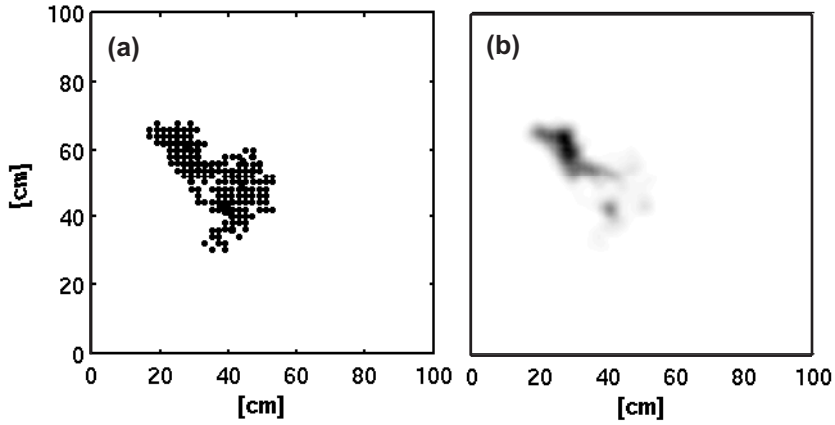

Figure 4.4: Utilisation distribution derived by the kernel estimator method. **(a)** Positions visited by one robot in 1000 steps. **(b)** Utilisation distribution. The total area covered amounts to $565cm^2$ if 95% of the distribution are taken.

Kernel estimator

Around each data point, a kernel function is placed. The values of these distributions of the whole data set are added up at each point of the observation area. This yields a continuous distribution function which is normalised to 1 (Figure 4.4). Thus, the utilisation probability for any point in the observation area can be determined. The whole area used by an individual can be inferred by regarding a core distribution of, e.g., 95%, by cutting off 5% of the tail of the distribution. Thereby, the smallest area enclosing 95% of the utilisation distribution is determined (Powell, 2000).

In the following, I introduce the kernel estimator method using the bivariate normal distribution as kernel function K that is superimposed on each data point (Equation 4.1). Similar functions can be used as kernel leading to comparable

results (Silverman, 1986).

$$K(\mathbf{x}) = \frac{1}{2\pi} \exp^{-\frac{\mathbf{x}'\mathbf{x}}{2}} \tag{4.1}$$

$\mathbf{x}$ denotes an arbitrary point in the plain. The probability of stay in any location of the observed area, i.e. the utilisation function $\hat{f}(\mathbf{x})$, can then be estimated according to Equation 4.2.

$$\hat{f}(\mathbf{x}) = \frac{1}{nh} \sum_{i}^{n} K[\frac{\mathbf{x} - \mathbf{X}_i}{h}] \tag{4.2}$$

The number of measurements n of bivariate data points $\mathbf{X}_i$ enter into the utilisation function. The value of the smoothing parameter h is crucial for the resulting utilisation distribution (Silverman, 1986; Worton, 1989). The smoothing parameter determines the width of the kernel function K. Low smoothing leads to a representation of all details in the data set while with high smoothing, any gaps and the roughness in the distribution are not represented. The least squares cross validation allows the choice of h to be adapted to the data set (Equation 4.3, Silverman, 1986). For this method, the function M_1 is minimised over h using the data set $\mathbf{X}_i$. In the minimisation, the convolution $K^{(2)}$ of the kernel K with itself is used. The value h as determined by this minimisation leads to a medium smoothing of the data.

$$\begin{aligned} M_1(h) &= \frac{1}{n^2h^2} \sum_{i}^{n} \sum_{j}^{n} K^*[\frac{\mathbf{X}_i - \mathbf{X}_j}{h}] + \frac{2}{nh^2} K(0) \\ K^* &= K^{(2)} - 2K \end{aligned} \tag{4.3}$$

Problems: The smoothing parameter h has to be chosen which poses a problem comparable to the choice of the grid spacing in the histogram method. Although the least squares cross validation allows a fit to the data without preassumptions, the comparability of several data sets becomes unclear if h is determined independently for each set. Additionally, the minimisation procedure $M_1(h)$ does not yield reasonable values of h if identical data points exist in the data set, i.e. if the individual had been observed in the same position two or more times. The computation of the kernel estimator method is expensive compared to the other methods presented here.

Advantages: The kernel estimator method can handle large bivariate data sets. It provides the same advantages as the histogram method. In addition, no preassumptions about the distribution of the data are needed (compare the cell spacing in the histogram method), and the resulting utilisation distribution is continuous.

4.5.2 Methods applied

The observed robots' positions mostly did not approach a convex shape. Thus, the minimum convex polygon method was inappropriate for my data. The histogram as well as the kernel estimator method work especially well with a reasonable large data set which is the case for the robot experiments. Hence, I analysed the bivariate data sets using both methods.

I recorded the positions of the robots each time they completed a step, i.e. as soon as they finished a translation. The length of a translation was restricted. Due to the restricted movement scheme (compare Section 3.5.3), a single step did not exceed $3cm$ and only fell short of $2cm$ if an obstacle was close-by. Thus, I can preassume that the positions are distributed approximately uniformly at a spacing of $2cm$. Hence, the histogram method was applied using this grid spacing.

For the kernel estimator, the smoothing parameter h was determined for each data set, whereby only a random subset of 200 (from 1000) differing data points was fed in the least squares cross validation (Equation 4.3). The determined values for h were averaged over the data sets with identical parameters. The averaged value of h was used for the kernel estimator method. The effects observed in the results presented below are independent of the method used. However, the kernel estimator method yields an infinite distribution. If the area has to be determined, a core of the utilisation distribution, e.g., 95% of the distribution, has to be chosen subjectively (Powell, 2000). Since the grid spacing in the histogram method was determinable according to the experimental setup, the area estimated by this method appears to be more accurate. Hence, only the results from the histogram method are shown in the following.

4.5.3 Quantification of the overlap

The home range of the robots denotes the whole area used during the whole experiment (in most cases 1000 steps, in long-term experiments, 10000 steps; compare Section 4.6). The territory is defined as the part of the home range that is exclusively used by the resident (compare Section 3.2). The area used by two or more individuals is referred to as overlap. Three measures of overlap are described in the literature (Smith and Dobson, 1994; Powell, 2000): (a) the area of overlap in relation to the whole home range of the individual, (b) the part of time (number of position measurements) spent in the overlap area by each individual, and (c) the probability of meeting the other individual(s) in the area of overlap. The measure (c) can be calculated as the index I_p of pairwise overlap O between the home

ranges of the individuals i and j (Equation 4.4; Smith and Dobson, 1994).

$$I_p = \sum_{k \in O} p_{ki} \sum_{k \in O} p_{kj} \tag{4.4}$$

While the measures (a) and (b) are asymmetrical, i.e. differ for the individuals of a pair, the probability of meeting each other in the area of overlap (measure (c)) is equal for both individuals, and is based on the assumption that the individuals visit the overlap area independently from each other. For the overlap between individual home ranges, I calculated all three measures. The area of overlap is usually located in the periphery of the home range where the probability of stay is reduced compared to the central areas. Thus, the measure (a) is likely to overestimate the overlap between home ranges in contrast to the other measures. The effects as presented in the results (Section 4.7) are observable with all three measures. For the plots shown, I used measure (b), the probability of stay in an area of overlap.

4.5.4 Statistics

The three dependent variables, home range size, amount of overlap, and territory size were tested by one-way ANOVAs. In order to determine differences between means, Tuckey's honestly significant difference criterion was applied. Interactions between the used memory structure and the experimental conditions were determined using two-way ANOVA. If no effect of memory structure was found, the data of grid and graph structure were pooled.

4.6 Experimental design

The robots were set in the arena which was previously unknown to them. The effect of different parameters of the territorial behaviour as well as different environmental influences were tested. The data was pooled for multiple experiments with identical settings. The simulation and its parameters are described in Chapter 3. The experiments 1 and 2 are concerned with the influences of internal (cognitive) factors on the behaviour while the experiments 3 to 5 treat the external influences. The last two experiments, 6 and 7, are concerned with the time dynamics of the home ranges and territories.

4.6.1 Experiment 1: Learning rate

According to the model of territory establishment, the attractiveness of a place increases with each visit if no competitor is met. In contrast, the attractiveness is reduced due to competitor encounters (compare Section 3.3.3). The learning rate of the attractiveness is determined by the variables R_p and R_f, respectively, of the attractiveness equation (Equation 3.1). Thereby, high values of R_p or R_f reflect a low learning rate and vice versa. If both positive visits and fights influence the attractiveness value, I will refer to this as the competitive model. As controls, either one or both of the learning parameters were removed from the model. Thus, either the influence of positive visits, of fights, or of both disappeared. The positive model excludes the influence of competitor encounters. This corresponds to the variable R_f set to infinity. Comparably, the negative model neglects positive visits, i.e. R_p is assigned with an infinite value. If no learning occurs at all, the robots perform a random walk.

Competitive model. The influence of the learning rate on the establishment of home ranges and territories was tested by applying values of R_p ranging from 0.5 (high learning rate) to 20 (low learning rate). The same value range was applied to the learning rate concerning the fights, R_f. The effect of learning rates was tested using the graph and the grid structure. For the other model parameters, the default values were used, as denoted in the Tables 3.3, 3.4, and 3.5.

Positive model. The learning of competitor encounters was suppressed ($R_f = \infty$). Thus, competitors only influenced the other robots' behaviour as mobile obstacles. The positive model was tested with values of R_p ranging from 0.5 to 20. As in the competitive model, the default values were applied to the other model parameters.

Negative model. In this case, the positive visits do not influence the attractiveness value ($R_p = \infty$). The negative model was tested with R_f-values between 0.5 and 20, and with default values of the remaining model parameters.

Random walk. The random walk is the control for the space use achieved without learning. Both R_p and R_f were set to infinity. The movements were only influenced by the obstacles, whereby the competitors act as mobile obstacles.

The different parameter sets tested in the different models are listed in the Table 4.1. All the experiments concerning the learning rate were conducted in the empty arena. The robots were placed at fixed initial positions as depicted in Figure 4.6a.

Table 4.1: Experiment 1. Tested parameter combinations of the attractiveness equation (see Equation 3.1).

R_p	R_f	P_{max}	F_{max}	A_0
Competitive model				
0.5	3.0	3.0	3.0	0.2
1.0	3.0	3.0	3.0	0.2
3.0	3.0	3.0	3.0	0.2
5.0	3.0	3.0	3.0	0.2
10.0	3.0	3.0	3.0	0.2
20.0	3.0	3.0	3.0	0.2
3.0	0.5	3.0	3.0	0.2
3.0	1.0	3.0	3.0	0.2
3.0	10.0	3.0	3.0	0.2
3.0	20.0	3.0	3.0	0.2
Positive model				
0.5	∞	3.0	-	0.2
1.0	∞	3.0	-	0.2
3.0	∞	3.0	-	0.2
5.0	∞	3.0	-	0.2
10.0	∞	3.0	-	0.2
20.0	∞	3.0	-	0.2
Negative model				
∞	0.5	-	3.0	0.2
∞	1.0	-	3.0	0.2
∞	3.0	-	3.0	0.2
∞	10.0	-	3.0	0.2
∞	20.0	-	3.0	0.2
Random walk				
∞	∞	-	-	0.2

4.6.2 Experiment 2: Memory retrieval

The amount of memory used for each movement decision is given by the N-neighbourhood (compare Section 3.5.3). I tested the influence of the amount of memory retrieval on the individual space use applying the values $N = \{1, 2, 3, 4, 5\}$. The other model parameters were set to their default value as defined in Tables 3.3, 3.4, and 3.5.

4.6.3 Overview: Internal factors

The interaction between memory retrieval and learning rate were observed by varying both R_p and N simultaneously. The relation between territory and home range size was regarded for the different learning models and for a higher amount of memory retrieval.

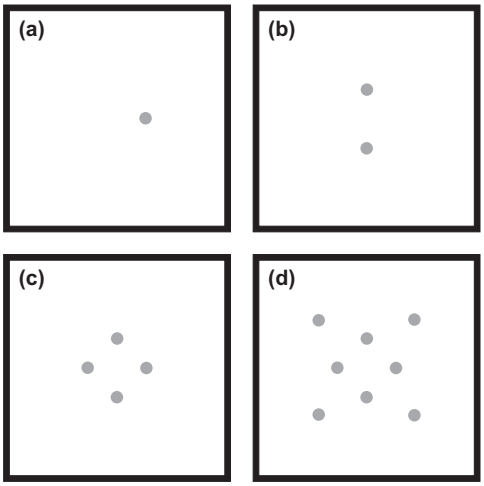

Figure 4.5: Experiment 3. Starting positions of the robots in the experiments testing the effects of competitor number. **(a)** Solitary robot. Only one of four starting positions used is shown. **(b)** Two robots. One of two applied starting configurations depicted. **(c)** Four robots. **(c)** Eight robots. Only the home ranges of the inner four robots were evaluated.

4.6.4 Experiment 3: Competitor number

One to eight agents were placed in the arena at a time. In the trials with eight individuals, only the ranges of four of them were evaluated. The starting positions were assigned as follows: a single agent was placed either north, east, south or west (example in Figure 4.5a), two agents were placed in the positions north and south from the mid of the arena (Figure 4.5b) or in positions east and west of it. Four agents were placed in positions in north, south, east and west (Figure 4.5c). These starting positions were also used for the four focal individuals if eight competitors were present (Figure 4.5d).

4.6.5 Experiment 4: Arena size

The available space for the territory establishment was manipulated by adjusting the arena size. The ranges of four robots were investigated. The robots were placed in square environments of three different sizes. Arena sizes of $1m^2$, $0.5m^2$ and $0.25m^2$ were tested. The full arena size ($1m^2$) does not restrict the size of the robots' home ranges. This still holds true for half the size ($0.5m^2$). Brought down to the quarter of the available space, four home ranges as established by a solitary robot in the full arena would fill up the space. For the other model parameters, the default values were applied (Tables 3.3, 3.4, and 3.5).

4.6.6 Experiment 5: Habitat structuring

The effects of environmental structuring on the pattern of space use was investigated placing four agents in four different environments (Figure 4.6): (a) Empty arena without obstacles, (b) all obstacles clustered in the centre of the arena (centred layout), (c) obstacles placed along the virtual borders of the arena's quadrants (quadrant layout) whereby the gaps between the obstacles could be easily passed by the agents, and (d) obstacles placed at random locations in the arena (random layout) using five different random layouts. Apart from the empty arena, the total area covered by obstacles was equal in the different environments. For all arena layouts, the starting positions of the individuals were identical. I hypothesised that in the quadrant layout, the territory boundaries would tend to line up with the obstacles. In order to test this hypothesis, I quantified the area used by each individual in the four quadrants of the arena.

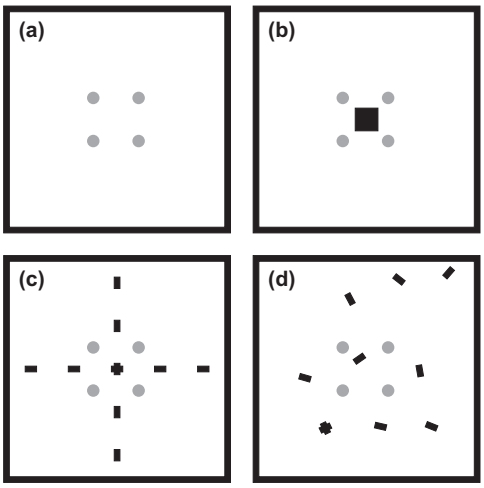

Figure 4.6: Experiment 5. Arena with different obstacle layouts. The gray circles mark the robots at their start positions, the black rectangles are the obstacles. **(a)** Empty arena. **(b)** Centred layout. **(c)** Quadrant layout. **(d)** Random layout (one of five random obstacle distributions is shown).

4.6.7 Overview: External factors

The relation between territory and home range size marks the exclusivity of space use. A comparison of this relation is given for solitary individuals, individuals in higher population densities, and individuals establishing ranges in habitats structured by obstacles.

4.6.8 Experiment 6: Residents and newcomers

Four individuals were allowed to establish home ranges in the empty arena. The individuals performed 1000 steps. In the first part of the experiment, a naive individual, the newcomer, was introduced in the arena at the position taken by one of the residents after its 800th step. The five individuals performed another 1000 steps. In the second part, one of the residents was removed after 1000 steps. The newcomer was placed at the last position taken by the removed resident. The four individuals present performed 1000 steps. Then, the former resident was reintroduced at the position it last visited before its removal. Again, the five individuals accomplished another 1000 steps.

I applied the default model parameters in the experiments with the newcomer (compare Tables 3.3, 3.4, and 3.5). The sizes of home range and territory as well as the drift of the home ranges was determined and compared between permanent residents, reintroduced resident, and newcomer.

4.6.9 Experiment 7: Long-term experiments

The development of the home ranges was investigated in long-term experiments. Instead of terminating the trials after 1000 steps, the space use of the individuals was observed over 10000 steps. The experiments with the elongated run-time were conducted with both memory structures and with an amount of memory retrieval of $N = 1$ and $N = 3$. For the other model parameters, the default values were applied (compare Tables 3.3, 3.4, and 3.5). I quantified the drift of the ranges used by the individuals. For this task, I calculated the overlap (probability of stay; compare Section 4.5.3) of the range used during 200 steps with the whole range visited previously by the same individual. If an individual confined its space use completely to previously explored areas, this measure amounts to 1, while 0 would indicate that the individual did not revisit any known place.

4.7 Results

4.7.1 Experiment 1: Learning rate

Competitive situation

Attractiveness decline. The rate of attractiveness decline is defined by the variable R_f. In Figure 4.7, the influence of the learning rate R_f concerning the competitor encounters is depicted. Obviously, R_f had little influence on home range and territory sizes. However, if competitor encounters were not learned at all, i.e. $R_f = \infty$ (positive model), the home range size was significantly smaller than for $R_f \leq 3$ for both memory structures (Figure 4.7a; ANOVA: $F_{11,228} = 5.36$, $p < 0.0001$). Though the memory structures did not differ in pairwise comparisons, the effect of the memory structure was revealed by two-way ANOVA (effect of memory structure: $F_{1,228} = 11.12$, $p = 0.001$, and of R_f: $F_{5,228} = 9.08$, $p < 0.0001$).

Comparably, the mean territory size was significantly smaller for $R_f = \infty$ than in the case of $R_f = 0.5$ or 1 if the grid structure was used. No significant differences were found in pairwise comparisons with the graph structure (Figure 4.7b; ANOVA: $F_{11,228} = 4.46$, $p < 0.0001$). Again, the memory structures dif-

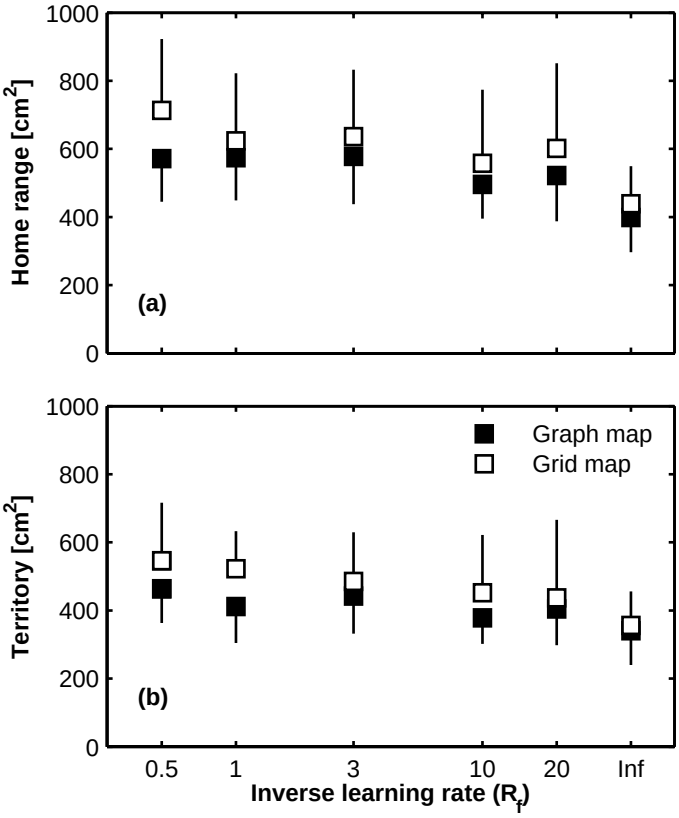

Figure 4.7: Experiment 1. Mean range sizes ($\pm$ SD, $n = 20$) dependent on the inverse learning rate of competitor encounters (R_f). An infinite value of R_f denotes that competitor encounters do not influence the attractiveness value (positive model). Note the logarithmic scaling of R_f. **(a)** Home ranges. **(b)** Territories.

fered significantly (two-way ANOVA, effect of memory structure: $F_{1,228} = 12.09$, $p = 0.0006$, and of R_f: $F_{5,228} = 6.68$, $p < 0.0001$).

Attractiveness increase. In Figure 4.8a, the home range size is shown as a function of R_p, and compared to the range used in the negative model which corresponds to an infinite value of R_p, i.e. only the competitor encounters altered

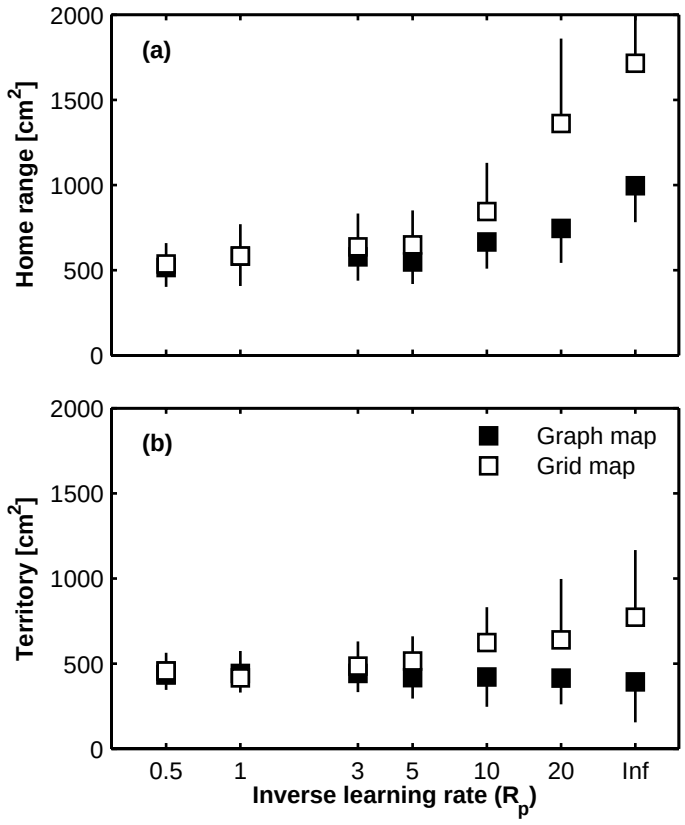

Figure 4.8: Experiment 1. Mean range sizes ($\pm$ SD, $n = 20$) dependent on the inverse learning rate (R_p) of positive visits in the competitive situation. If $R_p = \infty$, only the competitor encounters influence the attractiveness of places, i.e. no learning of place-related information occurs (negative model). Note the logarithmic scaling of R_p. **(a)** Home ranges. **(b)** Territories.

the attractiveness of places (negative model). While the home ranges measured with the graph map did not differ significantly as long as $R_p < 20$, the range increased significantly with increasing value of R_p if the grid map was used. The home ranges obtained by the negative model were significantly larger than those

measured with values of R_p ranging from 0.5 to 20 for both memory structures (ANOVA: $F_{13,266} = 46.37$, $p < 0.0001$). The two structures differed significantly for $R_p = 20$ and the negative model. In both cases, the grid led to higher home range sizes than the graph structure (two-way ANOVA, effect of memory structure: $F_{1,266} = 76.77$, $p < 0.0001$, and R_p: $F_{6,266} = 71.15$, $p < 0.0001$).

Since the overlap increased in proportion to the size of the home range, the area of the territories remained widely stable with decreasing learning rate (Figure 4.8b). Using the grid structure, the territories were significantly larger in the negative model than for $R_p \leq 5$. No significant differences in territory size were found when using the graph structure. This includes the negative model (ANOVA: $F_{13,266} = 6.12$, $p < 0.0001$). In pairwise comparisons, the memory structures only differed significantly for $R_p = 20$ and in the negative model (two-way ANOVA, effect of memory structure: $F_{1,266} = 31.74$, $p = 0.0001$, and R_p: $F_{6,266} = 2.96$, $p = 0.0082$).

Positive model

In the positive model, i.e. if competitor encounters did not influence the attractiveness of places, the learning rate had a similar effect on the individuals' space use as observed in the competitive model (Figure 4.9a). The home range sizes increased with a decreasing learning rate. An infinite value of R_p in the positive model results in random walk since the attractiveness value of a visited place remains unaltered (compare Section 4.6.1). The home ranges established in random walk were significantly larger than with $R_p \leq 20$ (ANOVA: $F_{13,266} = 88.07$, $p < 0.0001$). For the grid structure, the home range sizes additionally differed from each other if $R_p = 10$ and $R_p = 20$, and from the home range sizes measured with lower values of R_p. The memory structures had a significant effect on the home range size if $R_p \geq 10$ (two-way ANOVA, effect of memory structure: $F_{1,266} = 61.66$, $p < 0.0001$, and R_p: $F_{6,266} = 154.15$, $p < 0.0001$).

Again, the territories did not change boldly in size (Figure 4.9b). Only for the grid structure, the territory size reached with $R_p = 20$ significantly exceeded the territory size for $R_p \leq 5$ (ANOVA: $F_{13,266} = 8.44$, $p < 0.0001$). The memory structures only had a significant effect on territory size for $R_p = 20$ (two-way ANOVA, effect of memory structure: $F_{1,266} = 9.76$, $p = 0.002$, and R_p: $F_{6,266} = 12.94$, $p < 0.0001$).

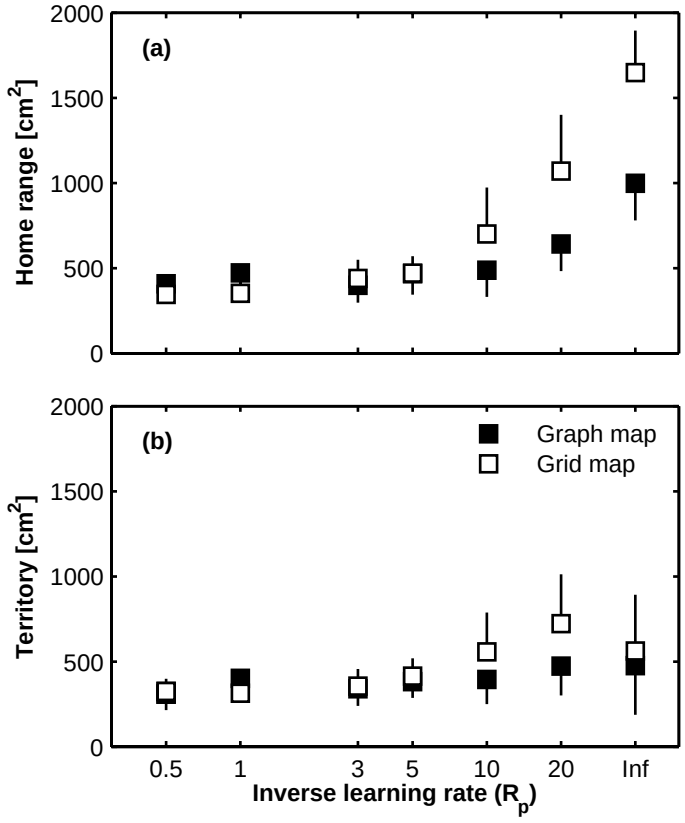

Figure 4.9: Experiment 1. Mean range sizes ($\pm$ SD, $n = 20$) dependent on the inverse learning rate (R_p) in the positive model, i.e. the competitors do not influence the attractiveness value. Here, random walk ($R_p = \infty$) serves as control. Note the logarithmic scaling of R_p. **(a)** Home ranges. **(b)** Territories.

Comparison of learning models

In Figure 4.10, the effects of different learning models are summarised. In the competitive and the positive learning model, the home ranges were notedly smaller than in the negative model and in random walk (Figure 4.10a). However, the territory sizes scarcely differed between the models (Figure 4.10b). Hence, territories,

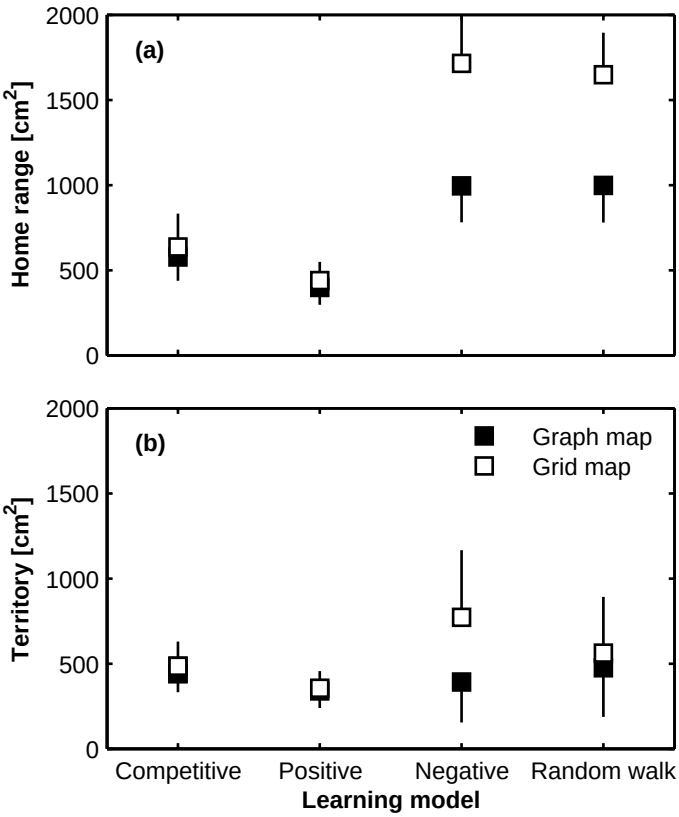

Figure 4.10: Experiment 1. Mean range sizes ($\pm$ SD, $n = 20$) with different models of attractiveness alteration. Data shown for competitive model: $R_p = R_f = 3$; positive model: $R_p = 3$, $R_f = \infty$; negative model: $R_p = \infty$, $R_f = 3$; random walk: $R_p = R_f = \infty$. The learning of positive visits (R_p) influence the range sizes stronger than the learning of fights (R_f). **(a)** Home ranges. **(b)** Territories.

i.e. exclusive ranges, were established with all learning rates applied, but the individuals achieved them by less roaming if they relied on higher learning rates. The learning of positive visits was thereby the crucial factor.

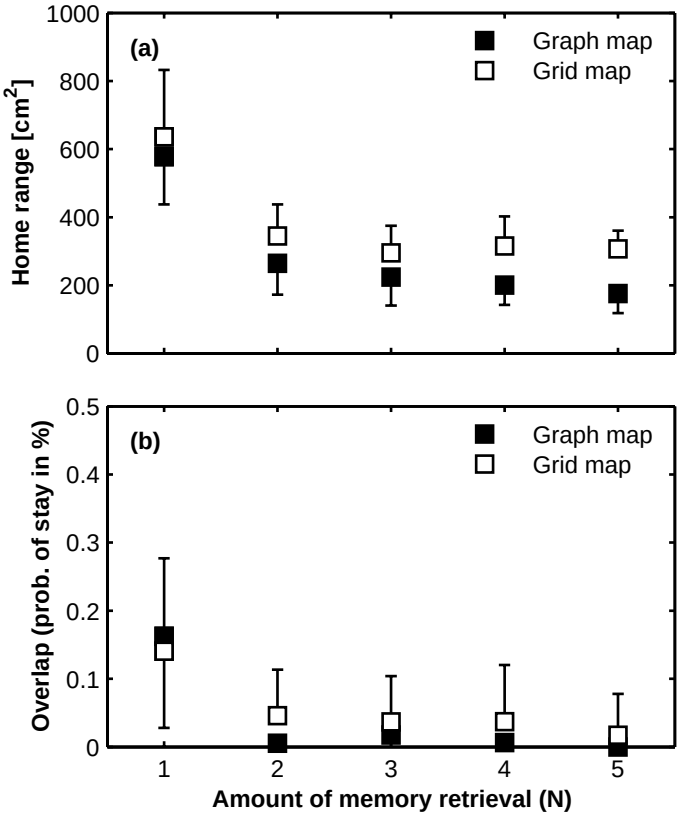

Figure 4.11: Experiment 2. **(a)** Mean home range size ($\pm$ SD, $n = 20$) dependent on the amount of memory retrieval (N). **(b)** Mean part of time (or number of steps) spent in overlap areas ($\pm$ SD, $n = 20$).

4.7.2 Experiment 2: Memory retrieval

If only the immediate neighbours in the memory structure were used for each decision ($N = 1$), the mean area of the home ranges was significantly larger than for all other amounts of memory retrieval tested (Figure 4.11a). No further significant decrease was observed for $N \geq 2$ within the same memory structure (ANOVA:

$F_{9,190} = 44.85$, $p < 0.0001$). For $N = 4$ and $N = 5$, the home ranges formed using the graph structure were significantly smaller than those observable with the grid structure in the same conditions (two-way ANOVA, effect of memory structure: $F_{1,190} = 39.37$, $p < 0.0001$, and of N: $F_{4,190} = 90.18$, $p < 0.0001$).

In conditions with smaller home ranges, the individuals spent less time in overlap areas. For $N = 1$, an average overlap (probability of stay) of $16.2 \pm 13.5\%$ and $14.0 \pm 13.7\%$ with graph and grid memory, respectively, was observed. For all higher N, the overlap approached zero (Figure 4.11b).

4.7.3 Overview: Internal factors

Both parameters of information processing, the learning rate of positive visits (inverse R_p) and the amount of memory retrieval (N), reduced the home range size if increased. In order to investigate how these two factors act together, both were varied simultaneously. In Figure 4.12, the contour lines denote constant home range sizes. Both memory structures are presented separately. The development of the home range size illustrates that the effects of learning rate and memory retrieval can compensate or amplify each other, respectively.

The relation between territory and home range size clarifies the exclusivity of space use (Figure 4.13). The closer the relation approaches 1 (the diagonal in the Figure), the smaller the proportion of overlap relative to the home range. High cognitive abilities, i.e. high learning rates and high memory retrieval, led to the optimisation of this relation.

4.7.4 Experiment 3: Competitor number

Solitary individuals established home ranges even in the absence of competitors. For all numbers of individuals tested, the area of the home ranges did not differ with respect to the memory structure used (two-way ANOVA, effect of memory structure: $F_{1,152} = 0.2$, $p = 0.6551$, and of competitor number: $F_{3,152} = 13.61$, $p < 0.0001$). Increasing competitor numbers resulted in larger home ranges (Figure 4.14a). Solitary individuals established significantly smaller home ranges than individuals in competitive situations with four or eight competitors present in the environment. The home ranges formed if two individuals were set in the arena at a time were significantly smaller than the home ranges with eight competitors (ANOVA: $F_{3,156} = 108.24$, $p < 0.001$).

The territory sizes matched in the solitary condition and with two and four competitors. In the experiments with eight competitors, the largest home ranges

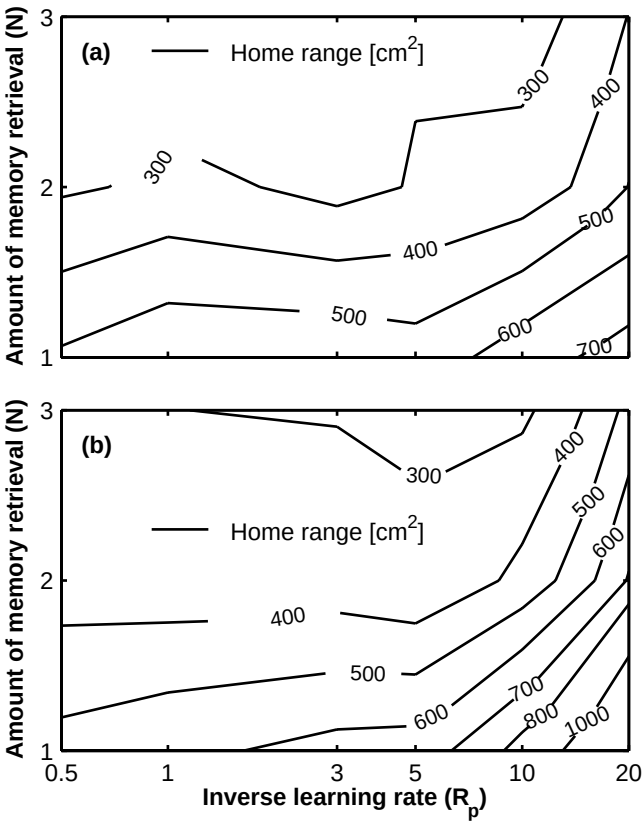

Figure 4.12: Experiment 2. Interaction of the amount of memory retrieval N with the inverse learning rate R_p. The contour lines depict constant home range sizes ($n = 20$). **(a)** Graph structure. **(b)** Grid structure.

were found while the mean territory size was significantly lower than for the other conditions (Figure 4.14b, ANOVA: $F_{3,156} = 60.57$, $p < 0.001$).

The number of steps that fell in an area of overlap increased with the number of individuals in the environment (Figure 4.15). The probability to stay in an overlap area was significantly higher with eight competitors in the environment than with less individuals present. Additionally, the overlap was also higher with four

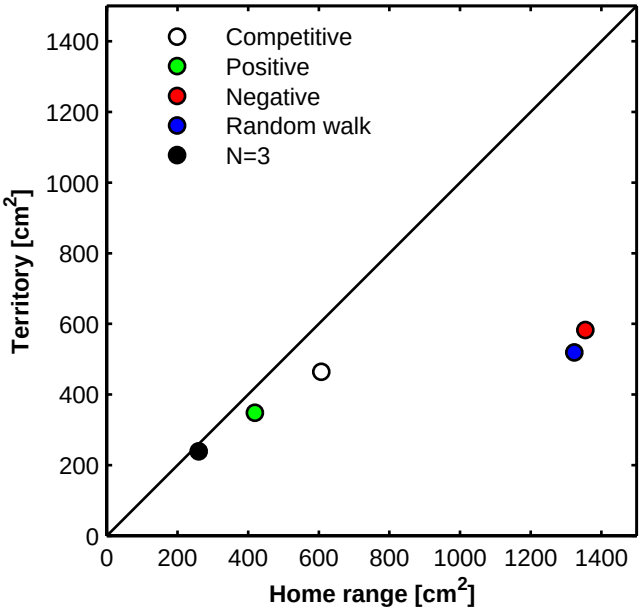

Figure 4.13: Internal factors. Relation between territory and home range sizes. Data of grid and graph structure are pooled. The territory cannot exceed the size of the home range, i.e. all values fall beneath the diagonal. Data points close the diagonal mark cognitive abilities that allow the establishment of highly exclusive ranges. The data from the four learning models in Experiment 1 are depicted as well as the data from an amount of memory retrieval $N = 3$ taken from Experiment 2.

individuals than with two. The overlap with two competitors present in the arena did not differ significantly from zero (ANOVA: $F_{3,156} = 60.57$, $p < 0.0001$).

4.7.5 Experiment 4: Arena size

Instead of reducing the space available per individual by introducing more individuals in the environment, the size of the environment was reduced in the experiments. The mean home range and territory sizes dependent on the arena size are shown in Figure 4.16. The data of grid and graph memory structure were pooled.

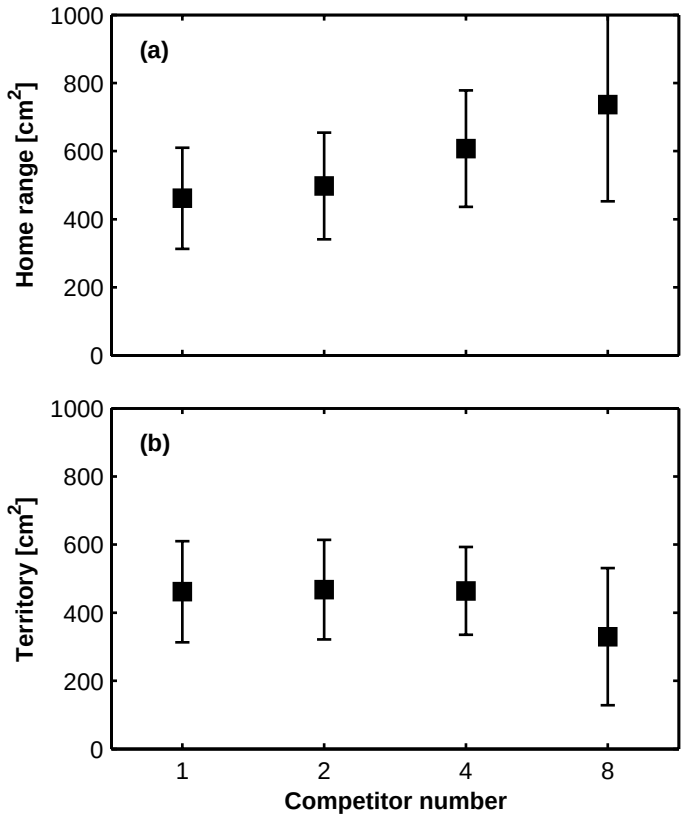

Figure 4.14: Experiment 3. Mean range sizes ($\pm$ SD, $n = 40$) dependent on the competitor number. **(a)** Home range. **(b)** Territory. The data of both memory structures are pooled.

If the individuals could only roam in an area of $0.25m^2$, the mean home range size was significantly reduced compared to an area of $1m^2$ (Figure 4.16a; ANOVA: $F_{2,117} = 5.63$, $p = 0.0046$). The territory size dropped more rapidly, yielding significantly different mean sizes for all three arena sizes (Figure 4.16b; ANOVA: $F_{2,117} = 73.03$, $p < 0.0001$). With $0.25m^2$ available to the four individuals in the environment, the territory sizes were nearly quartered compared to a square meter of space available.

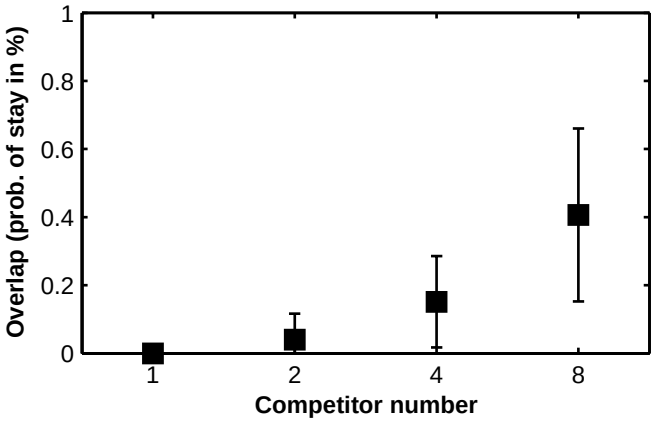

Figure 4.15: Experiment 3. Mean part of time (steps) spent in overlap areas ($\pm$ SD, $n = 40$) dependent on the competitor number. The data of both memory structures are pooled.

Regarding the overlap between the individuals, the probability of staying in an area used by more than one individual was significantly increased in the smallest arena as compared to the other two arena sizes (Figure 4.17; ANOVA: $F_{2,117} = 26.45$, $p < 0.0001$). Note that $0.25m^2$ approximately matches the size of four home ranges as established by solitary individuals in an empty arena (compare Figure 4.14).

4.7.6 Experiment 5: Habitat structuring

In the four different arena layouts tested, the area of the home range did not depend on the memory structure used by the individuals (two-way ANOVA, effect of memory structure: $F_{1,152} = 1.34$, $p = 0.2489$, and of arena layout: $F_{3,152} = 5.46$, $p = 0.0014$). In the case of the quadrant layout of the arena, the robots used significantly smaller ranges than in the empty and centred layouts (Figure 4.18a). The mean home range size in the random layout fell between the values of the other layouts and was not significantly different from any of them (ANOVA: $F_{3,156} = 5.48$, $p = 0.0013$).

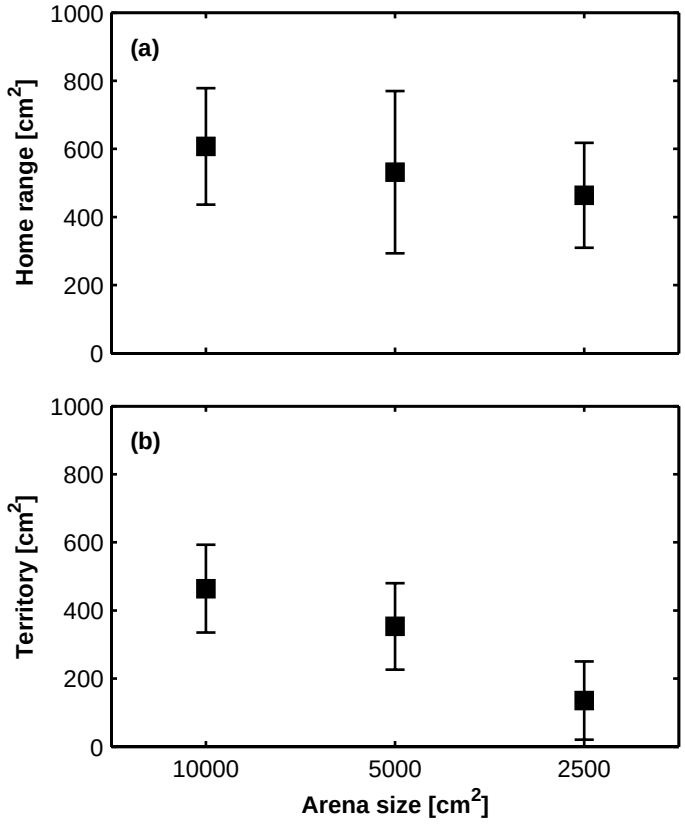

Figure 4.16: Experiment 4. Mean range sizes ($\pm$ SD, $n = 40$) dependent on arena size. **(a)** Home range. **(b)** Territory. The data of both memory structures are pooled.

The time or steps spent in areas of overlap between the home ranges of the individuals was smallest in the quadrant layout of the environment, differing significantly from the highest overlap found in the random layout (Figure 4.18b, ANOVA: $F_{3,156} = 3.86$, $p = 0.0107$). The territory size declined significantly in the random as compared to the empty and centred layouts, the other means did not differ significantly (data not shown, ANOVA: $F_{3,156} = 4.62$, $p = 0.004$).

In the quadrant layout, $91.2\% \pm 13.8\%$ of the home range fell in a single quad-

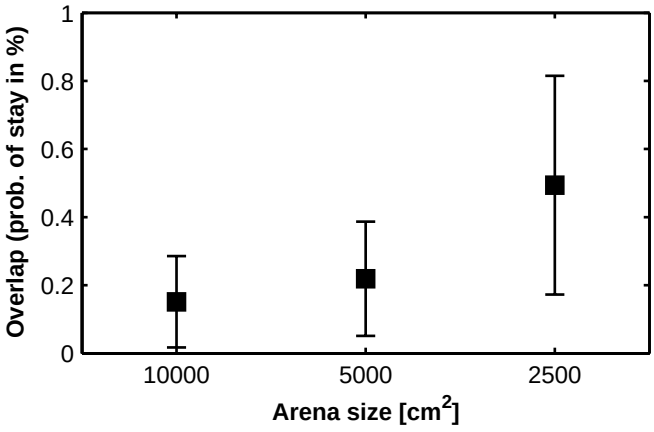

Figure 4.17: Experiment 4. Mean part of time (steps) spent in overlap areas ($\pm$ SD, $n = 40$) dependent on arena size. The data of both memory structures are pooled.

rant, exceeding significantly the means for the other layouts (Figure 4.19, ANOVA: $F_{3,156} = 7.81$, $p < 0.001$). There was no difference found between the memory structures used by the individuals (two-way ANOVA, effect of memory structure: $F_{1,152} = 0$, $p = 0.9693$, and of arena layout: $F_{3,152} = 7.65$, $p = 0.0001$).

4.7.7 Overview: External factors

In Figure 4.20, the relations between territory and home range sizes in the Experiments 3 to 5 are depicted. Highly exclusive ranges fall close to the diagonal. In high population densities, i.e. with eight competitors in the large arena, or four competitors in the smallest arena, the relation vastly deviated from 1. In the other conditions, the individuals approached a high ratio. Note that a solitary individual always reaches a ratio of 1 since it cannot have overlapping areas with other individuals. In the regularly structured quadrant layout, the territories also nearly reached the size of the home ranges.

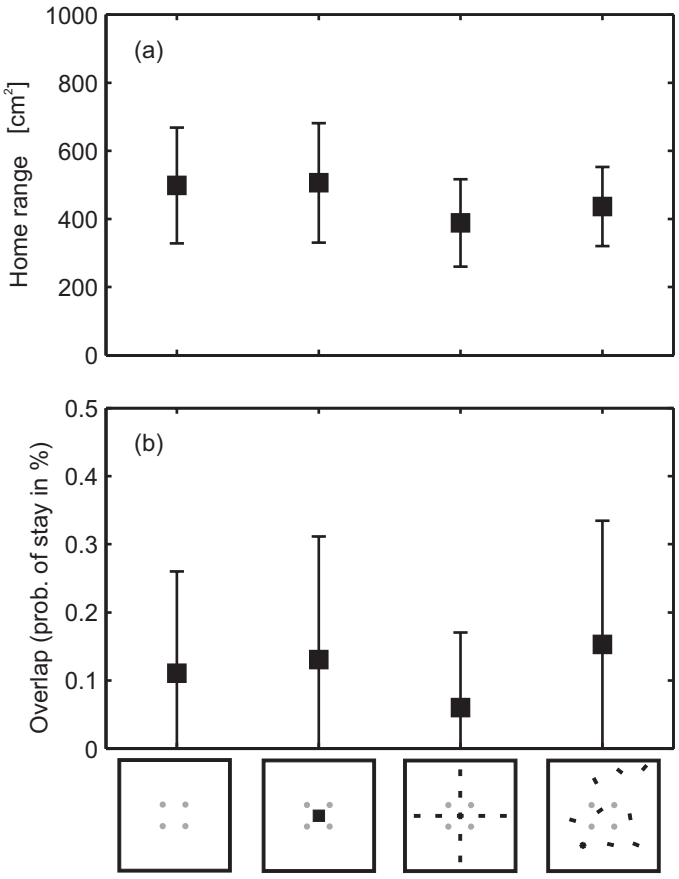

Figure 4.18: Experiment 5. **(a)** Mean home range size ($\pm$ SD, $n = 20$) dependent on the physical structuring of the environment. **(b)** Mean part of time (or number of steps) spent in overlap areas ($\pm$ SD, $n = 20$). The data of five random obstacle layouts is pooled. The data of both memory structures are pooled.

4.7.8 Experiment 6: Residents and newcomers

An individual (the newcomer) was introduced in the environment 1000 steps after the others in the home range of the focal resident. The home range sizes of the residents grew continuously during the experiment. The development of the new-

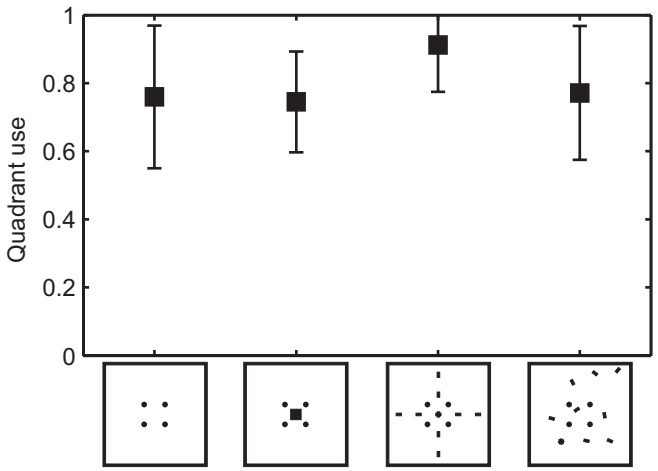

Figure 4.19: Experiment 5. Contribution of the largest part of the home ranges that falls in one of the arena's quadrants (means $\pm$ SD, $n = 40$). The data of five random obstacle layouts is pooled. Data for both memory structures pooled.

comer's home range did not differ from the residents (data not shown). The drift of the home ranges of the newcomer and focal resident did not differ from the other residents. The time spent in overlap areas was increased during the first 200 steps after the introduction of the newcomer (Figure 4.21a).

In the second part of the experiment, the focal resident was first substituted by a newcomer, and reintroduced in the environment later. As seen above, the home range sizes and the drift of the home ranges behaved according to the number of steps accomplished and was not dependent on the treatment. In Figure 4.21b, the overlap during the whole 3000 steps is depicted. The newcomer and the focal resident are highlighted by red and blue markers, respectively. The newcomer had a high probability to roam in overlap areas during the first 200 steps after his introduction, and the overlap was increased when the focal resident was reintroduced. Note that the overlap was also higher during the first 200 steps of each experiment, i.e. when all individuals were naive.

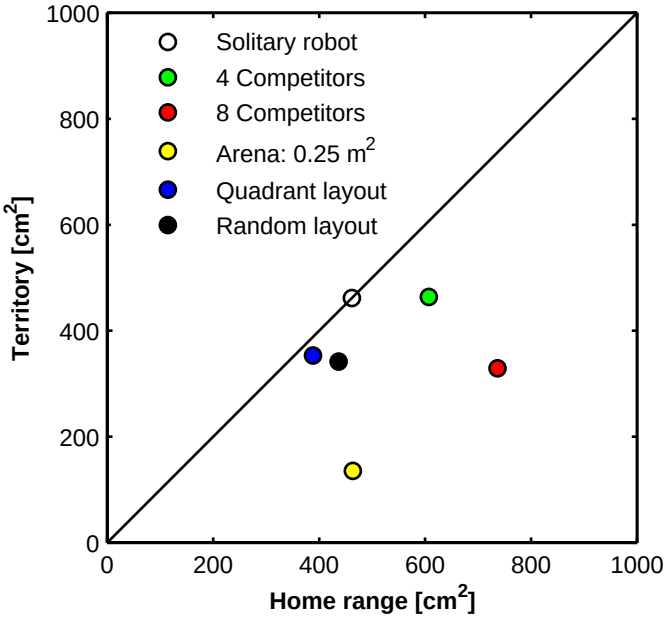

Figure 4.20: External factors. Relation between territory and home range sizes. Data of grid and graph structure are pooled. The territory cannot exceed the size of the home range, i.e. all values fall beneath the diagonal. Data points close the diagonal mark highly exclusive ranges. The data for different population densities (Experiments 3 and 4) as well as environmental structurings (Experiment 5) are shown.

4.7.9 Experiment 7: Long-term experiments

The increase of the whole area visited by the robots was observed over 10000 steps. In Figure 4.22, the overall home range size development in intervals of 1000 steps is presented for two different amounts of memory retrieval, $N = 1$ and $N = 3$. The home ranges did not reach a maximum size even in 10000 time steps. This held true for both memory structures as well as the two values of N applied. The ranges visited if the grid structure was used exceeded the ranges as used applying the graph memory.

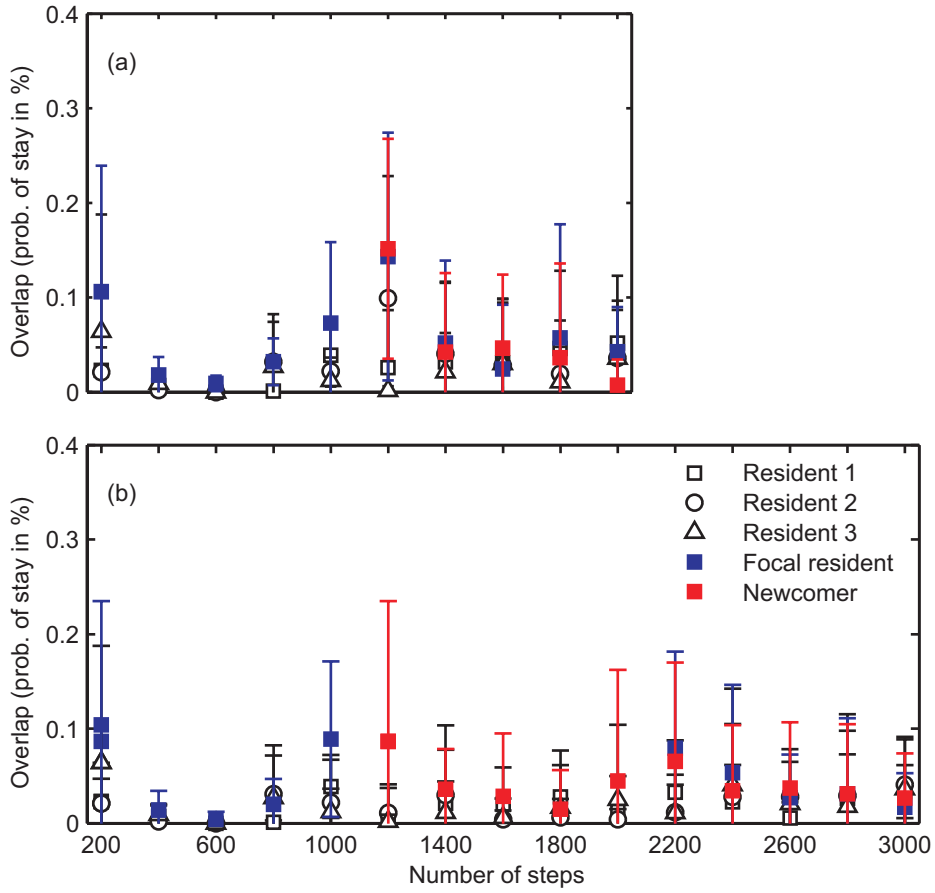

Figure 4.21: Experiment 6. Part of time (means $\pm$ SD, $n = 20$) spent in an area of overlap by individuals introduced in the arena at different times. **(a)** Four individuals established home ranges during 1000 steps. Afterwards, a newcomer is introduced in the home range area of a focal resident. **(b)** Four individuals accomplished 1000 steps. Then, one resident was substituted by a newcomer. The previously removed focal resident was reintroduced at its last position after another 1000 steps.

The probability that an individual will stay in previously explored areas was significantly higher for $N = 3$ than for $N = 1$ (Table 4.2; paired t-test: $p < 0.0001$

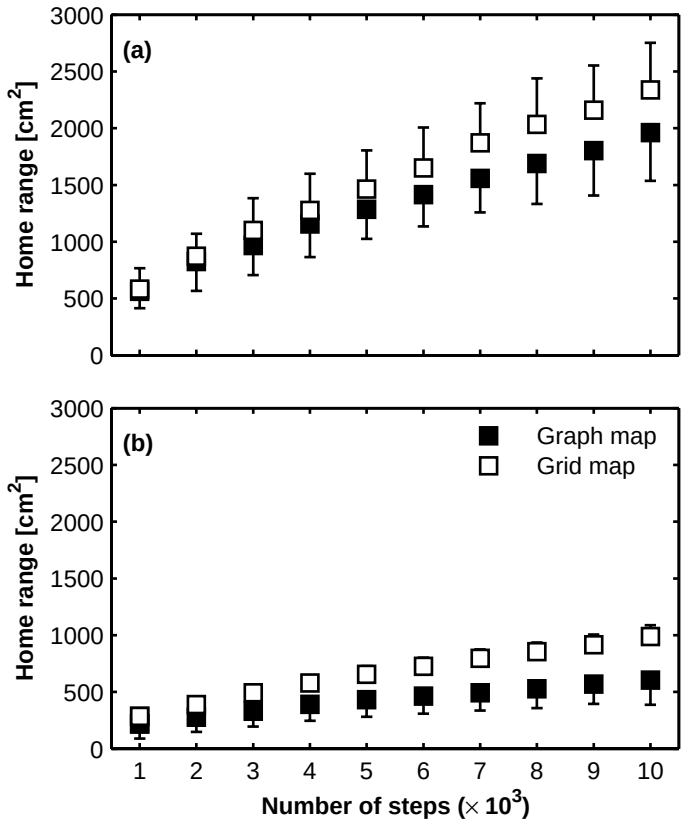

Figure 4.22: Experiment 7. Mean home range size ($\pm$ SD, $n = 20$) observed over 10000 steps. **(a)** Amount of memory retrieval $N = 1$. **(b)** $N = 3$.

for grid and for graph structure). Note that the variance of the probability of stay also dropped for $N = 3$ as compared to $N = 1$. The range used during an interval of 200 steps initially increased. After 5000 steps, it reached a constant value in all conditions tested.

Table 4.2: Experiment 7. Probability (means $\pm$ SD) that an individual will revisit previously explored places during 10000 steps.

	Grid structure	Graph structure
$N = 1$	$0.88\% \pm 0.17\%$	$0.88\% \pm 0.18\%$
$N = 3$	$0.96\% \pm 0.04\%$	$0.97\% \pm 0.08\%$

4.8 Discussion

4.8.1 Learning rate

In the simulation, the individuals learned about their environment by building up a spatial representation associated with a notion of the quality of the places, i.e. the attractiveness of the places (compare Chapter 3; Schmolke and Mallot, 2002b). The attractiveness value was changed according to the experiences at the place and could either increase due to repeated positive visits or decrease if a competitor was encountered (Experiment 1).

Attractiveness decline. The learning rate of competitor encounters had a low impact on the individuals' space use. However, if the encounters had no influence on the attractiveness of places, home range and territory sizes decreased. Thus, the learning of negative incidents did play an important role in the model while the learning rate was of low influence. Unknown areas of the environment were designated with a low attractiveness value. Most encounters with competitors occurred in previously unknown areas. Thus, the initially low attractiveness value approached zero upon the first encounter independent of the learning rate R_f. The corresponding place was subsequently avoided. Comparably, in the model presented by Stamps and Krishnan (1999), a low influence of R_f on home range and territory size was found.

Stamps and Krishnan (1999) assumed that the division of space develops due to the avoidance of the interference competition. However, the model might even apply if only exploitation competition is at work. The presence of another individual can be used as marker for reduced resource availability. Hence, the area is avoided or, in terms of the model, is assigned with a decreased attractiveness. The interaction itself is not modelled and not essential for the division of space between the individuals.

Attractiveness gain. In contrast to the learning rate of negative incidents, the learning rate of positive incidents has a strong influence on the individuals' space use. The home ranges of the simulated agents decreased if they learned at a higher rate. If the attractiveness values remained completely unaltered due to positive visits (negative model), the ranges were two to three times larger than with fast learning of positive incidents. In contrast, the area used exclusively remained mostly stable over different learning rates (Schmolke and Mallot, submitted).

If the influences of competitor encounters were excluded, i.e. the attractiveness value only changed due to positive visits, similar results were obtained. In this positive model of learning, the home range and territory sizes were persistently smaller than in the competitive model. Both positive and competitive learning model revealed a similar development of the range sizes: decreasing learning rates resulted in increasing home range sizes and fairly constant territory sizes. Thus, a higher learning rate (inverse R_p) allowed the individuals to achieve an exclusive area of similar size with distinctly reduced amount of roaming. The comparison of the different learning models clarifies the relation between home range size and territory size (see Figures 4.10 and 4.13). These findings of the simulation are in accordance with the model analysis of Stamps and Krishnan (1999). They also described clearly increased range sizes if no learning took place.

Especially with low learning rates (high values of R_p), the space used by single individuals was frequently disjoint, i.e. the individuals shifted their space use. Previously explored areas could become unreachable for an individual if the link between them and the individual's current position was designated with attractiveness values close to zero. Nevertheless, those areas were not prone to forget, but remained unaltered in memory. The sequence of events at the places was not stored, filling the memory with the information independent of the time passed since the information was obtained.

The effects of learning in the model suggest a fitness gain due to fast learning. However, a moderate learning rate leads mostly to similar results as a high learning rate.

4.8.2 Memory retrieval

The agents in the model retrieved different amounts of information from memory for each decision (Experiment 2). In the lowest amount of memory retrieval, only the information associated to the places reachable in the next step provided the basis for the decision. With higher amounts of memory retrieval, the information of more distant nodes was additionally taken into account. As soon as each decision

was based on more than the most proximate information, the home ranges drastically decreased in size. The overlap between the ranges of the competitors nearly vanished. Inclusion of more memorised information in the decision processes did not provoke further changes in space use (Schmolke and Mallot, submitted).

The effect of memory retrieval is thus comparable to the effect of learning rate. In both cases, the space use became more confined with higher information processing. The alteration is most pronounced if low is compared to medium information processing. The two cognitive factors could be balanced out (compare Figure 4.12).

The simulated memory retrieval can be compared to the working memory capacity of animals. In a model of optimal foraging, Bélisle and Cresswell (1997) revealed that the capacity of the working memory strongly influenced the foraging success. In my model, a higher memory retrieval allows the individuals to keep track of a previously explored area even if they moved out of it recently.

4.8.3 Population density

With an increasing number of competitors, the individuals in the model had difficulties to stabilise areas of high attractiveness (compare Figure 3.8 and 3.9). This consequence of the model implicitly simulates the decreasing reward of defending a territory in the presence of an increasing number of competitors. Indeed, the individuals roaming solitarily in the environment used a more confined area than individuals in competitive situations. The individuals stabilised their exclusively used area until the intruder pressure became too high (Experiment 3; Schmolke et al., 2004; Schmolke and Mallot, submitted). Similar results were also obtained in the model without spatial memory (Stamps and Krishnan, 1999).

This alteration of space use can be compared to the conditional territoriality in bellbirds (Craig and Douglas, 1986). However, my simulation does not necessarily assume competition through interference of the individuals. As discussed above, encounters with competitors might merely repel the individuals from the corresponding area. This is only possible as long as enough space is available to the individuals in order to avoid each other. Otherwise, no exclusive areas can be obtained anymore as it is the case in conditional territoriality. In addition, the fidelity to a confined area is less worthwhile since, for instance, food availability becomes unpredictable. The larger home ranges may reflect such decreased benefit of site fidelity.

The increase in population density was also simulated by reducing the available space (Experiment 4). In this case, the home ranges slightly decreased while the

territories showed a sharp decline with shrinking size of the environment. Comparably to rising population density due to a higher competitor number, the overlap between the home ranges increased. Thus, the conclusions drawn from the increasing competitor number also apply for a decreasing arena size. However, in a small arena, the individuals additionally often approached the arena walls. The avoidance of the competitors was thus aggravated, and the territory sizes even shrank faster than in larger environments.

4.8.4 Habitat structuring

Due to the explicit modelling of the individuals with their sensors and of the environment, it was possible to test the influences of the structuring of the physical environment on the individuals' space use (Experiment 5). In the environment depicted in Figure 4.6c, the robots confined their space use according to regularly arranged obstacles. The overlap with the competitors' ranges approached zero (Schmolke et al., 2004; Schmolke and Mallot, submitted).

The internal representation of the environment allowed the individuals to adjust their space use according to the physical structuring of the environment. Similar effects were shown in animal experiments (Eason and Stamps, 1992; Eason et al., 1999; LaManna and Eason, 2003). However, only landmarks or visual barriers were provided in the animal experiments while my agents had to face physical obstacles. In order to test the influence of landmarks, vision and visual memory should be introduced in my model.

The alignment of territorial boundaries according to external cues allows the memorisation of the boundary locations by comparably simple rules. No metric information would have to be included in the internal spatial representation. As discussed in Section 3.7, a graph-like memory structure would allow the establishment of territories without explicit representation of metric distances. The border locations of the territories could be recognised by characteristic visual cues or even due to simple rules (as the encounter of an obstacle), and thus, no metric position information about the border location has to be memorised. This would reduce the complexity of the memory. The usage of simple rules for the establishment of territory borders has been proposed by Mesterton-Gibbons and Adams (2003). The conventional borders sites do not only demand comparably low information processing abilities, but also reduce the investment in the establishment and maintenence of the boundaries.

4.8.5 Territory dynamics

The introduction of a newcomer in an environment already inhabited by residents did not result in distinct disadvantages for the newcomer (Experiment 6). In European robins, a resident advantage could be found in the contest for a patch. Tobias (1997) removed individuals from their territories for varying periods of time. The territory was mostly immediately claimed by another bird. The former resident was able to reclaim its territory if reintroduced after a few days. In my model, both the newcomer and the resident are able to maintain their ranges. No individual could actually be driven out of the experimental arena, instead the competitors were able to avoid each other.

If the simulation was run for a long period, i.e. 10000 steps, the home ranges of the residents still did not reach a maximum size (Experiment 7). About 12% of the individuals' steps were visits to previously unknown areas. With an increased amount of memory retrieval ($N = 3$), those visits were reduced to less than 5%. Since unknown areas were associated with an attractiveness above zero, visits to unknown areas occurred. The results of the long-term experiments suggest a constant drift of the activity range of the individuals while the range used during a fixed time interval remained stable. Analysed over the whole experiment, the home ranges grew constantly. This reflects the information content of the spatial memory of the individuals since no forgetting has been modelled.

White et al. (1996) presented a model of wolf territoriality including a den site and border markings as it is the case in wolfs during the breeding of the pubs. However, if the den site was removed from the model, simulating the winter condition when the young wolfs join the pack, the pack was moving more extensively through the territory. The buffer zone between the territories of two packs was more likely to be entered. Thus, a den site is a strong factor in order to prevent the drift of the activity range. Additionally, landmarks might come into play. As discussed above, landmarks provide reliable cues for the localisation of the territory borders. In my experiments, the individuals were not bound to a certain site, and the territory borders could not be settled according to external cues.

Chapter 5

Conclusions and outlook

5.1 Conclusions

Territorial behaviour is based on the ability of spatial learning. An individual has to assess its own position, and associate it with experiences gathered at this place before. Additionally, it has to learn the relations between places. In order to solve these problems, animals rely both on measurements of egomotion and on external position cues. I introduced a path integration system which can be used as an estimate of the own position in relation to a starting point. The accuracy of the system was increased by combining it with a polarisation compass as external orientation measurement. Compass orientation using the polarisation pattern of the sky or other means are common in animals. The polarisation compass is a solution applicable to miniature robots due to its low claim in energy supply, number of sensors, and size.

For the exploration of an area without a defined spatial goal, as it is the case in territoriality, the information gathered has to be included in a memory structure wherein the relations of the known places are represented. Such a spatial memory is usually referred to as cognitive map. I presented two different possible realisations of a map-like spatial memory. In both memory structures, position information and non-spatial information was stored. With both memory structures, the individuals were able to establish territories. The simulation approach allowed the comparison of the internal state of the individuals with their behaviour. The grid structure claims a higher memory capacity since the whole available space is represented, including unknown places. In contrast, only known places appear in the graph memory which leads to lower computational costs. Though initially designed for

way-finding tasks, the graph representation is suited as basis for territoriality, and, additionally, provides the advantage of reduced computational costs as compared to the grid.

In addition to the two different structures of the spatial memory, the individuals relied on varying learning rates as well as amounts of information retrieved from memory for each movement decision. These cognitive factors strongly influenced the space use of the individuals. Faster learning and higher memory retrieval led to more compact territories and less overlapping space use of the competitors. However, this development was not linear, but flattened when reaching high extends. Thus, as soon as cognitive abilities can sustain a behaviour, they should not be refined any further in animals. Instead, according to the model, very high cognitive performances claim high computational power, but do not result in a distinctly improved behavioural performance.

Solitary individuals had more compact territories than individuals in competitive situations. As soon as an individual could establish an area of high attractiveness, visits outside this area have a low probability. However, if strongly disturbed by competitors, i.e. frequent attractiveness reductions, the individuals had to switch to other areas. In high population densities, this resulted in high overlap areas between the individuals and small territories. The competition could be tempered by the introduction of obstacles in the environment that predefined territory boundaries. Regularly arranged obstacles that left enough space for the formation of a territory between them reduced the overlap between the individual ranges. The individuals tended to stay in the areas predefined by the obstacles.

The model assumes that every patch of the environment yields the same fitness value for the individuals. However, fitness and resources were not explicitely modelled. Thus, the individuals did not have to cover a minimal area in order to maintain their energy intake. Fights only are implicitly modelled by the loss of attractiveness, but do not influence subsequent interactions. The individuals are assumed to have similar resource holding potentials, resulting in fights between equal competitors. Stamps and Krishnan (2001) included asymmetric fights in their model. Highly aggressive individuals were able to claim larger ranges. Nonetheless, the basic results of the model were comparable to the results gained with the assumption of equal competitors.

The inclusion of resource availability and fighting costs would allow to measure the efficiency of space use directly by the fitness of the individuals. Using a game-theoretic approach, different strategies of territory establishment could be introduced in a population. The factors determining a strategy as evolutionary sta-

ble could thus be derived. Morrell and Kokko (2005) presented a two-dimensional model of territory formation, and determined evolutionary stable strategies under different conditions, e.g., varying costs of fights.

The inclusion of forgetting in the simulation would implicate a more parsimonious memory. Places visited at least once are represented in the memory even if they got out of the reach of the individual. On the other hand, areas labelled as unattractive due to competitor encounters are lost for the individual forever although the competitor might have left the area.

Nonetheless, I observed steady territory sizes over a wide range of parameters tested in the model. Opposite to the stability of the exclusively used range, the non-exclusively used area was strongly affected by internal and external influences. An increased area of overlap is equivalent to stronger competition and to increased travel distances due to the growth of the whole range. Hence, the model shows that simple information processing mechanisms can account for the establishment and maintenence of efficient space use although the underlying ultimate causes, i.e. fitness and resource availability, were not modelled.

The model shows that behaviour is strongly influenced by the underlying cognitive abilities. The simulation approach allowed the manipulation of specified information processing abilities independent of other characteristics of the individuals and the environment. The consideration of such abilities is important in order to judge optimality of behaviour. It can be neither assumed that animals are able to assess all information relevant for their decisions nor that they use the information available to them completely. Additionally, a high amount of information used for decisions does not appear to increase the efficiency of behaviour markedly compared to an intermediate information use.

In summary, the simulation suggests a graph-like spatial memory as basis of territorial behaviour. The cognitive abilities underlying behaviour should be expected to be modularly adapted to the animal's ecological niche. A medium amount of information processing as needed for the behaviour would thereby be most favourable in order to save neuronal complexity. The cognitive abilities are crucial for the understanding of animal behaviour. It cannot be assumed that animals assess or use all information available to them. This holds true from the sensors to highly abstract cognitive processing. Instead of admitting thoroughly as much information in their decisions as possible, it might very frequently suffice for animals to follow more or less simple rules in order to achieve a behaviour that roughly approaches optimality.

5.2 Outlook

As I pointed out above, the simulation could be made more realistic by adding certain aspects. First, the robots in the simulation do not navigate completely autonomously. The combination of a visual system with the presented path integration system would allow them to built their internal representation exclusively with information gathered through realistic sensory systems. This includes the detection of the competitors. The graph formation based on visual homing and metric information from path integration presented by Hübner and Mallot (2002) will be used for such an approach. First tests with this extended simulation were successful. The autonomous navigation would allows to quantify the influences of imperfect information on the behaviour. Additionally, whether environmental cues can be efficiently used as locations of boundaries could be tested more thoroughly.

A second improvement to the model would be the inclusion of a forgetting function. Forgetting would imply that the sequence of events at a place plays a role. The attractiveness values of places visited a long time ago would slowly approach the default attractiveness of unknown places again. In the graph representation, such places would even be prone to be forgotten completely, i.e. they would disappear from memory. Forgetting should follow an exponential function (Rubin and Wenzel, 1996; White, 2002) which would be applied to the attractiveness value in my simulation. With the forgetting, the individuals would further decrease the memory claim of the graph representation. Additionally, I would expect that the individuals show a higher place fidelity since they rely more on recently collected information at places closer to the current position than information about places visited long ago.

The encounters between competitors are assumed to end in a draw, i.e. the individuals all display the same fighting abilities. This is usually not the case in animals. Thus, as a third point, asymmetrical fights should be included in the simulation. This would imply that individuals with higher fighting abilities should gain more space, and "defend" their territory more effectively. In the simulation, this would mean that their territories are less influenced by competitors, and thus, the space use of the "stronger" individuals should show a lower drift, or be more compact, respectively, under the pressure of competitors.

As a fourth point, the inclusion of the individual fitness would allow predictions about the most successful spatial strategies underlying territorial behaviour. The individuals would loose energy over time, fights would additionally reduce their strength. In order to compensate this loss, they would have to collect resources. Such resources would be explicitely modelled, and, accordingly, could be

dispersed variably in the environment. The relation between minimal territory sizes and population densities would become predictable with the model. The effects of exploitation and interference competition would become separable by varying the costs of fights (as compared to the positive and competitive learning model of the attractiveness in the current version of the simulation; compare Chapter 4). The performance of cognitive abilities could be rated according to the abilities of the individuals to establish and maintain exclusive ranges, or by their fitness value. Including also costs for the cognitive machinery, evolutionary stable strategies of spatial cognition within territoriality could be determined.

Bibliography

Adams ES, 1998. Territory size and shape in fire ants: A model based on neighborhood interactions. Ecology 79:1125–1134.

Adams ES, 2001. Approaches to the study of territory size and shape. Ann Rev Ecol Syst 32:277–303.

Aiello LC, Wheeler P, 1995. The expensive-tissue hypothesis: the brain and the digestive system in human and primate evolution. Curr Anthropol 36:199–221.

Arbib MA, Lieblich I, 1977. Motivational learning of spatial behavior. In: Systems neuroscience (Metzler J, ed.), New York: Academic Press. 221–239.

Arkin RC, 1989. Motor schema-based mobile robot navigation. Int J Robot Res 8:92–96.

Armstrong DP, 1992. Correlation between nectar supply and aggression in territorial honeyeaters: causation or coincidence? Behav Ecol Sociobiol 30:95–102.

Beecher MD, Campbell SE, Nordby JC, 1998. The cognitive ecology of song communication and song learning in the song sparrow. In: Cognitive Ecology: The Evolutionary Ecology of Information Processing and Decision Making (Dukas R, ed.), Chicago: University of Chicago Press, chap. 5. 175–199.

Begon M, Harper JL, Townsend CR, 1990. Ecology: Individuals, Populations, and Communities. Blackwell Scientific.

Bélisle C, Cresswell J, 1997. The effects of a limited memory capacity on foraging behavior. Theor Popul Biol 52:78–90.

Benhamou S, Seguinot V, 1995. How to find one's way in the labyrinth of path integration models. J theor Biol 174:463–466.

Bennett ATD, 1996. Do animals have cognitive maps? J Exp Biol 199:219–224.

Bolhuis JJ, Macphail EM, 2001. A critique of the neuroecology of learning and memory. Trends Cogn Sci 5:426–433.

Borenstein J, Everett HR, Feng L, Wehe D, 1997. Mobile robot positioning: Sensors and techniques. J Robotic Syst 14:231–249.

Borenstein J, Feng L, 1994. Umbmark - a method for measuring, comparing, and correcting dead-reckoning errors in mobile robots. Tech. Rep. UM-MEAM-94-22, University of Michigan.

Borenstein J, Feng L, 1996. Measurement and correction of systematic odometry errors in mobile robots. IEEE T Robotic Autom 12:869–880.

Both C, Visser ME, 2000. Breeding territory size affects fitness: an experimental study on competition at the individual level. J Anim Ecol 69:1021–1030.

Both C, Visser ME, 2003. Density dependence, territoriality, and divisibility of resources: From optimality models to population processes. Am Nat 161:326–336.

Bradbury JW, 1977. Lek mating behavior in the hammer-headed bat. Z Tierpsychol 45:225–255.

Braitenberg V, 1984. Vehicles. Experiments in Synthetic Psychology. MIT Press, Cambridge, Mass.

Brown WM, 2001. Natural selection of mammalian brain components. Trends Ecol Evol 16:471–473.

Burt WH, 1943. Territoriality and home range concepts as applied to mammals. J Mammal 24:346–352.

Cartwright BA, Collett TS, 1983. Landmark learning in bees. experiments and models. J Comp Physiol A 151:521–543.

Cartwright BA, Collett TS, 1987. Landmark maps for honeybees. Biol Cybern 57:85–93.

Chapman MR, Kramer DL, 1996. Guarded resources: the effect of intruder number on the tactics and success of defenders and intruders. Anim Behav 52:83–94.

Chelazzi G, 1992. Reptiles. In: Animal homing (Papi F, ed.), London: Chapman and Hall, chap. 6. 235–261.

Clarke MF, Dasilva KB, Lair H, Pockington R, Kramer DL, McLaughlin R, 1993. Site familiarity affects escape behaviour of the eastern chipmunk *Tamias striatus*. Oikos 66:533–537.

Colombo M, Broadbent NJ, Taylor CSR, Frost N, 2001. The role of the avian hippocampus in orientation in space and time. Brain Res 919:292–301.

Craig JL, Douglas ME, 1986. Resource distribution, aggressive asymmetries and variable access to resources in the nectar feeding bellbird. Behav Ecol Sociobiol 18:231–240.

Davies NB, 1978. Territorial defense in the speckled wood butterfly (*Pararge aegeria*): the resident always wins. Anim Behav 26:138–147.

Dukas R, ed., 1998a. Cognitive Ecology: The Evolutionary Ecology of Information Processing and Decision Making. Chicago: University of Chicago Press.

Dukas R, 1998b. Evolutionary ecology of learning. In: Cognitive Ecology: The Evolutionary Ecology of Information Processing and Decision Making (Dukas R, ed.), Chicago: University of Chicago Press, chap. 4. 129–174.

Dukas R, 1999. Costs of memory: ideas and predictions. J theor Biol 197:41–50.

Dukas R, 2004. Evolutionary biology of animal cognition. Annu Rev Ecol Evol Syst 35:347–374.

Dyer FC, 1991. Bees acquire route-based memories but not cognitive maps in a familiar landscape. Anim Behav 41:239–246.

Eason PK, Cobbs GA, Trinca KG, 1999. The use of landmarks to define territorial boundaries. Anim Behav 58:85–91.

Eason PK, Stamps JA, 1992. The effect of visibility on territory size and shape. Behav Ecol 3:166–172.

Elfes A, 1987. Sonar-based real-world mapping and navigation. IEEE J Robotic Autom 3:249–265.

Etienne AS, Maurer R, Seguinot V, 1996. Path integration in mammals and its interaction with visual landmarks. J Exp Biol 199:201–209.

Flombaum JI, Santos LR, Hauser MD, 2002. Neuroecology and psychological modularity. Trends Cogn Sci 6:106–108.

Franz MO, Mallot HA, 2000. Biomimetic robot navigation. Robot Auton Syst 30:133–153.

Franz MO, Schölkopf B, Mallot HA, Bülthoff HH, 1998a. Learning view graphs for robot navigation. Auton Robot 5:111–125.

Franz MO, Schölkopf B, Mallot HA, Bülthoff HH, 1998b. Where did I take that snapshot? Scene-based homing by image matching. Biol Cybern 79:191–202.

Franz NM, Wcislo WT, 2003. Foraging behavior in two species of *Ectatomma* (Formicidae: Ponerinae): individual learning of orientation and timing. J Insect Behav 16:381–410.

Freake MJ, 2001. Homing behaviour in the sleepy lizard (*Tiliqua rugosa*): the role of visual cues and the parietal eye. Behav Ecol Sociobiol 50:563–569.

von Frisch K, 1965. Tanzsprache und Orientierung der Bienen. Berlin, Heidelberg: Springer-Verlag.

Gallistel CR, 1990. The organization of learning. Cambridge, MA: MIT Press.

Getty T, 1987. Dear enemies and the prisoner's dilemma: Why should territorial neighbors form defensive coalitions? Am Zool 27:327–336.

Giraldeau LA, 1997. The ecology of information use. In: Behavioural Ecology: An Evolutionary Approach (Krebs JR, Davies NB, eds.), Oxford: Blackwell Science, chap. 3. 4th ed., 42–68.

Gordon DM, 1989. Ants distinguish neighbors from strangers. Oecologia 81:198–200.

Gould JL, 1980. Sun compensation by bees. Science 207:545–547.

Gould JL, 1986. The locale map of honey bees: Do insects have cognitive maps? Science 232:861–863.

Grant JWA, Gaboury CL, Levitt HL, 2000. Competitor-to-resource ratio, a general formulation of operational sex ratio, as a predictor of competitive aggression in Japanese medaka (Pisces: Oryziidae). Behav Ecol 11:670–675.

Grimm V, 1999. Ten years of individual-based modelling in ecology: what have we learned and what could we learn in the future? Ecol Model 115:129–148.

Haefner JW, Crist TO, 1994. Spatial model of movement and foraging in harvester ants (*Pogonomyrmex*) (I): The roles of memory and communication. J theor Biol 166:299–313.

Hampton RR, Sherry DF, Shettleworth SJ, Khurgel M, Ivy G, 1995. Hippocampal volume and food-storing behavior are related in parids. Brain Behav Ecol 45:54–61.

Healy S, 1992. Optimal memory: toward an evolutionary ecology of animal cognition? Trends Ecol Evol 7:399–400.

Healy S, Braithwaite V, 2000. Cognitive ecology: a field of substance? Trends Ecol Evol 15:22–26.

Healy S, de Kort SR, Clayton NS, 2005. The hippocampus, spatial memory and food hoarding: a puzzle revisted. Trends Ecol Evol 20:17–22.

Healy SD, Hurly TA, 1995. Spatial memory in rufous hummingbirds (*Selsphorus rufus*)–a field test. Anim Learn Behav 23:63–68.

Heinze J, Foitzik S, Hippert A, Hölldobler B, 1996. Apparent dear-enemy phenomenon and environment-based recognition cues in the ant *Leptothorax nylanderi*. Ethology 102:510–522.

Hölscher C, 2003. Time, space and hippocampal functions. Rev Neurosci 14:253–284.

Hübner W, Mallot HA, 2002. Integration of metric place relations in a landmark graph. In: ICANN 2002, LNCS 2415 (Dorronsoro JR, ed.). Springer-Verlag Berlin Heidelberg, 825–830.

Jacobs LF, 2003. The evolution of the cognitive map. Brain Behav Evol 62:128–139.

Jacobs LF, Gaulin SJC, Sherry DF, Hoffman GE, 1990. Evolution of spatial cognition: Sex-specific patterns of spatial behavior predict hippocampal size. Proc Natl Acad Sci USA 87:6349–6352.

Jacobs LF, Schenk F, 2003. Unpacking the cognitive map: the parallel map theory of hippocampal function. Psych Rev 110:285–315.

Jerison HJ, 2001. The evolution of neural and behavioral complexity. In: Brain evolution and cognition (Roth G, Wullimann MF, eds.), New York: Wiley, chap. 18. 523–553.

Judson OP, 1994. The rise of the individual-based model in ecology. Trends Ecol Evol 9:9–14.

Kawata M, 1997. Exploitative competition and ecological effective abundance. Ecol Model 94:125–137.

Kerth G, Wagner M, König B, 2001. Roosting together, foraging apart: information transfer about food is unlikely to explain sociality in female bechstein's bats (*Myotis bechsteinii*. Behav Ecol Sociobiol 50:283–291.

Kirschfeld K, 1972. Die notwendige Anzahl von Rezeptoren zur Bestimmung der Richtung des elektrischen Vektors linear polarisierten Lichts. Z Naturforsch 27 b:578–579.

Knaden M, Wehner R, 2003. Nest defense and conspecific enemy recognition in the desert ant *Cataglyphis fortis*. J Insect Behav 16:717–730.

Kuipers B, 2000. The spatial semantic hierarchy. Artif Intell 119:191–233.

Labhart T, 1980. Specialized photoreceptors at the dorsal rim of the honeybee's compound eye: Polarizational and angular sensitivity. J Comp Physiol A 141:19–30.

LaManna JR, Eason PK, 2003. Effects of landmarks on territorial establishment. Anim Behav 65:471–478.

Lambrinos D, Möller R, Labhart T, Pfeifer R, Wehner R, 2000. A mobile robot employing insect strategies for navigation. Robot Auton Syst 30:39–64.

Langen TA, Tripet F, Nonacs P, 2000. The red and the black: habituation and the dear-enemy phenomenon in two desert *Pheidole* ants. Behav Ecol Sociobiol 48:285–292.

Laverty TM, Plowright RC, 1988. Flower handling by bumblebees: a comparison of specialists and generalists. Anim Behav 36:733–740.

Lewis MA, White KAJ, Murray JD, 1997. Analysis of a model for wolf territories. J Math Biol 35:749–774.

Macphail EM, Bolhuis JJ, 2001. The evolution of intelligence: adaptive specializations *versus* general process. Biol Rev 76:341–364.

Maher CR, Lott DF, 1995. Definitions of territoriality used in the study of variation in vertebrate spacing systems. Anim Behav 49:1581–1597.

Mallot HA, 1999. Spatial cognition: Behavioral competences, neural mechanisms, and evolutionary scaling. Kognitionswiss 8:40–48.

Marler CA, Moore MC, 1991. Supplementary feeding compensates for testosterone-induced costs of aggression in male mountain spiny lizards, *Sceloporus jarrovi*. Anim Behav 42:209–219.

Marler CA, Walsberg G, White ML, Moore MC, 1995. Increased energy expenditure due to increased territorial defense in male lizards after phenotypic manipulation. Behav Ecol Sociobiol 37:225–232.

Maynard Smith J, 1982. Evolution and the Theory of Games. Cambridge University Press.

Menzel EW, 1973. Chimpanzee spatial memory organization. Science 182:943–945.

Menzel R, Greggers U, Smith A, Berger S, Brandt R, Brunke S, Bundrock G, Hülse S, Plümpe T, Schaupp F, Schüttler E, Stach S, Stindt J, Stollhoff N, Watzl S, 2005. Honey bees navigate according to a map-like spatial memory. Proc Natl Acad Sci USA 102:3040–3045.

Mery F, Kawecki TJ, 2004. An operating cost of learning in *Drosophila melanogaster*. Anim Behav 68:589–598.

Mesterton-Gibbons M, Adams ES, 2003. Landmarks in territory partitioning: A strategically stable convention? Am Nat 161:685–697.

Moravec H, Elfes A, 1985. High resolution maps from wide angle sonar. In: Proceedings of the IEEE International Conference on Robotics and Automation. St. Louis, MO, 116–121.

Morrell LJ, Kokko H, 2003. Adaptive strategies of territory formation. Behav Ecol Sociobiol 54:385–395.

Morrell LJ, Kokko H, 2005. Bridging the gap between mechanistic and adaptive explanations of territory formation. Behav Ecol Sociobiol 57:381–390.

Mouritsen H, Feenders G, Liedvogel M, Kropp W, 2004a. Migratory birds use head scans to detect the direction of the earth s magnetic field. Curr Biol 14:1946–1949.

Mouritsen H, Janssen-Bienhold U, Liedvogel M, amd J Stalleicken GF, Dirks P, Weiler R, 2004b. Cryptochromes and neuronal-activity markers colocalize in the retina of migratory birds during magnetic orientation. Proc Natl Acad Sci USA 101:14294–14299.

O'Keefe J, Nadel L, 1978. The hippocampus as a cognitive map. Oxford: Clarendon Press.

Papi F, Wallraff HG, 1992. Birds. In: Animal homing (Papi F, ed.), London: Chapman and Hall, chap. 7. 263–319.

Peck SL, 2004. Simulation as experiment: a philosophical reassessment for biological modeling. Trends Ecol Evol 19:530–534.

Pereira HM, Bergman A, Roughgarden J, 2003. Socially stable territories: The negotiation of space by interacting foragers. Am Nat 161:143–152.

Pipe AG, 2000. An architecture for learning "potential field" cognitive maps with an application to mobile robotics. Adapt Behav 8:173–204.

Powell RA, 2000. Animal home ranges and territories and home range estimators. In: Research techniques in animal ecology: controversies and consequences (Boitani L, Fuller TK, eds.), New York: Columbia University Press. 65–110.

Pravosudov VV, Clayton NS, 2002. A test of the adaptive specialization hypothesis: population differences in caching, memory, and the hippocampus in black-capped chickadees (*Poecile atricapilla*). Behav Neurosci 116:515–522.

Pusey AE, Packer C, 1997. The ecology of relationships. In: Behavioural Ecology: An Evolutionary Approach (Krebs JR, Davies NB, eds.), Oxford: Blackwell Science, chap. 11. 4th ed., 254–283.

Real LA, 1993. Toward a cognitive ecology. Trends Ecol Evol 8:39–41.

Reid ML, Weatherhead PJ, 1988. Topographical constraints on competition for territories. Oikos 51:115–117.

Ries L, Debinski DM, 2001. Butterfly responses to habitat edges in the highly fragmented prairies of Central Iowa. J Anim Ecol 70:840–852.

Rodríguez F, López JC, Vargas JP, Broglio C, Gómez Y, Salas C, 2002. Spatial memory and hippocampal pallium through vertebrate evolution: Insights from reptiles and teleost fish. Brain Res Bull 57:499–503.

Rossel S, Wehner R, 1986. Polarization vision in bees. Nature 323:128–131.

Rossiter SJ, Jones G, Ransome RD, Barratt EM, 2002. Relatedness structure and kin-biased foraging in the greater horseshoe bat (*Rhinolophus ferrumequinum*). Behav Ecol Sociobiol 51:510–518.

Rubin DC, Wenzel AE, 1996. One hundred years of forgetting: A quantitative description of retention. Psychol Rev 103:734–750.

Sanada-Morimura S, Minai M, Yokoyama M, Hirota T, Satoh T, Obara Y, 2003. Encounter-induced hostility to neighbors in the ant *Pristomyrmex pungens*. Behav Ecol 14:713–718.

Schmolke A, Basten K, Mallot HA, 2004. Effects of intruders and environments on spatial behavior: a simulation study. In: Dynamic Perception (Ilg UJ, Bülthoff HH, Mallot HA, eds.). Akad. Verl.-Ges. Aka, Berlin, 39–44.

Schmolke A, Mallot HA, 2002a. Polarisation compass for robot navigation. In: Fifth German Workshop on Artificial Life (Polani D, Kim J, Martinetz T, eds.). Akad. Verl.-Ges. Aka, Berlin, 163–167.

Schmolke A, Mallot HA, 2002b. Territory formation in mobile robots. In: Proceedings of the Eighth International Conference on Artificial Life (Standish RK, Bedau MA, Abbass HA, eds.). Cambridge, MA: MIT Press, 256–259.

Schmolke A, Mallot HA, submitted. Cognitive ecology of space use: a simulation study of territoriality.

Schölkopf B, Mallot HA, 1995. View-based cognitive mapping and path planning. Adapt Behav 3:311–348.

Schultz CB, Crone EE, 2001. Edge-mediated dispersal behavior in a prairie butterfly. Ecology 82:1879–1892.

Shettleworth SJ, 2001. Animal cognition and animal behaviour. Anim behav 61:277–286.

Shettleworth SJ, 2003. Memory and hippocampal specialization in food-storing birds: challenges for research on comparative cognition. Brain Behav Evol 62:108–116.

Sih A, Mateo J, 2001. Punishment and persistence pay: a new model of territory establishment and space use. Trends Ecol Evol 16:477–479.

Silverman BW, 1986. Density estimation for statistics and data analysis. London, New York: Chapman & Hall.

Smith AT, Dobson FS, 1994. A technique for evaluation of spatial data using asymmetric weighted overlap values. Anim Behav 48:1285–1292.

Stamps J, 1994. Territorial behavior: Testing the assumptions. Adv Stud Behav 23:173–232.

Stamps JA, 1995. Motor learning and the value of familiar space. Am Nat 146:41–58.

Stamps JA, Krishnan VV, 1990. The effect of settlement tactics on territory sizes. Am Nat 135:527–546.

Stamps JA, Krishnan VV, 1994a. Territory acquisition in lizards: I. first encounters. Anim Behav 47:1375–1385.

Stamps JA, Krishnan VV, 1994b. Territory acquisition in lizards: II. establishing social and spatial relationships. Anim Behav 47:1387–1400.

Stamps JA, Krishnan VV, 1995. Territory acquisition in lizards: III. competing for space. Anim Behav 49:679–693.

Stamps JA, Krishnan VV, 1997. Functions of fights in territory establishment. Am Nat 150:393–405.

Stamps JA, Krishnan VV, 1998. Territory acquisition in lizards. IV. obtaining high status and exclusive home ranges. Anim Behav 55:461–472.

Stamps JA, Krishnan VV, 1999. A learning-based model of territory establishment. Q Rev Biol 74:291–318.

Stamps JA, Krishnan VV, 2001. How territorial animals compete for divisible space: A learning-based model with unequal competitors. Am Nat 157:154–169.

Temeles EJ, 1994. The role of neighbours in territorial systems: when are they 'dear enemies'? Anim Behav 47:339–350.

Thrun S, 1998. Learning metric-topological maps for indoor mobile robot navigation. Artif Intell 99:21–71.

Thrun S, Bücken A, 1996. Integrating grid-based and topological maps for mobile robot navigation. In: Proceedings of the Thirteenth National Conference on Artificial Intelligence, AAAI, Portland, Oregon. AAAI Press, Menlo Park, California USA, 944–950.

Tobias J, 1997. Asymmetric territorial contests in the European robin: the role of settlement costs. Anim Behav 54:9–21.

Tolman EC, 1948. Cognitive maps in rats and men. Psychol Rev 55:189–208.

Trullier O, Wiener SI, Berthoz A, Meyer JA, 1997. Biologically based artificial navigation systems: review and prospects. Prog Neurobiol 51:483–544.

Webb B, 2000. What does robotics offer animal behaviour? Anim Behav 60:545–558.

Wehner R, 1982. Himmelsnavigation bei Insekten. Neurophysiologie und Verhalten. Naturforsch Ges Zürich.

Wehner R, 1992. Arthropods. In: Animal homing (Papi F, ed.), London: Chapman and Hall, chap. 3. 45–144.

Wehner R, 2003. Desert ant navigation: how miniature brains solve complex tasks. J Comp Physiol A 189:579–588.

Wehner R, Menzel R, 1990. Do insects have cognitive maps? Annu Rev Neurosci 13:403–414.

Wehner R, Srinivasan MV, 1981. Searching behaviour of desert ants, genus *Cataglyphis* (Formicidae, Hymenoptera). J Comp Physiol A 142:315–338.

White KAJ, Lewis MA, Murray JD, 1996. A model for wolf-pack territory formation and maintenance. J theor Biol 178:29–43.

White KG, 2002. Temporal generalization and diffusion in forgetting. Behav Proc 57:121–129.

Wiltschko W, Wiltschko R, 2001. Light-dependent magnetoreception in birds: the behaviour of european robins, *Erithacus rubecula*, under monochromatic light of various wavelengths and intensities. J Exp Biol 204:3295–3302.

de Winter W, Oxnard CE, 2001. Evolutionary radiations and convergences in the structural organization of mammalian brains. Nature 409:710–714.

Winter Y, Stich KP, 2005. Foraging in a complex naturalistic environment: capacity of spatial working memory in flower bats. J Exp Biol 208:539–548.

Wohlgemuth S, Ronacher B, Wehner R, 2001. Ant odometry in the third dimension. Nature 411:795–798.

Wohlgemuth S, Ronacher B, Wehner R, 2002. Distance estimation in the third dimension in desert ants. J Comp Physiol A 188:273–281.

Worton BJ, 1989. Kernel methods for estimating the utilization distribution in home-range studies. Ecology 70:164–168.

Appendix A

Implementation details

A.1 Territory behaviour

In the following, I introduce the main classes of the territorial behaviour. I provide a short description of the tasks each class fulfils and mention the most important functions of the classes. I explicitely state if a class does not apply for both the real and the simulated robots.

A.1.1 Attractiveness

Calculation of the attractiveness value applying Equation 3.1 within the function **new_attract**. Constants of the equation are read from the initialisation file.

A.1.2 Occupancy

Calculation of the occupancy probability of the grid. From the current sensor data, the grid range covered by the sensors is derived. This sub-grid is merged with the global occupancy grid. The positions of the infrared sensors relative to the robot's centre are provided. The sensor model as introduced in Section 3.5.2 is implemented here. The cell spacing of the occupancy grid is predefined.

Functions:

actual_submap Builds a small occupancy grid from the current infrared sensor data. The returned occupancy grid is aligned with the global occupancy grid

and centred around the cell in which the robot is currently positioned.

merge_submaps Merges the sub-map gained by the previous function with the corresponding section of the global occupancy grid. The occupancy values in each cell are calculated using Equation 3.4 as implemented in the following function.

new_cell_value Incremental calculation of the occupancy probability given two estimates (compare Equation 3.4).

calc_overlap Calculates the overlap between each grid cell and the free or occupied area, respectively, as derived from the sensor data (compare Section 3.5.2 and Figure 3.2).

get_sensorRect Calculation of the area that is detected as free or occupied, respectively, by each sensor.

A.1.3 BaseMap

Spatial memory structure. This is the base class for the two memory structures applied, the graph (**TerritoryGraph**) and the grid (**TerritoryGrid**). The updates of the memory as well as the choice of the next destination are implemented here.

Functions (virtual in BaseMap):

save_map Writing the whole structure to a file.

read_map Reading the memory from file.

update_map Updating the memory by current local data. This includes the position, the attractiveness of the current place, the information about obstacles (the occupancy of the surrounding in case the grid is used) and the presence of competitors.

nextNode Decision for the destination of the subsequent step.

Additional functions in TerritoryGraph:

TerritoryGraph uses the class **MetricGraph** which stores the connections between the nodes.

catchment_area Checks if the robot has entered the catchment area of a node.

goto_heading Retrieves the nodes from memory that belong to the N-neighbourhood of the current node. The attractiveness panorama is assembled using the following function. From the panorama, a movement direction is chosen stochastically.

attractPanorama Builds the attractiveness panorama according to the attractiveness values and distances of the nodes in the N-neighbourhood (compare Section 3.5.2 and Equation 3.5).

obstacle_edges Determines the position of obstacles in relation to the robot. In case an obstacle is close-by, the current node labelled as explicitely unconnected to the nodes behind the obstacle ("non-edges" in the graph, compare Section 3.5.2).

add_node_to_Matrix A new node is added to the graph if a previously unknown place is visited. The nodes and connections between them are stored in **MetricGraph**.

Additional functions in TerritoryGrid:

heritedAttractiveness Calculation of the directional attractiveness according to the N-neighbourhood (compare section 3.5.2).

get_submap Retrieves the section of the occupancy grid that currently corresponds the to infrared sensor range. This sub-grid is merged with the current grid as calculated from the sensor data, see **Occupancy**:merge_submaps.

write_submap Changes the occupancy values as stored in the global grid according to the updated sub-grid.

A.1.4 TerritoryNode

An instance of this class provides the memory container that is connected to each node in the graph structure or cell in the grid. The following data is stored: position, occupancy probability (for the grid), attractiveness value, infrared sensor data, number of positive and negative visits. All functions of this class either set or retrieve these data.

A.1.5 FileMan

This class handles the data storage in files and the loading of files in case a robot is revived from a previous session. While the memory is only written to file after a predefined number of steps (**write_file**), the current robot's position is written to file after each step (**savePosition**). The file names include the number of steps accomplished, the number of the robot and the type (*.map for the memory content, *.pos for the robot's positions).

A.1.6 TerritoryBehave and SimBehave

These classes control the single robots, i.e. for each robot, an instance of the classes is provided. **TerritoryBehave** is used for the real Khepera robots while **SimBehave** controls the simulated robots.

Functions:

move / get_destination Retrieves the destination of the next step from **BaseMap** and controls the robot's movement to this location.

updates Retrieval of all available information after each step. This information changes the memory content via the classes introduced above.

A.1.7 TerritoryControl

This class controls all real Khepera robots and the tracking system. The user interface to this control class is provided by **GuiTerritory**. The image as captured by the tracking camera is shown on the graphical user interface. The bottoms change a state variable that is scanned by the control class after each step.

A.1.8 sim

This is the heart of the Khepera simulation. The class controls all robots as **TerritoryControl** and provides the user interface. Additionally, it initialises the simulated environment. It provides the interface between the robots and their environment.

A.2 Control of the real Khepera robots

A.2.1 ComHand

Control of a robot and the tracking system. Since the robots are contacted via the radio module, transmissions occasionally fail. This class is designed to bridge transmission problems. Only if the communication fails several times in a row, the robot is assumed to be unreachable. Comparably, the tracking of a robot is repeated several times if it fails. For each robot in use, an instance of **ComHand** is produced. The robot identity is adjusted in **TKhepera** (see below). The classes introduced here were also used for the evaluation of the polarisation compass.

Functions:

move Command to the robot to move forward or backward for a defined distance.

rotate Command to the robot to rotate by a defined angle.

stop Any movement of the robot is interrupted.

reached Checks if the robot reached its position.

set_speed_profile Determines the maximum speed the robot will reach during translations and the acceleration.

motor_position Reads out the motor counters of the robot.

reset_motor_counters Resets the counters of the robot's step motors.

read_IR Reads out the data of the active infrared sensing.

read_ambient_IR Reads out the ambient infrared light as measured by the infrared sensors.

read_cam Reads out the data of the linear camera device.

read_analysers Reads out the data of the polarisation sensors.

set_LED Switches the LEDs on or off. The LEDs are the signals used by the tracking system to detect the robot's position and heading. Only one robot can be detected at a time, thus, the LEDs have to be switched off after the tracking of one robot.

walk_to The call combines a rotation and a translation command that will steer the robot to a defined goal position.

track_position / get_tracker_pos Retrieve the robot's arena position from the tracking system.

get_averaged_tracker_pos Averages the robot's arena position over several measurements. This allows a more precise position measurement.

reset_com_counter The failed communications with the robot are counted and communication is given up if this counter reaches a defined threshold value. This function resets the counter.

reset_tracker_counter The number of unsuccessful tracking attempts are reset to zero.

A.2.2 TKhepera

Interface to the Khepera robots. Functions for the Khepera control as listed in the manual are provided. Most functions are reimplemented in **ComHand**. For the territorial behaviour, it is important to communicate with a defined robot. This is achieved by adjusting the robot identity in each function call. The current robot ID is set with the function **activate_robot**.

A.2.3 TEnv

This class exclusively triggers the tracking of the robot using the function **search_robot**. The class **ImgCapture2** reads out the camera image while **CalTracking** calculates the robot's position by detecting the LEDs in the image. The image distortion is corrected.

A.3 Simulation environment

The code of the simulation environment is adapted from the Khepera simulator as provided by Olivier Michel (compare 3.5.1). The code is not written in C++ as the rest, but in C. I will list the functions that are important for the territorial behaviour and altered (or added) accordingly.

A.3.1 sim

This subsumes the overall control of the simulation and the main function (see above).

Functions:

OpenProgram Initialisation of the environment with the robots as well as the graphical user interface. Links to **SimBehave** in order to retrieve the parameters from the initialisation files.

main Note that only the options *STEP_ROBOT* and *RUN_ROBOT* are linked to the territorial behaviour. All settings of the environment and the robots are defined before program start in the initialisation files as described below.

A.3.2 robot

This file includes all the functions and variables that are needed to define and run a single robot.

Functions:

CreateRobot Produces a struct that defines a robot.

IRSensorDistanceValue Calculates the responses of the infrared sensors by using the information of obstacle location from the environment (**world**) and the infrared sensor model as described in Section 3.5.1.

A.3.3 multirobots

Subsumption of all robots. The sequential access to the robots is controlled as well as their mutual influences.

Functions:

CreateMultiRobots Produces a struct that subsumes all robots that are currently running in the arena.

MultiInitSensors Controls the infrared sensors of all robots including potential mutual influences between the robots.

MultiRobotRun Controls the movements of all robots. Each robot accomplishes a full step; the robots are executed one after the other.

RobotDetection Checks if another robot is closer than 15cm to the robot currently in focus.

A.3.4 world

Definition of the environment with the obstacles. It provides the interface to the robots in order to calculate their sensor responses.

Functions:

CreateObject Produces a struct that defines a single obstacle.

CreateEmptyWorld Creates the arena bare of any obstacles (even the walls).

ReadWorldFromFile Reads the *world* file and sets the obstacles accordingly.

getEdges Calculates the edges of an obstacle. This function is essential for the determination of the robots' infrared sensor response.

A.3.5 graphics

In this file, all functions related to the graphical user interface are subsumed. I added the function **DrawMultiLittleRobots** which draws the robots on the graph-

ical user interface. The robots are provided with a yellow number each that reflects their identity number. The other functions are mostly originally taken form the Khepera simulator.

A.4 Initialisation files

On program start, an initialisation file is read in. This file defines the variables of the experiment that apply for all robots at a time. Additionally, it contains the names of the initialisation files as used for each robot. This allows different settings for the robots. The initialisation files are written im XML and the classes **veXml** and **veStrUtils** are used to extract the data.

A.4.1 Global initialisation file

Parameters:

fileName Name of the result files. Robot number, step number and a file name extension is appended to this file name (compare **FileMan**).

worldName Name of the file that defines the arena layout, i.e. the number and positions of the obstacles. This parameter does not apply if the real robots are used.

tracker Determines if the tracker is used for the position information in the real robots. This variable does not apply if the simulated robots are used.

robotNum Number of robots.

contSession If this parameter is set to 1, a previous session is restarted. Set the parameter to zero to start a completely new session.

prevRobots If **contSession** is set to 1, this parameter defines the number of robots in the previous session. It is possible to reload less robots than were running in the previous session. This parameter does not apply if **contSession** is set to 0.

steps Number of steps that will be accomplished in the session. The session is interrupted automatically as soon as the steps are accomplished.

interval Defines the number of steps during an interval. After each interval, all data is saved automatically and the session is continued. Note that **steps** should be dividable by **interval**.

StartPosition Array of position data composed of the x and y coordinate in mm of the start position and the heading in degree. There have to be provided as many positions as robots started. This parameter does not apply for the real robots.

map Name of the initialisation file for a single robot. For each robot, one file name has to be given.

calfile / imgfile Name of the calibration files for the tracking system. These parameters do not apply if the simulation environment is used.

iniK Name of the files containing the calibration data for each robot as gained by the UMBmark method and the optimisation of the polarisation sensors (compare Section 2.2.3 and 2.3). This parameter does not apply if the simulation environment is used.

A.4.2 Individual initialisation files

For each robot, an individual initialisation file is defined. The names of these files are listed in **maps** of the global initialisation file.

Parameters:

map Identification number of the memory structure that will be used; 1 marks the grid, 2 the graph structure.

node_length Amount of memory retrieval. The number denotes the N-neighbourhood applied (compare Section 3.5.3).

Rp / Rf / Pmax / Fmax Parameters of Equation 3.1.

defaultAttract Attractiveness value of unknown places.

gridSize Number of cells in one row of the grid structure.

cellSize Edge length in cm of a single cell in the grid structure.

min / max Minimal and maximal step length in cm if the graph structure is used. If the step length should be constant as in the presented experiments, both values are set equally.

radius Radius in cm of the catchment area of a node in the graph structure (compare Section 3.5.2).

accuracy Sample separation in degree of the attractiveness panorama (compare Section 3.5.3).

Danksagung

Besonders herzlich möchte ich mich bedanken bei meinem Doktorvater, Herrn Prof. Dr. Hanspeter A. Mallot, für die Überlassung des Themas, für die stets große Aufgeschlossenheit in allen fachlichen Fragen und für die Freiheit, die ich bei der Gestaltung meines Themas genossen habe. Die Ermutigung zu Aktivitäten außerhalb der Doktorarbeit sowie die uneigennützige Förderung meiner Zukunftspläne weiss ich sehr zu schätzen.

Großer Dank geht an Wolfgang Hübner und Wolfgang Stürzl, die mich in die Künste des Programmierens eingeführt haben und auf deren Quellcode ich zurückgreifen durfte. Ihre Hilfe bei der Überwindung von Rechner- und rechnerischen Problemen war unabdingbar für das Gelingen dieser Arbeit. Kai Basten möchte ich danken für die Implementierung des Graphen im Rahmen seiner Diplomarbeit.

Die Mitarbeiter des Lehrstuhls kognitive Neurowissenschaft hatten immer ein offenes Ohr für wissenschafliche, technische und organisatorische Fragen. Vielen Dank für die gute Zusammenarbeit und alles, das nichts mit Wissenschaft zu tun hatte.

Für sehr hilfreiche Kommentare zum Manuskript der Arbeit möchte ich mich bedanken bei Hanspeter Mallot, Jan Wiener, Sabine Gillner und Johannes Thiele.

Die Arbeit wurde durch die finanzielle Unterstützung der DFG im Rahmen des SFB 550 und des Graduiertenkollegs Kognitive Neurobiologie ermöglicht.

Ein ganz besonderer Dank kommt meinen Eltern zu, die meine Interessen immer unterstützt haben und mir zur Seite stehen, wo immer es möglich ist - bei weitem nicht nur mit einem guten Tropfen aus dem Badischen.

Curriculum vitae

Amelie Schmolke
* 21. Mai 1975 in Freiburg i. Br.

Forschung

seit 2003	Stipendiatin im Graduiertenkolleg Kognitive Neurobiologie
seit 2001	Doktorarbeit (Kognitive Neurowissenschaften, Universität Tübingen): *Territorial Robots: A Model Approach to the Ecology of Spatial Cognition*
2000-2001	Projektarbeit (MPI für biologische Kybernetik, Tübingen): *A Camera-Based Tracking System for Miniature Robots*
1999-2000	Diplomarbeit (Tierphysiologie, Universität Freiburg): *Das Polarisationssehen der Honigbiene: Der differentielle Einsatz der POL-Regionen*
1998-1999	Forschungspraktikum (Tierphysiologie, Universität Groningen, Niederlande): *Long-term Effects of Social Stress on the Expression of Corticotropin-Releasing Factor by Measuring mRNA in various Regions of the Rat Brain*

1998	Projekt als wissenschaftliche Hilfskraft (Tierphysiologie, Universität Freiburg): *Elektrophysiologie des* Drosophila-*Auges zur Charakterisierung von Mutanten*
1997	Forschungspraktikum (Tierphysiologie, Universität Bayreuth): *Der Einfluss des sozialen Status auf Verhalten und Immunsystem der Ratte*

Schule und Studium

2000	Diplom in Biologie. Hauptfach: Tierphysiologie / Verhaltensbiologie, Nebenfächer: Informatik, Genetik und Entwicklungsbiologie
1994-2000	Studium der Biologie und Informatik an der Universität Freiburg
1994	Abitur am Deutsch-Französischen Gymnasium, Freiburg